

Comparative DNA-Protein Interaction and Epithelial Tight Junctions Modulation Potential of Immunosuppressive Regime

Dissertation

for the award of the degree

Doctor rerum naturalium (Dr.rer.nat.)

(Division of Mathematics and Natural Sciences)

of the Georg-August-Universität Göttingen

within the doctoral program Biology

of the Georg-August University School of Science (GAUSS)

Submitted by

Niamat Khan

from Gul Shah Khel (Distt. Kohat), Pakistan

Göttingen, 2015

Thesis Committee

Prof. Dr. Uwe Groß
University Medical Center Göttingen
Institute of Medical Microbiology, George-August-University
Kreuzberggring 57, 37075, Göttingen, Germany

Prof. Dr. Stefanie Pöggeler
Institute of Microbiology and Genetics
Dept. Genetics of Eukaryotic Microorganisms
Georg-August University, Grisebachstr.8, 37077, Göttingen, Germany

Prof. Dr. Abdul R. Asif
Clinical Proteomics, Diagnostics, Quality Management
Institute of Clinical Chemistry / UMG-Laboratories
University Medical Center, George-August-University
Robert-Koch-Str. 40, D-37075, Göttingen, Germany

Members of the Examination Board (in alphabetical order)

Prof. Dr. Ralf Dressel
Department of Cellular and Molecular Immunology
University Medical Center, George-August-University
Robert-Koch-Str. 40, D-37075 Göttingen

PD Dr. Wilfried Kramer
Institute for Microbiology and Genetics
Dept. of Molecular Genetics, George-August-University
Grisebachstr. 8, 37077 Göttingen, Germany

PD Dr. Marko Rohlf's
J.F. Blumenbach Institute of Zoology and Anthropology
George-August-University, Berliner Str. 28, 37073 Goettingen, Germany

Prof. Dr. Ernst A. Wimmer
Johann-Friedrich-Blumenbach-Institute of Zoology and Anthropology
Dept. of Developmental Biology GZMB, Georg-August-University Goettingen
Justus-von-Liebig-Weg 11, 37077 Goettingen, Germany

Date of the oral examination: 14th January, 2016

DECLARATION

I hereby declare that the Ph.D. thesis entitled “Comparative DNA-Protein Interaction and Epithelial Tight Junctions Modulation Potential of Immunosuppressive Regime” has been written independently, with no other sources than quoted, and no portion of the work referred to in the thesis has been submitted in support of an application for another degree.

Niamat Khan

Table of Contents

| | |
|---|------|
| List of Figures | vii |
| List of Tables | viii |
| List of Abbreviations | ix |
| 1 General introduction: | 1 |
| 1.1 Mycophenolic acid..... | 1 |
| 1.1.1 Pharmacodynamics of MPA | 1 |
| 1.1.2 Pharmacokinetics | 2 |
| 1.1.3 Adverse side effects of MPA | 2 |
| 1.2 Rationale for the proposed research..... | 4 |
| 2 Mechanism of Tight Junction Regulation in Leak-Flux Diarrhea | 5 |
| 2.1 Abstract..... | 6 |
| 2.2 Introduction:..... | 6 |
| 2.3 Mechanisms of Leak-Flux diarrhea | 8 |
| 2.3.1 Myosin Light Chain Kinase (MLCK) Pathway | 9 |
| 2.3.2 Certain bacterial pathogens exploit MLCK Pathway to disturb TJ assemblage. | 10 |
| 2.3.3 Phosphoinositide 3 kinases (PI3K) pathway..... | 13 |
| 2.3.4 Signal Transducer and Activator of Transcription (STAT) Pathway | 13 |
| 2.3.5 P38MAPK pathway | 13 |
| 2.3.6 Protein kinase C (PKC) pathway | 14 |
| 2.3.7 JunD pathway..... | 18 |
| 2.3.8 <i>Salmonella</i> and TJ regulation..... | 18 |
| 2.3.9 EGFR/JNK pathway | 19 |
| 2.3.10 <i>Clostridium perfringens</i> enterotoxin (CPE) and TJ regulation..... | 19 |
| 2.3.11 Concluding remarks | 20 |
| 2.4 Acknowledgements..... | 20 |
| 3 Transcriptional Regulators of Claudins in Epithelial Tight Junctions | 21 |
| 3.1 Abstract..... | 21 |
| 3.2 Introduction..... | 21 |
| 3.2.1 Claudin 1:..... | 23 |
| 3.2.2 Claudin 2..... | 24 |
| 3.2.3 Claudin-3, Claudin-4, and Claudin-5 | 25 |
| 3.2.4 Claudin-7..... | 25 |

| | | |
|--------|---|----|
| 3.2.5 | Claudin-15..... | 26 |
| 3.2.6 | Claudin 19..... | 26 |
| 3.3 | Conclusion: | 27 |
| 3.4 | Acknowledgement: | 27 |
| 4 | Immunosuppressant MPA modulate tight junction through epigenetic activation of MLCK/MLC-2 pathway via p38MAPK..... | 28 |
| 4.1 | Abstract..... | 28 |
| 4.2 | Introduction..... | 29 |
| 4.3 | Material and Methods | 31 |
| 4.3.1 | Experimental Design..... | 31 |
| 4.3.2 | Chemicals/Reagents | 31 |
| 4.3.3 | Primer Design | 32 |
| 4.3.4 | Cell Culture..... | 32 |
| 4.3.5 | Caco-2 monolayer integrity assays | 32 |
| 4.3.6 | RNA expression analysis | 33 |
| 4.3.7 | Dot Blot..... | 34 |
| 4.3.8 | Western blot..... | 35 |
| 4.3.9 | Chromatin immunoprecipitation (ChIP) | 36 |
| 4.3.10 | Data Analysis | 36 |
| 4.3.11 | Statistics | 37 |
| 4.4 | Results..... | 38 |
| 4.4.1 | MPA increases global histone (H3K9 and H4K8) acetylation in Caco-2 Cells..... | 38 |
| 4.4.2 | MPA treatment activates MLCK and MLC-2 while inactivates occludin at epigenetic level in Caco-2 cells..... | 38 |
| 4.4.3 | MPA treatment activates p38MAPK and ATF-2 at epigenetic level in Caco-2 cells..... | 39 |
| 4.4.4 | Inhibition of p38MAPK via SB counteracts the altered expression of MLCK, MLC-2, and occludin genes in MPA-treated Caco-2 cells. | 39 |
| 4.4.5 | p38MPAK inhibition partially reverses MPA-induced TJs dysfunction | 40 |
| 4.4.6 | Inhibition of p38MAPK through SB demolishes increased promoter activity of downstream targets of p38MPAK in MPA-treated Caco-2 cells..... | 43 |
| 4.5 | Discussion | 46 |
| 4.6 | Conclusions..... | 48 |
| 4.7 | Competing Interests | 49 |
| 4.8 | Author's contribution..... | 50 |

| | | |
|--------|---|----|
| 4.9 | Acknowledgments..... | 50 |
| 5 | Active and repressive chromatin associated proteome after MPA treatment and the role of midkine in epithelial monolayer permeability | 51 |
| 5.1 | Abstract..... | 51 |
| 5.2 | Introduction..... | 52 |
| 5.3 | Material and Methods | 53 |
| 5.3.1 | ChIP-O-Proteomics..... | 53 |
| 5.3.2 | mRNA Expression Assay: | 55 |
| 5.3.3 | Cell cytotoxicity assays..... | 55 |
| 5.3.4 | Caco-2 monolayer integrity | 56 |
| 5.4 | Results and discussion: | 56 |
| 5.5 | Conflict of Interest | 64 |
| 5.6 | Acknowledgement | 64 |
| 6 | MPA modulates tight junctions' permeability via midkine/PI3K pathway in Caco-2 cells: A possible mechanism of leak-flux diarrhea in organ transplanted patients | 65 |
| 6.1 | Abstract..... | 65 |
| 6.2 | Introduction..... | 66 |
| 6.3 | Material and Methods | 67 |
| 6.3.1 | Cell Culture..... | 67 |
| 6.3.2 | Inhibitory Assays | 68 |
| 6.3.3 | Experimental design..... | 68 |
| 6.3.4 | Cell cytotoxicity assays..... | 68 |
| 6.3.5 | Caco-2 cells monolayer integrity | 68 |
| 6.3.6 | Primer Design: | 69 |
| 6.3.7 | Expression Assay: | 69 |
| 6.3.8 | Western blot..... | 69 |
| 6.3.9 | ChIP Assay: | 70 |
| 6.3.10 | Immunofluorescence microscopy of TJs proteins:..... | 70 |
| 6.3.11 | Statistics | 71 |
| 6.4 | Results..... | 71 |
| 6.4.1 | MPA induces midkine-dependent epigenetic activation of PI3K, Cdx-2 and Cludin-2 (Cldn-2) genes and repression of claudin-1(Cldn-1) gene..... | 71 |
| 6.4.2 | MPA activates Cdx-2 expression via midkine/PI3K pathway..... | 74 |

| | | |
|-------|--|-----|
| 6.4.3 | MPA-mediated altered expression of Cldn-1 and Cldn-2 are prevented by midkine or PI3K inhibitors. | 75 |
| 6.4.4 | p38MAPK pathway is activated by Midkine/PI3K signaling in MPA treated Caco-2 cells. 76 | |
| 6.5 | Discussion | 80 |
| 6.6 | Conclusion | 85 |
| 6.7 | Conflict of Interest | 86 |
| 6.8 | Acknowledgement | 86 |
| 7 | Summary | 88 |
| 8 | Reference List | 93 |
| 9 | Acknowledgment | 117 |
| 10 | Curriculum Vitae - Niamat Khan..... | 118 |

List of Figures

| | |
|---|----|
| FIGURE 1.1: PHARMACODYNAMICS OF MPA IN LYMPHOCYTES | 3 |
| FIGURE 2.1: TJS PRESENT AT THE APICAL-LATERAL REGION AND CONTROL PARACELLULAR MOVEMENTS ACROSS EPITHELIAL MONOLAYER. | 8 |
| FIGURE 2.2: SCHEMATIC REPRESENTATION OF TJ REGULATION VIA PI3K AND MLCK PATHWAYS ACTIVATED BY MPA, PROINFLAMMATORY CYTOKINES AND ENTEROPATHOGENIC E. COLI (EPEC). | 11 |
| FIGURE 2.3: STRATEGIES USED BY PROINFLAMMATORY CYTOKINE AND BACTERIAL TOXINS TO REGULATE TJ VIA P38MAPK AND PKC PATHWAYS. | 17 |
| FIGURE 4.1: MPA TREATMENT INCREASES GLOBAL HISTONE ACETYLATION IN CACO-2 CELLS. | 41 |
| FIGURE 4.2: CAUSES EPIGENETIC ACTIVATION OF MLCK/MLC-2 PATHWAY AND TIGHT JUNCTION GENES (OCCLUDIN). | 42 |
| FIGURE 4.3: P38MAPK REGULATES MLCK/MLC-2 PATHWAY AND ITS INHIBITION PARTIALLY PREVENTS MPA-INDUCED TJS DYSFUNCTION. | 44 |
| FIGURE 4.4: INHIBITION OF P38MAPK COUNTERACTS MPA-MEDIATED EPIGENETIC REMODELING. | 45 |
| FIGURE 4.5: P38MAPK INHIBITION PRESERVES NORMAL MLCK/MLC-2 GENE EXPRESSION IN CACO2 CELLS TREATED WITH MPA. | 46 |
| FIGURE 4.6: PROPOSED MECHANISM OF MPA-INDUCED TJS ASSEMBLY DEREGULATION IN CACO-2 CELLS MONOLAYER. | 49 |
| FIGURE 5.1: SCHEMATIC OVERVIEW OF CHIP-O-PROTEOMICS EXPERIMENTAL STEPS | 60 |
| FIGURE 5.2: INFLUENCE OF MPA ON THE EXPRESSION AND ACTIVATION OF MIDKINE GENE AND CACO-2 CELLS MONOLAYER INTEGRITY. | 61 |
| FIGURE 5.3: INFLUENCE OF MIDKINE INHIBITOR (IMDK) ON MIDKINE EXPRESSION AND CELL VIABILITY OF MPA-TREATED CACO-2. | 62 |
| FIGURE 6.1: INFLUENCE OF MPA ON PI3K/AKT PATHWAY AND PI3K/AKT DEPENDENT MODULATION OF TJS PERMEABILITY. | 72 |
| FIGURE 6.2: REGULATORY EFFECT OF MPA TREATMENT ON THE PROMOTER OF OTHER GENES INVOLVE IN THE REGULATION OF TJ PERMEABILITY. | 74 |
| FIGURE 6.3: CYTOTOXIC EFFECTS OF PI3K INHIBITOR (AMG) IN CO-TREATMENT WITH MPA ON CACO-2 CELLS. | 75 |
| FIGURE 6.4: ACTIVATION OF CDX-2 GENE VIA MIDKINE/PI3K PATHWAY AFTER MPA TREATMENT. | 77 |
| FIGURE 6.5: INFLUENCE OF MIDKINE MEDIATED PI3K PATHWAY ON TJ STRUCTURAL PROTEINS (CLAUDIN-1, -2) IN MPA TREATED CACO-2 CELLS. | 78 |
| FIGURE 6.6: PROMOTER ACTIVITY OF CLAUDIN-1 AND CLAUDIN-2 GENES. | 79 |
| FIGURE 6.7: MIDKINE/PI3K DEPENDENT ACTIVATION OF P38MAPK PATHWAY AFTER MPA TREATMENT. | 80 |
| FIGURE 6.8: PROPOSED MECHANISM OF MPA-INDUCED TJ ASSEMBLY DEREGULATION IN CACO-2 CELLS MONOLAYER. | 85 |
| FIGURE 7.1: CHROMATIN IMMUNOPRECIPITATION. | 89 |
| FIGURE 7.2: TJS REGULATION. | 90 |
| FIGURE 7.3: PROPOSED AND EXPERIMENTAL EVIDENCE FOR MPA MEDIATED TJS DISRUPTION: | 91 |

List of Tables

| | |
|--|----|
| TABLE 3.1 REGULATORS OF CLAUDINS | 27 |
| TABLE 4.1: PROMOTOR ASSAY AND MRNA EXPRESSION PRIMER LIST. | 37 |
| TABLE 5.1: DIFFERENTIAL PROTEOMIC AFTER MPA TREATMENT AT HISTONE MODIFICATIONS (H3K4ME3 & H3K27ME3) | 63 |
| TABLE 6.1: LIST OF PRIMERS OF MIDKINE/PI3K RELATED GENES | 87 |

List of Abbreviations

| | | | |
|--------------------|--|--------------|---|
| 2 ^{-ΔΔCT} | Comparative threshold cycle (CT) method | Esp | Effector proteins |
| A/C | Attaching and effacing | ETS | E26 transformation-specific sequence |
| AcMPAG | Acyl glucuronide of mycophenolic acid | FCS | Fetal calf serum |
| ANOVA | Analysis of variance | FD4 | FITC-dextran (4KDa) |
| aPKC | Atypical protein kinase C | FITC-dextran | Fluorescein isothiocyanate-conjugated dextran |
| BS | binding sites | foxO | Forkhead box |
| C.difficile | Clostridium difficile | GEF-H1 | |
| Caco-2 | Colon carcinoma | GI | Gastrointestinal |
| CD | Crohn's disease | GMP | Guanosine monophosphate |
| CDK2 | cyclin-dependent kinase 2 | HA/P | Heamgglutinin/protease |
| cdx | caudal-related homeobox | HEK-293 | human embryonic kidney-293 |
| ChIP | Chromatin immunoprecipitation | Hnf4α | hepatocyte nuclear factor 4 alpha |
| ChIP-O-Proteomics | Chromatin immunoprecipitation-O-Proteomics | IAA | Iodoacetamide |
| Cmax | Maximal plasma concentration | IBDs | inflammatory bowel diseases |
| CPE | Clostridium perfringens enterotoxin | IL-1β | Interleukin-1 β |
| CrD | Crohn's disease | IL-6 | Interleukin-6 |
| d | Days | iMDK | Inhibitor of midkine |
| Dlg1 | Drosophila discs large tumor suppressor | IMP | Inosine monophosphate |
| DMEM | Dulbecco's Modified Eagle's medium | IMPDH | Inosine monophosphate dehydrogenase |
| DMSO | Dimethyl sulfoxide | IMPDH-2 | inhibitor of inosine 5'-monophosphate dehydrogenase-2 |
| DNA | Deoxyribonucleic Acid | JAMs | Junctional adhesion molecules |
| dNTPs | Deoxynucleotide triphosphates | JNK | c-Jun N-terminal kinases |
| DTT | Dithiothreitol | LDH | lactate dehydrogenase |
| EC-MPS | Enteric-coated mycophenolate sodium | LFD | Leak flux diarrhea |
| EGFR | epidermal growth factor receptor | LIGHT | Lymphotoxin-like inducible protein that competes with glycoprotein D for herpes virus entry on T-cell |
| ELF3 | E74-like factor 3 | LPS | Lipopolysaccharide |
| EM | Epithelial monolayer | MAGI-1 | membrane-associated guanylate kinase |
| EPEC | Enteropathogenic Escherichia coli | MAPK/ERK | mitogen-activated protein kinase/extra cellular signal |

| | | | |
|-----------|---|--------------|--|
| MEK/ERK | regulated kinase mitogen-activated protein kinases/extracellular signal- regulated kinases | TFA | Trifluoroacetic acid |
| MLC-2 | myosin light chain-2 | TFs | Transcription factors |
| MLCK | myosin light chain kinase | TJs | tight junctions |
| MLCP | Myosin light chain phosphorylation | TNF α | Tumor necrosis factor alpha |
| MMF | Mycophenolate mofetal | TRED | Transcriptional regulatory element database |
| MPA | mycophenolic acid | UC | ulcerative colitis |
| MPAG | Mycophenolic acid glucuronide | UGTs | Uridine diphosphate- glucuronosyltransferases |
| mRNA | Messenger ribonucleic acid | UV | Ultra violet |
| MUPP-1 | multi-PDZ domain protein-1 | v | Volume |
| MYPT1 | | WPC1 | Whey protein concentrate 1 |
| P38MAPK | P38 mitogen-activated protein kinase | Zn | Zinc |
| PAR-6 | partitioning defective 6 homolog alpha | ZO-1 | Zonula occludens-1 |
| PATJ | PALS1-associated TJ | ZOT | Zonula occludin toxin |
| PBS | Phosphate buffer saline | | |
| PDZ | PSD95 Dlg1 ZO-1 | | |
| PI3K | PhosphoInositide-3 Kinase | | |
| PKC | Protein kinase C | | |
| PP1 | Protein phosphatase 1 | | |
| PP2A | Protein phosphatase 2A | | |
| PSD95 | postsynaptic density protein | | |
| PTEN | phosphatase and tensin homolog | | |
| Rab-13 | Ras-related protein Rab-13 | | |
| Rab-3b | Ras-related protein Rab-3B | | |
| ROCK | Rho-associated protein kinase | | |
| SDS | Sodium dodecyl sulfate | | |
| SGLT1 | Na ⁺ /glucose cotransporter 1 | | |
| siRNA | small interference RNA | | |
| Sp/XKLF | specificity protein/Krüppel- like factor | | |
| Sp-1 | Specificity protein-1 | | |
| STAT | Signal transducer and activator of transcription | | |
| TcdA/B | Toxin A/B | | |
| Tcf/Lef-1 | T-cell factor/lymphoid enhancing factor-1 | | |
| TEER | Trans epithelial electrical resistance | | |

1 General introduction:

1.1 Mycophenolic acid

Mycophenolic acid (MPA) is an active agent of *Penicillium brevicopactum* and was discovered by an Italian physician Bartolomeo Gosio in 1893 as an antibiotic against *Bacillus anthracis*. Currently, MPA is available in two generic forms (*enteric-coated mycophenolate sodium (EC-MPS) myfortic®*; Novartis Pharma AG, Basel, Switzerland; and *mycophenolate mofetil (MMF)*; CellCept, Roche, Grenzach-Wyhlen, Germany) and is prescribed to the organ transplanted patients with the aims to prevent allograft rejection [1;2].

1.1.1 Pharmacodynamics of MPA

Proliferating cells require pools of nucleotides including guanosine monophosphate (GMP) during DNA replication. Inosine monophosphate dehydrogenase (IMPDH)-2 is involved in the conversion of inosine monophosphate (IMP) into GMP via *de novo* pathway [3]. Highly proliferating cells such as B- and T-lymphocytes largely depends on the *de novo* pathway for the GMP synthesis [1]. However non-lymphocytes mainly acquire GMP via salvage pathway, where GMP is obtained from breaking down of RNA and DNA [1]. IMPDH-1 is expressed in all most all cell types, while IMPDH-2 is mainly expressed in proliferating active lymphocytes [1]. MPA competitively and reversibly inhibits the enzymatic activity of IMPDH-2 fivefold more than IMPDH-1, making it an effective immunosuppressive drug (ISD) (Fig. 1) [2]. MPA can prevent allograft rejection *via* three mechanisms: **a)** by inducing apoptosis in activated T-lymphocytes, consequently reduces clones of cells that respond to antigenic stimulation, **b)** by suppressing glycosylation and expression of some adhesion molecules, as a result, recruitment of immune cells decreases at the site of graft, and **c)** by depleting the cofactor of the inducible form of nitric oxide synthase ‘tetrahydrobiopterin’, in turn suppresses the production of NO and consequently peroxynitrite mediated tissue damage [1].

MPA has found its use in the treatment of autoimmune disorders (eyes and skin) [9;10], hypertension [11], lupus nephritis [3] as well as in neuromuscular autoimmune diseases [13;14]. As organ transplanted patients undergoing immunosuppressive therapy are more susceptible to

the infectious agents [4], the anti-bacterial [5], anti-viral [6] and anti-fungal [7] activities of MPA make it as a drug of choice for organ transplanted patients.

1.1.2 Pharmacokinetics

Upon oral administration, MMF is rapidly hydrolyzed by esterases into active form MPA and is absorbed in the stomach [8]. The EC-MPS requires neutral pH of intestine for solubility rather than acidic pH of stomach and is absorbed in small intestine [15;16]. MPA maximal plasma concentration (C_{max}) is acquired within 1.5-2.5 hrs after oral administration with mean bioavailability of 72% in case of EC-MPS [8]. While in the case of MMF, approximately 1-1.5 hrs is required to achieve C_{max} with mean bioavailability of 81% - 94 % [8]. Trough plasma concentration of MPA in the range of 1.0-3.5 mg/L indicates adequate therapy in liver transplant recipients [9]. Approximately 97-99 % MPA binds to the plasma albumin and less than three percent remains unbound which is responsible for the therapeutic activity in renal and heart transplanted patients [10].

MPA toxicity is reduced and excretion rate is increased by undergoing glucuronidation as a phase II metabolism. MPA is rapidly metabolized into MPA glucuronide (MPAG) by uridine diphosphate-glucuronosyltransferase (UGT), 7-O-glucoside by UGT287, acyl glucuronide MPA (AcMPAG) by UGTs (1A9, 1A7, 1A8, 1A10), and 6-O-desmethyl MPA by cytochrome P-450 3A45 enzyme which are expressed in liver, gastrointestinal (GI) tract and in kidney cells [19-21]. Following oral administration, the mean elimination half-life of MPA is ranged between 9 to 17 hrs [8]. Excretion of MPA mostly occurs through urine in MPAG (60-93%) metabolite form and approximately $\leq 3\%$ as MPA. Less than 6% is eliminated along with feces. Some portion of MPAG is recycled via enterohepatic circulation process. In this process MPAG is excreted from the liver cells in bile via multidrug resistance protein 2 (MRP2). GI tract bacteria deglucuronidate MPAG and convert it to MPA [5;22] which is again absorbed to the blood and is responsible for the second peak of MPA detected in plasma 6-12 hrs following oral administration [11].

1.1.3 Adverse side effects of MPA

On the one side, MPA is important for the prevention of allograft rejection, while on the other side its use is associated with some adverse effects such as neurological disturbances, cardio-

respiratory toxicity, metabolic disturbances, hematologic effects and gastrointestinal (GI) tract complications including diarrhea [4].

MPA-induced diarrhea of unknown etiology is frequently observed in transplanted patients, which results in dehydration and discomfort in the immune compromised patients ([28;29]). Approximately 62% and 79% of diarrhea incidences occurred in kidney transplanted patients following MMF and EC-MPA therapy, respectively [12]. Reducing the dose can decrease the chances of diarrhea incidence but concomitantly can increase the chances of acute allograft rejection [13]. It is difficult to assess quantitatively the overall diarrheogenic potential because drug based specific toxic effects cannot be dissociated from the potential contribution of other possible factors such as drug-drug interaction [13] and food-drug interactions [14] etc. Therefore it is necessary to investigate and understand the cellular mechanisms of MPA-induced diarrhea and to explore possible anti-diarrheal inhibitor(s) to use as a therapeutic agent during MPA therapy.

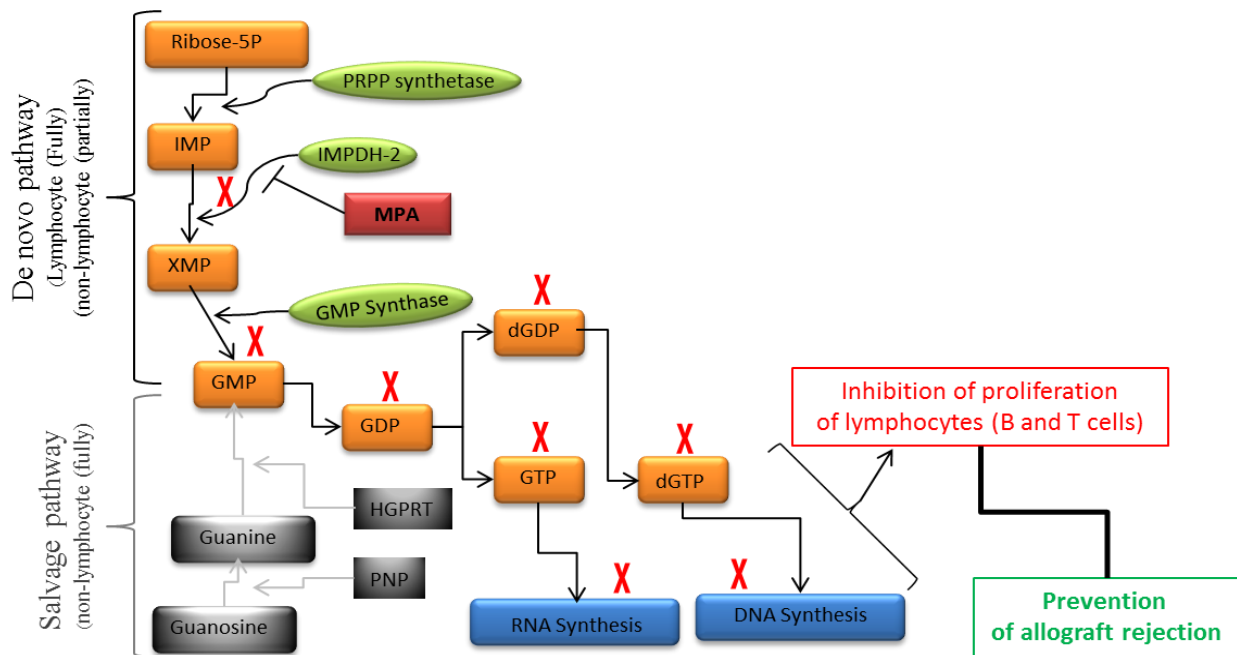


Figure 1.1: Pharmacodynamics of MPA in Lymphocytes. MPA blocks the enzymatic activity of IMPDH-2 which converts IMP into XMP via *de novo* pathway leading to depletion of XMP. XMP is required for the synthesis of GMP through GMP synthase. GMP is converted into GTP and dGTP via sequential rounds of phosphorylation. GTP is used in the transcription of RNA and “dGTP” in the replication of DNA. Therefore the synthesis of DNA and RNA are stopped, proliferation of lymphocytes is halted and as a result prevents allograft rejection (adapted from [2]).

1.2 Rationale for the proposed research

MPA impairs tight junctions (TJs) mediated small bowel barrier function [15] with not yet completely understood mechanism. TJ is a complex structure of multiple proteins that establish dynamic assembly between the adjacent cells of epithelial monolayer at apical region and selectively control paracellular movement of molecules and ions across the monolayer [16]. Several pathways such as protein kinase C (PKC) [33;34], phosphoinositide-3 kinase (PI3K) [17], myosin light chain kinase (MLCK) [18], Rho-associated protein kinase (ROCK) [19], and p38 mitogen-activated protein kinase (p38MAPK) [34;38] are activated in epithelial monolayer cells in response to various physiological and pathophysiological stimuli. The abnormal activation of one or more of these pathways can lead to the alteration of TJs proteins expression and/or distribution resulting in altered TJ assembly, increased permeability [20] and consequently causes diarrhea [21].

The present study was conducted to increase our understanding of the regulation and formation of TJs assembly using ChIP-o-Proteomics approach. To identify and characterize MPA-mediated TJs regulation, the following strategy was adopted.

1. Establishment of differentiated and polarized Caco-2 cells monolayers as TJs model followed by MPA treatment.
2. Immunoprecipitation of active and repressive chromatin followed by identification and quantification of DNA-binding proteins using mass spectrometry.
3. Amplification of ChIP-DNA with promoter specific primer pairs of target genes using real time PCR.
4. Characterization of genes involved in the regulation of cellular pathways and consequently alteration of TJs assembly.

2 Mechanism of Tight Junction Regulation in Leak-Flux Diarrhea

Niamat Khan^{1,2}, Muzna Zahur³ and Abdul R. Asif^{1,4*}

¹Institute for Clinical Chemistry / UMG-Laboratories, University Medical Centre, Robert-Koch-Str. 40, 37075, Goettingen, Germany. ²Department of Biotechnology & Genetic Engineering, Kohat University of Science and Technology, Kohat 26000, KPK, Pakistan. ³Department of Neurology, University Medical Centre, Waldweg 33, 37073, Goettingen, Germany. ⁴School of Biological Sciences, Quaid-i-Azam campus, University of the Punjab, Lahore, Pakistan.

* Author to whom correspondence should be addressed;

Submitted

Highlights

- Cellular signaling pathways tightly associated with tight junction regulation and consequently to the leak flux diarrhea as summarized in this review.
- Altered expression and/or localization of TJ proteins disturb TJs assembly and influence its ability to perform barrier function.
- Several cytokine, bacterial pathogen and immunosuppressant trigger common MLCK pathway to increase the TJ permeability.
- Bacterial toxins and/or oxidative stress trigger PKC dependent TJ permeability.
- MLCK, p38MPAK and PI3K pathways represent the principal forces behind tight junction assembly and its regulation.

2.1 Abstract

Intact and dynamic intercellular tight junctions (TJs) are crucial structural components that maintain epithelial barrier function and protect human body against interfering toxic and infectious agents. Inflammatory bowel diseases (IBD) such as ulcerative colitis (UC) and Crohn's disease (CrD) lead to increased loss of solutes and electrolytes resulting in leak flux diarrhea (LFD). LFD is backed by epithelial barrier dysfunction due to the altered regulation of TJ assembly through the disease mediated stimuli. Tight junctions receive intracellular signals and convert them to regulate their assembly and function. Most debated mechanism to increased TJ permeability are a) altered MLC-2 dependent F-actin cytoskeleton through myosin light chain kinase (MLCK); b) cdx-2 and src dependent increase of claudin-2 and redistribution of claudin-1 through P13K; c) decreased expression of pore-sealing claudin-4 through P38MAPK. Moreover, Protein kinase C (PKC) and protein phosphatases regulate TJ assembly via altered phosphorylation and dephosphorylation of occludin protein. This review describes the pathways that are involved in the regulation of TJs assembly via leak-flux mechanisms that consequently leads to leak flux diarrhea.

Key Words: Tight Junctions, Cellular Pathways, Gastrointestinal Disturbance, Leak-flux diarrhea

2.2 Introduction:

Gastrointestinal (GI) tract has the tremendous capacity to absorb electrolytes and water from the gut under normal condition where daily 8-9 liters of fluid are standing and only 100-200 ml is eliminated with waste (stool) [21]. Altered movement of electrolytes and water molecules and change in osmotic gradient is the hall mark of diarrhea [21] causing severe dehydration if not treated. Diarrhea is a common observation in many GI tract disturbances [22]. It has been estimated that within 18 months, an average individual in an industrialized country has at least one incident of acute diarrhea [23].

Mechanistically diarrhea can be divided into five different types, (i): motility disorder-dependent diarrhea: If the food particles moves too quickly and there are not sufficient time to absorb sufficient nutrients and water. This hypermotility diarrhea is caused by an excessive amount of

coarse foods or highly seasoned irritating food. In contrast, prolonged presence of the food particles in the bowel lumen causes bacterial overgrowth leading to hypomotility diarrhea [24] which is normally observed together with pancreatic insufficiency or bile-salt malabsorption. (ii) Osmotic diarrhea: Lactase deficiency and laxative abuse result in the accumulation of non-absorbable water-soluble substances or poorly absorbed substances (e.g., lactulose, hexitols, sorbitol, and mannitol) in the small intestine that can draw water from the body into the bowel leading to osmotic diarrhea [24-26]. (iii) Malabsorptive diarrhea: It is caused by insufficient absorption of food nutrients (e.g. glucose, galactose) across the GI tract [24]. Mutation in the Na⁺/glucose cotransporter (SGLT1) gene [27] and infection of the ubiquitous intestinal parasites Giardia [28] are mostly responsible for this malabsorption. (iv) Secretory diarrhea: It is due to the impaired absorption of electrolyte (e.g., Na⁺ or Cl⁻) [29]. Different types of bacterial toxins such as; enterotoxins produced by E. coli [24] can activate such diarrheal condition. (v) **Leak flux diarrhea (LFD)**: In this type of diarrhea, epithelial monolayer permeability is increased due to the altered TJ that allows solutes and fluid to flow back from circulation into the gut lumen [30;31]. Dysregulated paracellular permeability due to uncontrolled paracellular movement impedes normal physiological epithelial function [32]. Patients with GI tract disturbances mostly suffer from inflammation-induced leak-flux diarrhea [33]: Mechanistic studies of different types of GI tract disorders such as IBD (CrD, UC) show a key role of TJ-dependent altered permeability of epithelial monolayers [34] in disease progression.

TJs are multiprotein complexes with dynamic structures at the apical region between two adjacent differentiated and polarized cells of epithelial monolayer that form the lining of the gut and many other organs of the human body [35]. TJs seal the paracellular space and act as a selectively permeable barrier that allow absorption of electrolytes, solutes and solvents molecules across the epithelial monolayer from the intestinal lumen into the circulation thus provides effective defense by preventing translocation of intraluminal toxin, antigen and gut flora (**Figure 2.1**) [36]. Intercellular part of TJ consists of four different types of transmembrane proteins families: claudins [35], occludin [37], junctional adhesion molecules (JAMs)[38] and tricellulin [39]. In fact, paracellular space is sealed by the interaction of protruding extracellular domain of these proteins between adjacent cells. These interactions can either be in *cis* or *trans* form and may be hemophilic or heterophilic [36]. Cytoplasmic or intracellular domain of these

proteins interact with various types of adaptors, scaffolds and signaling proteins to mechanically link and anchor the TJ with the actin cytoskeleton [40].

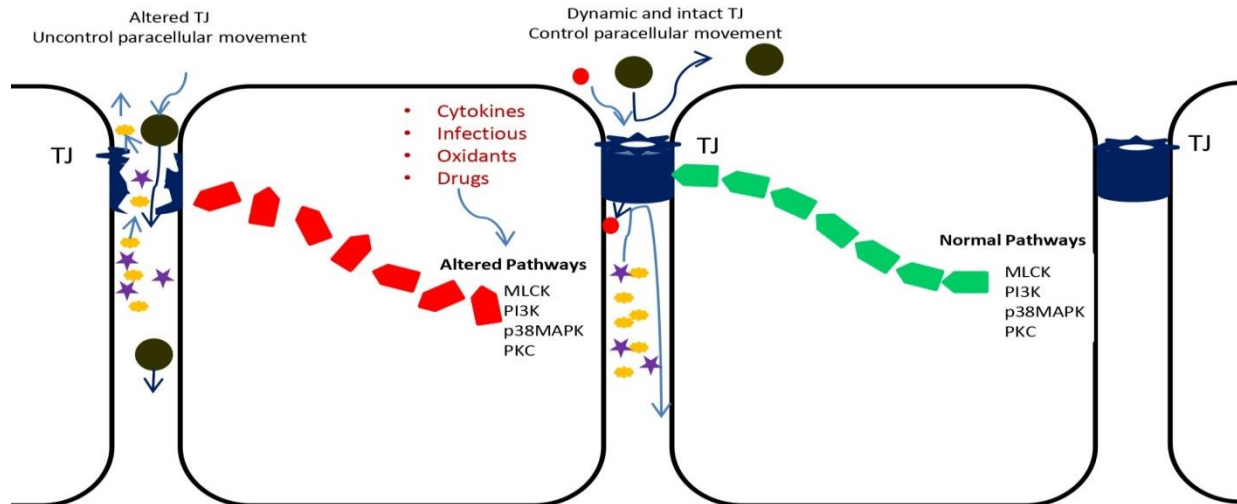


Figure 2.1: TJs present at the apical-lateral region and control paracellular movements across epithelial monolayer. Paracellular movement is associated with selective movement of electrolytes, nutrients and water molecules between intercellular spaces of adjacent epithelial cells. TJ structural proteins are regulated by means of kinases, phosphatases through different cellular signaling pathways, resulting alteration of TJ assembly and increased paracellular movements across epithelial monolayer. Green arrows indicate normal pathway and red arrows altered pathways.

The dynamic function of TJ is modulated either through direct regulations of TJ proteins or indirectly through changes in cytoskeleton of cells by means of kinases[41;42], phosphatases [43;44] and other signaling molecules [36]. *In vitro* [45] and *in vivo* [46] studies commonly employ transepithelial electrical resistance (TEER) and paracellular flux of macromolecules such as mannitol or dextran [47] to determine the TJ integrity. The present review will focus on TJ regulations and signaling pathways that mediate TJ through leak-flux mechanisms i.e., by increased epithelial permeability resulting diarrhea in different human diseases.

2.3 Mechanisms of Leak-Flux diarrhea

Inflammatory bowel diseases such as UC and CrD lead to an increased loss of solutes and electrolytes that results in leak flux diarrhea associated with epithelial barrier dysfunction due to

the altered regulation of TJ assembly [34]. Brief accounts of different cellular pathways that are involved in this phenomenon are given below.

2.3.1 Myosin Light Chain Kinase (MLCK) Pathway

MLCK is a serine/threonine kinase that alters TJ assembly and increases paracellular movement through the contraction of F-actin base cytoskeleton via phosphorylated MLC-2. MLCK phosphorylates MLC-2 at serine-19 and this phosphorylation is correlated with myosin ATPase activity that favours contractile movement of myosin against actin and produce contraction in cytoskeleton of the cells [48] which consequently reorganize the TJ assembly. Myosin light chain phosphorylation (MLCP) reverses this reaction by dephosphorylating MLC-2 that helps to decrease tension within the cell's cytoskeleton [49]. Increased expression and activity of MLCK and phosphorylation of MLC-2 are observed in the biopsy specimen of ileal and colonic epithelia of IBD patients positively correlated with the degree of active inflammation [50]. MLCK pathway is the major mechanism of LFD and is linked to several exogenous and endogenous factors.

Several cytokines are involved in higher TJ permeability through MLCK pathways like elevated TNF α level that plays a critical role in IBD pathogenesis [51]. TNF α induces barrier dysfunction in intestinal epithelial monolayer [52] through MLCK mediated phosphorylation of MLC-2 that reorganizes perijunctional F-actin, redistributes occludin and ZO-1, and increases TJ permeability [53]. Occludin is one of the important components of TJ that contribute to barrier function [54;55]. In vitro studies suggest that the loss of occludin from TJ through endocytosis results in barrier loss [56;57]. In vivo model study revealed that TNF-induced MLCK activation triggers caveolin-1 (principal component of caveolae membranes and involved in receptor-independent endocytosis) dependent endocytosis of occludin that effect TJ assembly and function [18]. Pharmacological inhibition of endocytosis (by dynasore/M β CD) or caveolin-1 knockout prevents TNF-induced occludin internalization, TJ barrier loss and water secretion. While overexpression of occludin limited the barrier loss and consequently prevented water secretion [18]. In vivo studies have shown that anti-CD3 mAB injection activated T-cell systemically that resulted transient watery diarrhea mediated by TNF [58]. T-cell induced-TNF increases permeability, deepens antiabsorptive effect and reduces the enzymatic activity of NA⁺/K⁺-ATPase. This model suggests that TNF-mediated altered activity of NA⁺/K⁺-ATPase

impair electrolyte absorption that contributes to intestinal fluid losses in immune-mediated bowel disorder patients [59]. Enterocytes from jejunum of anti-CD3 mice reveal disruption of the TJ and visible perijunctional cytoskeletal condensation. Genetically knockout MLCK in vivo model or pharmacological inhibiting MLCK significantly reverses these symptoms [60]. Still another cytokine, Lymphotoxin-like inducible protein that competes with glycoprotein D for herpes virus entry on T cell (LIGHT) is a core member of TNF family and its expression is considerably increased in the mucosal biopsy specimen from active IBD patients [61]. LIGHT induces LT β R-dependent activation of MLCK and MLC-2, which in turn stimulates endocytosis of occludin through caveolar pathway [57]. The inhibition of MLCK (with membrane-permeant inhibitor of MLCK (PIK)) or caveolar endocytosis reversed the cytokine (TNF- α , IFN- γ , LIGHT) induced permeability in *in vitro* studies and TNF-dependent diarrhea was corrected in *in vivo* mouse model [57;62;63].

Moreover, recent reports showed that immunosuppressive drug, mycophenolic acid (MPA) exposure increased the TJs permeability and impaired TJ proteins via MLCK/MLC-2 pathway in Caco-2 cells monolayer that may be a possible mechanism of diarrhea in organ transplanted patients taking MPA as an immunosuppressant to prevent graft rejection [64].

2.3.2 Certain bacterial pathogens exploit MLCK Pathway to disturb TJ assemblage.

Enteropathogenic *Escherichia coli* (EPEC) is an extracellular attaching and effacing (A/E) pathogen that adheres to the surface of epithelial host cells and produce characteristic lesions [65]. EPEC uses a type-three secretion system (T3SS) to transfer over 20 secreted bacterial effector molecules [65] (such as EspG, EspF) to the host cell via a molecular syringe [66]. These effector molecules are known to exploit the MLCK pathway to trigger a broad range of cellular events that ultimately cause alteration in TJ assembly [47]. Among these effector molecules, EspG induces disruption of microtubules through activation of the microtubule-bound guanine

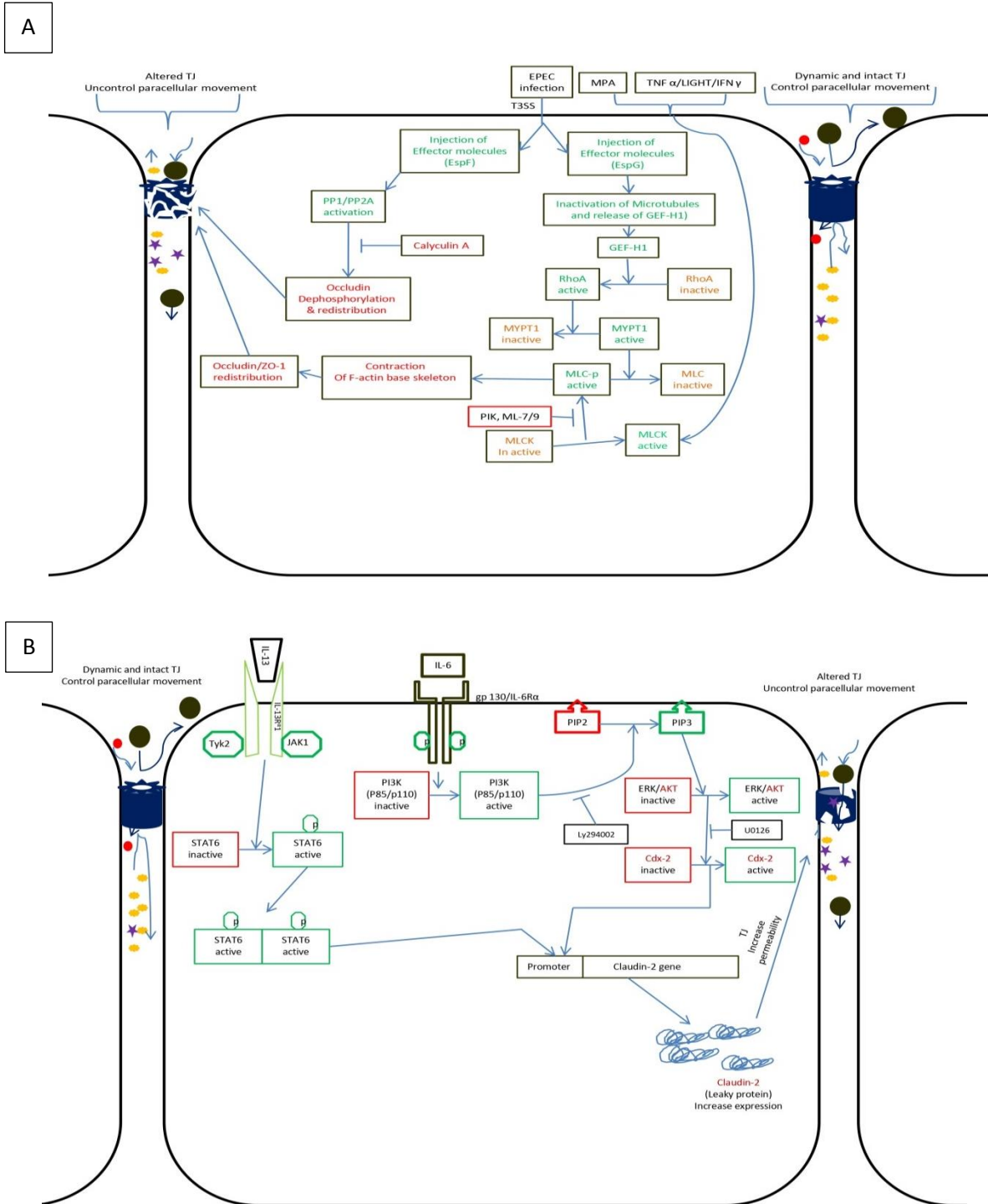


Figure 2.2: Schematic representation of TJ regulation via PI3K and MLCK pathways activated by MPA, proinflammatory cytokines and Enteropathogenic *E. coli* (EPEC). The outermost portion of the figure indicates activators of PI3K, STAT6 and MLCK pathways that lead to increase permeability of TJ. A. EPEC injects effector proteins (EspF, EspG) into the cytoplasm of host cells (epithelial cells) via T3SS. EspF mediates TJ disassembly by activating protein phosphatases that dephosphorylate occludin

and redistributes of occludin from TJ assembly. EspG inactivates microtubules and releases GEF-H1 factor. GEF-H1 activates RhoA that in turn inactivates MYPT1, consequently activated (phosphorylated) MLC increases in the cytoplasm. Activated-MLC triggers F-actin based cytoskeleton, resulting contraction of F-actin filaments and redistribution of TJ proteins (occludin & ZO-1). B. Proinflammatory cytokines IL-13 and IL-6 increase expression of leaky protein (claudin-2) via STAT6 and PI3K pathways.

nucleotide exchange factor (GEF-H1). However similar events are not observed in the epithelial cell infected with EPEC-mutant strain EspG1/2^{-/-} [67]. GEF-H1 activates RhoA upon releases from microtubules [68] and activated-RhoA inactivates MYPT1 via Rho-associated kinase (ROCK) [69;70], resulting increased phosphorylated MLC [71]. Thus infection of epithelial cells by EPEC stimulates the phosphorylation of MLC20 via MLCK, resulting in the contraction of F-actin base cytoskeleton [72] and finally decreased TEER and increased paracellular permeability of epithelial cell monolayer [73]. ZO-1 serves as an important linker molecule between the perijunctional actin and transmembrane proteins of TJ assembly, annular contraction in actin based cytoskeleton can dynamically affect paracellular permeability [74]. Interaction between transmembrane proteins (occludin, claudin-1) and peripheral membrane protein (ZO-1) of TJ, and restricted localization of these proteins in TJ assembly lost in the EPEC-infected T84 cells [75]. EPEC-infected mice also significantly decrease barrier function at early post infection in epithelial tissue of ileum and colon along with EspF-dependent redistribution of occludin in TJ assembly in these tissues [76]. ML-9, an inhibitor of MLCK, prevents EPEC-induced increase in T84 TJ permeability and partially restores TEER [77;78]. The partially restored TEER by ML-9 suggests the involvement of supplementary mechanisms, such as disorder of occludin from TJ assembly. EPEC-infection alters the localization (from TJ-associated domain to an intracellular compartment) of occludin and dephosphorylates occludin in T84 cells [79]. EspF (206 aa protein) is translocated into the host cells via T3SS and decrease TEER, increase permeability and redistribute occludin from TJ assembly in dose-dependent fashion [80]. Phosphorylation of occludin is obligatory for its localization to the TJ complex [81]. Gentamicin treatment of EPEC-infected monolayer (T84) cells results in normal localization and phosphorylation of occludin in TJ assembly as compared to non-pathogenic E. coli K-12 infected monolayer. Calyculin A, an inhibitor of protein phosphatase 1 (PP1) and protein phosphatases 2A (PP2A) that dephosphorylate occludin at serine and threonine residues, completely prevents the dissociation of occludin from TJ and decrease in TEER (**Figure 2.2 A**) [79].

2.3.3 Phosphoinositide 3 kinases (PI3K) pathway

This pathway is again linked to the elevated level of cytokines that play a key role in TJ permeability. Elevated Interleukin 6 (IL-6) is observed in the serum and tissue specimens of active IBD patients [82] and correlate with the severity of disease [83;84]. IL-6 increases the cation-selective epithelial TJ permeability through increased expression of leaky protein, claudin-2. IL-6 enhances transcriptional factor activity of cdx-2 via MEK/ERK and PI3K/ERK dependent pathways. Activated cdx-2 binds to the cdx-2 binding site in the promoter region of claudin-2 and increases its transcription. Increased claudin-2 protein participates in pore-formation and consequently increases TJ permeability. IL-6 induced increase expression of claudin-2 can be inhibited by blocking MEK/ERK and PI3K/Akt pathways through their specific inhibitors U0126 and LY294002 respectively (*Figure 2.2 B*) [85]. An eastern medicine Berberine, prevents TNF α -induced upregulation of claudin-2 and disassembly of claudin-1 via PI3K/AKT and tyrosine kinase src, in vitro and in vivo models [86].

2.3.4 Signal Transducer and Activator of Transcription (STAT) Pathway

Signal Transducer and Activator of Transcription play an important role in active transcription of many interleukin proteins. IL-13, produced by CD1-reactive NKT cells, has a significant role in the regulation of inflammation and induction of epithelial monolayer barrier disturbance in UC [87;88]. IL-13 binds to its receptors (IL-13R α 1/IL-4R α) and trigger signal cascade that induce phosphorylation of STAT6 in colonic cell lines that in turn increases the expression of claudin-2 (pore-forming claudin of TJ) [88;89]. Following phosphorylation, STAT6 dimerizes and translocates to the nucleus to activate transcription (*Figure 2.2 B*) [90]. Biopsy specimens of the UC patient show increase expression of claudin-2 protein, while STAT6-deficient mice showed decreased expression of claudin-2 [88;89].

2.3.5 P38MAPK pathway

P38MAPK pathway closely interconnected with MLCK pathway through phosphorylation cascades. CrD patient shows elevated level of interleukin-1 β (IL-1 β , a proinflammatory cytokine), in their colonic mucosa and the severity of intestinal inflammation is directly correlated to the level of IL-1 β elevation [91;92]. In vitro and in vivo studies showed IL-1 β -induce increased TJ permeability require p38 kinase-dependent activation and phosphorylation of activating transcription factor 2 (ATF-2). Following activation, ATF-2 translocates to the

nucleus and specifically binds to the promoter of MLCK and increases its activity (**Figure 2.3 A**). IL-1 β -induced epithelial TJ permeability can be prevented by inhibiting p38 kinase activity (p38 kinase specific inhibitor, SB-203580), knocking down the ATF-2 by (siRNA) or mutating the binding site of ATF-2 in the promoter region of MLCK [42].

Campylobacter jejuni (*C. jejuni*) is a major cause of bacterial food-borne diarrheal disease (GI disturbances) throughout the world [93]. *C. jejuni* infection induces phosphorylation of p38MAPK, ERK, hypophosphorylation and redistribution of occludin from TJ, redistribution of claudin-1, decreases expression of pore-sealing claudin-4 and rapid activation of NF- κ B and AP-1 in epithelial cells [94-96]. Lipopolysaccharide (LPS)-treated Caco-2 cells showed TJ damage by decreasing expression of occludin and ZO-1 via MAPK/ERK pathway. However, Somatostatin pretreatment decreases LPS-induced mRNA level of somatostatin receptor 5, phosphorylation of ERK1/2, blocks MAPK/ERK pathway and ameliorates LPS-dependent TJ damage [97]. EGF pretreatment prevents disruption of claudin-4 and translocation of *E. coli* C25, reduces jejunal colonization and distribution of *C. jejuni* to the liver and spleen of chicks [94].

2.3.6 Protein kinase C (PKC) pathway

PKC belong to serine/threonine specific kinases that are involved in the regulation of barrier function of epithelial and endothelial cells [98]. So far 12 different isozymes of PKC have been reported that are divided into three subfamilies namely; conventional PKC (cPKC α , β 1, β 2, γ) that are activated in a Ca^{++} and DAG dependent manner, novel PKC (nPKC δ , ϵ , θ , μ) requires only DAG for activation and atypical PKC (aPKC λ , ζ) activated without Ca^{++} and DAG [47;98].

Phosphorylation of occludin at serine, threonine and tyrosine residues play an important role in TJ assembly. Normal epithelial monolayer shows hyper phosphorylation [99] of occludin at serine [100] & threonine residues [101;102], most likely phosphorylated by different isoforms (i.e., λ , ζ) of atypical protein kinase C (PKC) that are present close to TJ assembly [103]. Occludin loss interaction with anchoring proteins i.e., ZO-1, -2, -3, after phosphorylation at tyrosine residue (**Figure 2.3 B**) [104]. Dephosphorylation of occludin at the same residues is reported to be implicated in disrupted TJ under different external stimuli (Ca^{++} depletion [81], phorbol esters [105] and EPEC infection [79]). PP2A and PP1 directly interact with the C-terminal tail of occludin and negatively regulate the assembly by dephosphorylating it at threonine and serine residue respectively [106]. Inhibition of PP2A or PP1 activity through either

by antisense oligonucleotide, siRNA or specific inhibitors (okadaic acid, fostriecin, calyculin-A) reverse these effects [107]. In addition, oxidative stress increases TJ permeability through kinases that phosphorylate tyrosine residue in TJ proteins (ZO-1 and occludin) [108]. Disruption of TJ assembly by oxidative stress is observed to be mediated by activation of c-Src and PI3K in the Caco-2 cells [109;110].

Ingestion of gluten-containing diets (wheat, rye, barely) can activate inappropriate immune response which leads to the drastic alteration of small intestinal epithelial architecture and consequently enhanced epithelial permeability in celiac disease [111]. Endoscopic biopsy specimens showed an upregulation of pore-forming claudin-2 and -15 and simultaneous down-regulation of tightening TJ proteins (occludin and pore-sealing claudin-3, -5, -7) in patients receiving gluten-containing diets as compared to the healthy controls [44]. In celiac disease, paracellular leakage occurred via altered subcellular distribution of Par-3 and atypical PKC Isotype-Specific Interacting Partner, whereas TJ structural proteins also exhibit changed expression. A celiac disease specimen displays an enhanced basolateral distribution of Par-3 and increased expression of PP-1 in epithelial cryptic cells which dephosphorylates the occludin. Par-3 moves to apical region of the cell and contributes to the organization of primordial junctions to belt-like TJs during polarization of the epithelial cells [112].

PKC α and PKC β activation pathway is triggered by *Clostridium difficile* (*C. difficile*) that releases two types of exotoxins called toxin A (TcdA) and toxin B (TcdB) [113] in the large bowel [114]. These toxins bind to gp96 [21] and chondroitin sulfate proteoglycan 4 [115] in epithelial cells respectively and translocate it into the cytosol. This translocation activates PKC α [116] and PKC β but inactivate Rho proteins (Rho, Rac, Cdc42) via transfer of a sugar moiety using UDP-glucose as a co-substrate [114]. All these changes result in alteration of actinomyosin ring [47] and translocation of adaptor protein (ZO-1) from TJ assembly (**Figure 2.3 B**) [116]. These toxin based adverse effects can be inhibited by PKC α/β antagonist (myristoylated PKC α/β peptide) that block RhoA glucosylation [116].

Vibrio cholerae (*V. cholerae*) enters with contaminated water into the small intestine of human that causes profuse diarrhea and leading to severe dehydration and delayed treatment can result death of the infected patients [117]. Hemagglutinin/protease (HA/P), RTX and zonula occludin toxin (ZOT) are toxins produced by *V. cholerae* and involved in the alteration of TJ assembly

[21] via different mechanisms. HA/P, an extracellular protease, cleaves integral membrane protein (occludin) and rearranged ZO-1, that are involved in the regulation of TJ assembly [118]. RTX crosslink the actin base cytoskeleton of the cells changing cell morphology (from columnar to round shape), resulting significantly decrease in TEER and increase in permeability (measured by FITC-dextran 3000) [119]. While ZOT, 44.8 KDa protein, is involved in the reversible regulation of TJ assembly via PKC dependent pathway [40]. ZOT is non-functional in its phage associated form [21]. It is cleaved into an active 12 KDa peptide [120]. Structure-function analysis reveals that amino acids (aa) located between 288-293; are biologically active portion of the ZOT at N-terminal and consist of 6 aa 'FCIGRL' called PAR2 activity motif [121]. Active peptide of ZOT binds to the apical receptor, zonulin [122] and internalized into cytoplasm [123] where PAR2 activity motif increase PKC-dependent phosphorylation of ZO-1 and myosin C1 (**Figure 2.3 B**) [40]. PAR2 Activity motif of ZOT increases PKC-dependent phosphorylation of serine and threonine residues present in protein binding domains of ZO-1 and alter the interaction of ZO-1-claudins and ZO-1-occludin resulting redistribution of occludin and ZO-1 in TJ [40]. ZOT also increase phosphorylation of myosin C1 and diminish myosin C1-ZO1 interaction [124] consequently increase TJ permeability. ZO-1 (225 KDa) is a phosphoprotein that consists of several protein binding domains such as; PKZ domains, src homology (SH) 3 domain, GUK domain [125] etc. These domains play a key role in the organization of TJ assembly complex [124;126]. Claudin family members interact with ZO-1 via PDZ domain to anchor with intracellular cytoskeleton [125] while occludin is bound to ZO-1 via unique 5 (present between SH3 and GUK domains) domain [127]. Finally ZO-1 bound integral membrane proteins of TJ (claudins and occludin) are linked to actin based cytoskeleton [126] via the C-terminal unique 225-aa proline-rich tail of ZO-1 [124].

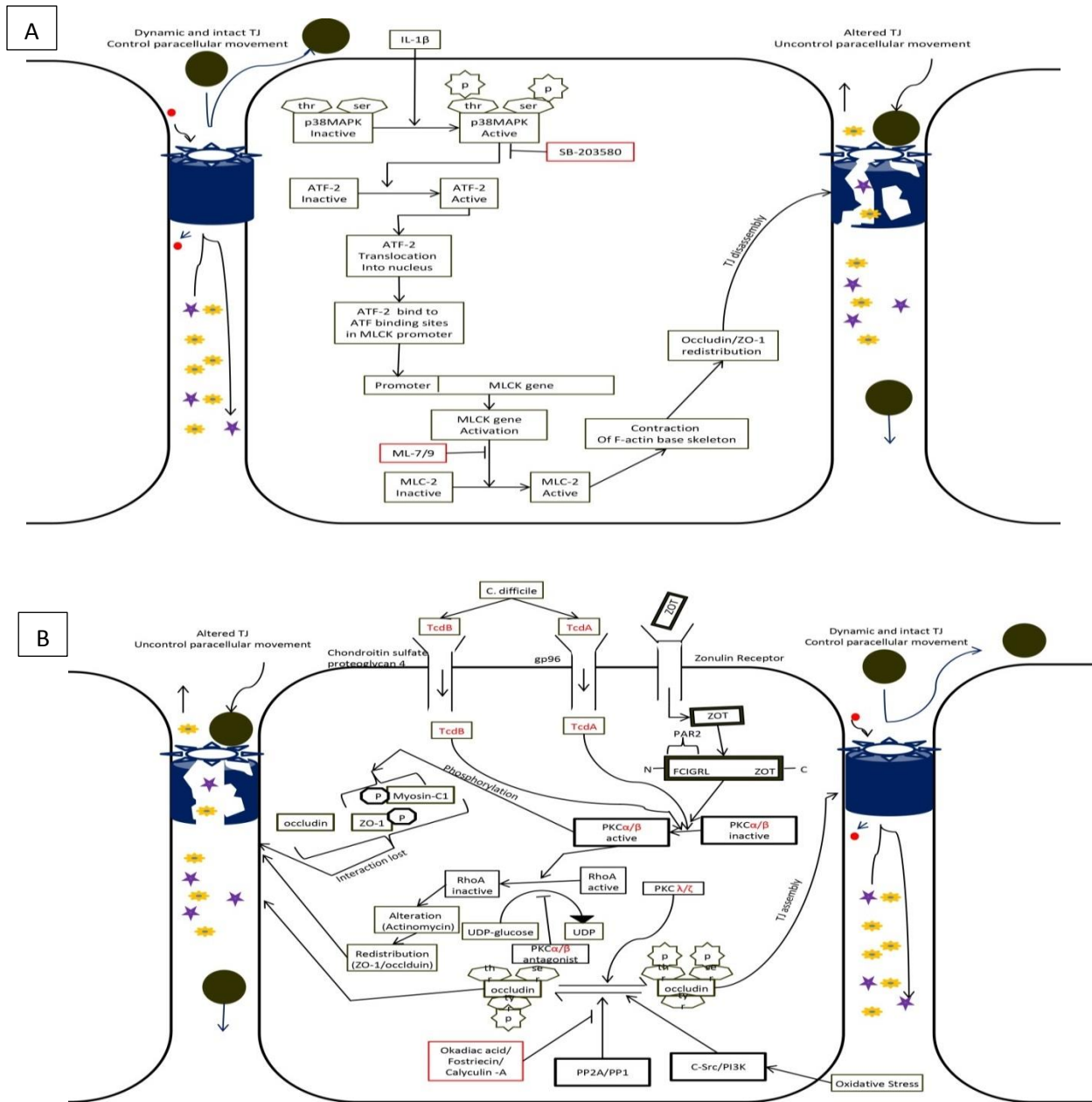


Figure 2.3: Strategies used by proinflammatory cytokine and bacterial toxins to regulate TJ via p38MAPK and PKC pathways. A. Transmembrane proteins (occludin, claudins) are anchored to F-actin based cytoskeleton via adaptor protein (ZO-1). IL-1 β activates P38MAPK-dependent MLCK, which acts on TJ-associated F-actin filaments via MLC-2 phosphorylation. Phosphorylated MLC-2 triggers myosin contraction that resultant redistribution of ZO-1 and its linked proteins of TJ consequently disrupt TJ assembly. **B.** Bacterial toxins (tcdA, tcdB, ZOT) bind and internalize by their relevant apical receptors of epithelial cells, activate PKC pathway. Disruption of TJ by PKC pathway occur either directly by phosphorylating TJ proteins (ZO-1, occludin) that result loss of interaction with other proteins or via

inactivation of Rho GTPases consequently contraction of F-actin cytoskeleton and redistribution of TJ protein.

2.3.7 JunD pathway

JunD is overexpressed in inflammatory intestinal mucosa of pediatric patients with IBD [128] and represses transcription and translation of TJ protein (ZO-1) in intestinal epithelial cells, in turn causing an increase in epithelial paracellular permeability [129]. Transcription is inhibited through direct binding with cAMP response element-binding protein (CREB)-binding site in the promoter region of ZO-1, while translation is inhibited by promoting the interaction of 3'-UTR of ZO-1 mRNA with RNA-binding protein TIAR (translation repressor) [130] in epithelial cells [129]. JunD-induced transcription and translation of ZO-1 was shown to be prevented by either mutating CREB-binding site in the promoter region of ZO-1 or by reducing TIAR expression through siRNA [129].

2.3.8 *Salmonella* and TJ regulation

Contaminated food and water are the major sources by which *Salmonella* gain entry into the human GI tract, causing gastroenteritis and infections and resulting significant morbidity and mortality worldwide [131]. *Salmonella* disrupts TJ assembly either directly via TJ structure protein regulation or indirectly through actin regulation. Infection of *Salmonella* AvrA-deficient strain disrupts TJ assembly via decrease expression of occludin-1, ZO-1 and claudin-1 in intestinal epithelial cells as compared to AvrA-sufficient strain [132]. Sodium butyrate enhance intestinal barrier function via specificity protein 1 (SP-1) transcription factor dependent increase expression of claudin-1 [133].

T3SS, encoded by *Salmonella* Pathogenicity Island-1 (SPI-1) [134;135], is activated upon contact with the host and injects around 12 effectors into the cytoplasm of host cells that modify cell signaling pathways of host cells [136;137]. Among these 12 SPI-1-secreted effectors, only SopB, SopE, SopE2 and Sip A disrupt Rho-dependent TJ assembly by redistributing ZO-1 and occludin in Caco-2/TC7 cell [131]. Comparing to wild type, different types of mutant strains of *Salmonella* (Δ sopB, Δ sopE/E2, Δ sipA, or Δ sipA/sopB, Δ sopB/E/E2 and Δ sipA/sopE/E2) were unable to disrupt F-actin based cytoskeleton, altered distribution of ZO-1 and occludin and increase permeability of polarized epithelial monolayer (Caco-2/TC7) [138]. Inhibition of protein geranylgeranylation, which is critical for the function of a number of proteins such as

RhoA and Rac [139], prevents TJ disruption by *Salmonella* [138]. Rho family GTPases (Rho, Cdc42, Rac) are key regulators of disrupting TJ structure and functions [140] via actin based cytoskeleton. Both SopE and SopE2 act as GEFs for activating Cdc42 and Rac1 [141;142], while SopB (a potent inositol phosphatase) stimulates Cdc42-dependent reorganization of F-actin based cytoskeleton via phosphoinositide fluxes [143]. SipA binds to F-actin and stabilizing F-actin filaments as well as enhancing the activity of actin-bundling proteins (T-plastin)[144].

2.3.9 EGFR/JNK pathway

Salmonella increases c-Jun dependent expression of TJ leaky protein (claudin-2) via EGFR/JNK pathway for invasion as learned from both in vitro (HT29C19A) and in vivo (C57BL6 mice) models. Inhibition of EGFR, an upstream regulator of JNK, with Gefitinib (EGFR inhibitor) or JNK with SP600125 (JNK inhibitor) block the *Salmonella*-induced expression of claudin-2. EGFR/JNK inhibitors could also block the increase expression of c-Jun (downstream target of JNK) in *Salmonella* infected epithelial cells [145] suggesting claudin-2, as a potential therapeutic target to prevent bacterial invasion.

2.3.10 *Clostridium perfringens* enterotoxin (CPE) and TJ regulation

C. perfringens causes GI infections by producing up to 16 different types of toxins, including enterotoxin (*Clostridium perfringens* enterotoxin (CPE) [146]). CPE has a C-terminal binding domain and N-terminal biologically active domain [147;148]. Following binding to the cell surface, CPE remains associated with the plasma membrane and increases membrane permeability [149]. CPE-induced increased permeability pore include a Ca⁺⁺ influx that trigger apoptotic/cell death pathways [150;151]. It also physically interacts with claudin-3 and -4 [152], and claudin-8, -14 [153] upon contact with CPE-sensitive enterocyte. Asparagine-149, present at the extracellular loop-2 in claudin-3, -4, -8 and -14 [154;155] plays an important role between the interaction of claudins and CPE [153;156]. These claudins work as CPE receptors [153] and therefore CPE interaction selectively removes claudin-4 from TJ with its concomitant degradation [156]. This morphological change of claudins in TJ correlates temporally with decreased TER and increased paracellular flux [157]. The colonic specimen of IBD patient shows downregulation of claudin-4 (pore-sealing protein of TJ) and upregulation of claudin-2 (pore-forming protein of TJ) [88;158]. This regulation of claudins-2 and 4, respectively contribute to defective barrier function of TJ that control paracellular movements across

epithelial monolayer, resulting leak-flux diarrhea in IBDs collagenous colitis patients [158]. On the other hand, whey protein concentrate 1 (WPC1) a natural source of TGF β in human nutrition TGF β provides natural barrier protection by reversing the downregulation of claudin-4 [159].

2.3.11 Concluding remarks

Compromised TJ integrity by modulation of signaling pathways is a key feature in numerous human diseases. Significant progress has been made over the past decades to better understand the molecular mechanisms of complex signaling pathways that are involved in the TJ regulation. However, an enormous amount of work still remains to be done to reconcile information in studying signaling pathways using in vitro and in vivo disease models. Particularly a systematic effort is required to exploit the true potential of emerging technologies like epigenetics, peptidomics and proteomics to identify novel signaling molecules and to explore better therapeutic intervention for the TJ assembly related human abnormalities.

2.4 Acknowledgements

The author is grateful for continued support of his mentor, and acknowledges supports from faculty member, department of Biotechnology and Genetic Engineering, and administrative staff, Kohat University of Science and Technology, Pakistan. We sincerely thanks to the researchers whose work are cited in this article and apologize to those whose work we could have cited, but did not due to space restrictions. The author is awarded PhD scholarship by Higher Education Commission (HEC), Pakistan/German Academic Exchange Program (DAAD).

3 Transcriptional Regulators of Claudins in Epithelial Tight Junctions

Niamat Khan^{1,2} and Abdul R. Asif^{1*}

¹Institute for Clinical Chemistry / UMG-Laboratories, University Medical Centre, Robert-Koch-Str. 40, 37075, Goettingen, Germany. ²Department of Biotechnology & Genetic Engineering, Kohat University of Science and Technology, Kohat 26000, KPK, Pakistan

* Author to whom correspondence should be addressed;

Published in “Mediators of Inflammation” Volume 2015 (2015), Article ID 219843, 6 pages
<http://dx.doi.org/10.1155/2015/219843>

3.1 Abstract

Human gastrointestinal tract is covered by a monolayer of specialized epithelial cells that constitute a protective barrier surface to external toxic and infectious agents along with metabolic and digestive functions. Intercellular junctions among epithelial cells, such as desmosomes, adheren, gap and tight junctions (TJs) not only provide mechanical integrity, but also limit movement of molecules across the monolayer. TJ is a complex structure composed of approximately 35 different proteins that interact with each other at the apical side of two adjacent epithelial cells. Claudin family proteins are important members of TJ with so far 24 known isoforms in different species. Claudins are structural proteins of TJ that help to control the paracellular movement by forming fence and barrier across the epithelial monolayer. Altered function of claudins is implicated in different form of cancers, inflammatory bowel diseases (IBDs) and leaky diarrhea. Based on their significant role in the molecular architecture of TJ, diversity and disease association, further understanding about claudin family proteins and their genetic/epigenetic regulators are indispensable.

Key words: Claudins, Promoter Binding, Epithelial Tight Junction, Transcription Factors, Inflammation

3.2 Introduction

Epithelial monolayer (EM) is the largest body tissue lining many organs in the human body. In the intestine, EM provides protection to the internal body from toxic and infectious agents while

at the same time facilitates absorption of digested food and water from the gut. Epithelial monolayer integrity and paracellular transport are the important features that can be protected and maintained with the help of epithelial barrier function [160]. Epithelial cells are connected with each other by four types of junctions i.e., desmosomes, gap junctions, adheren junctions and TJs [161-163]. Tight junctions are impermeable and control the movement of molecules and ions via a paracellular pathway. Until recently, tight junction functions were categorized as “fence” as they separate the apical and basolateral cell surface domain defining cell polarity or a “barrier” due to their control over solutes and liquid flow through the paracellular space between the epithelial cells [164-167]. However TJs are not restricted to the fence and barrier function, but have been defined to participate in signal transduction processes, gene expression, cell proliferation and differentiation [168-170]. Various unidentified external and internal regulators impair the normal function of TJs causing loss of water and solute in the passive manner that leads to leak-flux watery diarrhea. The unwanted invasion of noxious luminal antigens prolongs the existence of mucosal inflammatory processes. [171].

Tight junction (TJ) is a complex structure constituting of growing numbers of components, including integral membrane proteins (claudins, occludin, junctional adhesion molecules “JAMs”) and peripheral membrane proteins. The peripheral membrane proteins includes (1) scaffold PDZ (Post synaptic density protein (PSD95), Drosophila disc large tumor suppressor (Dlg1), and Zonula occludens-1 protein (ZO-1), multi-PDZ domain protein-1 (MUPP1), Membrane-associated guanylate kinase (MAGI-1); (2) no-PDZ expressing proteins such as cingulin, symplekin, atypical protein kinase C, Ras-related protein Rab-3B (Rab3b), Ras-related protein Rab-13 (Rab13), Phosphatase and tensin homolog (PTEN), 7H6 antigen; (3) cell polarity molecules ASIP/PAR-3, Partitioning defective 6 homolog alpha (PAR-6), PALS1-associated TJ protein (PATJ) [172;173]. Besides these proteins, tricellulin protein has recently been identified at the epithelial cell junctions with involvement in the barrier function [174].

Claudin family so far includes 24 reported members in different types of mammalian cells, among them 21 are known components of TJ in EM in the kidneys, liver, brain and intestine [175]. These are involved in various physiological processes such as regulation of paracellular permeability and conductance. Claudins are found in homo and heterotypic manner in single TJ [176;177]. They can be divided into two main categories; “pore-sealing” and pore forming

claudins. Claudin-1, -3, -4, -5, -7 and -19 are known as pore-sealing claudins and an increased expression of these claudin proteins lead to increased tightness of EM, increased transepithelial electrical resistance (TEER) and decreases solute permeability across the monolayer [178-182]. On the other hand, claudin-2 and -15 are considered as the “pore-forming claudins”, because of their ability to form paracellular anion/cation pores as well as water channels and therefore decrease epithelial tightness and increase solute permeability [176;183].

Epithelial barrier dysfunctions occur in inflammatory bowel diseases (IBDs) like crohn’s disease (CD) or ulcerative colitis (UC) that contribute to leaky flux diarrhea i.e., loss of solutes and water in increased amount dependent upon the components of TJ proteins. Downregulation of pore-sealing claudins (e.g., 4, 5, and 8) while upregulation of pore-forming claudin-2 are observed in active Crohn’s disease patients [184;185]. Similarly downregulation of pore-sealing claudin-4 is also associated to UC disease [185]. Numerous studies have reported leaky diarrhea in patients undergoing immunosuppressive therapy after organ transplantation [12;186-188]. Recently our group has reported mycophenolic acid (MPA)-mediated increased expression of myosin light chain kinase (MLCK) myosin light chain (MLC-2) as well as MLC-2 phosphorylation and redistribution of ZO-1 and occludin in Caco-2 as well as in HEK-293 cells [189;190] as a possible mechanism of diarrhea in patients undergoing immunosuppressive therapy. Transcription factors (TFs) play an important role in the gene regulation at the promoter level either working as an activator or repressor of a specific gene. Current review will focus major claudins family members and their regulators, which alter claudins gene activity at promoter level and therefore modulate TJs structure and function.

3.2.1 Claudin 1:

Claudin 1 protein is a key constituent of TJs and its altered expression is reported in a variety of cancers, most prominently colorectal cancers [176;191-193]. Promoter region (-1160 bps to -850 bps) of claudin-1 consists of putative binding sites for caudal-related homeobox (cdx-1, 2), GATA4 and T-cell factor/lymphoid enhancing factor-1 (Tcf/Lef-1) transcription factors. There is a direct correlation between claudin-1 and cdx-2 expression in human colon cancer patient [193]. Cdx-2 is a homeobox domain-containing nuclear transcription factor that plays an important role in intestinal development by regulating the proliferation and differentiation of intestinal cells [194-196], and it is expressed in all cells along the crypt villus axis. Cdx-2 transcriptional

activity is controlled through ERK, MAPK pathway which phosphorylates it at ser-60 position and resultantly reducing cdx-2 transcription activity in crypt and lower villus cells. On the other side, cyclin-dependent kinase 2 (CDK2) phosphorylates cdx-2 at Ser-281 which coordinate cdx-2 polyubiquitination and degradation by the proteasome [194;197-200]

Specificity protein 1 (Sp-1) is the first identified transcription factor of specificity protein/Krüppel-like factor (Sp/XKLF) family, consisting of 785 amino acids (aa) with molecular weight of 100 to 110 kDa. Sp-1's DNA binding domain is the most conserved among other domains of SP family members which is consisted of Cy2His2 Zinc (Zn) fingers. Mutational analysis has revealed that Zn fingers 2 and 3 are essential for DNA binding activity [201]. Sp-1 binds to the GC-rich elements [202] that are common regulatory elements in the promoters of numerous genes. Sp-1 binds its individual binding sites as a multimer and is capable of synergic activation of promoters containing multiple binding sites [203] and regulates transcription by dynamically recruiting and forming complexes with many factors associated with transcription [204]. Normally Sp-1 has been described as a transcriptional activator but it can also act as a repressor [205]. Claudin-1 promoter region (-138 to -76 bp) contains Sp-1 binding site and a mutation in this region results in a significant loss of claudin-1 transcription [206].

3.2.2 Claudin 2

Claudin-2, also known as leaky protein, forms paracellular water channels in TJs and mediates paracellular transport of water molecules across the EM. EM permeability is enhanced by increased expression of claudin-2 in TJs. It is also involved in many signaling pathways, including vitamin D receptor, epidermal growth factor receptor (EGFR), and c-Jun N-terminal kinases (JNK) signaling pathways, and contributes to inflammatory bowel disease and colon cancer [184;207-210]. Salmonella infection facilitates bacterial invasion across the EM by inducing claudin-2 expression and altering its localization in TJs which is reversible by specific inhibitors (EGFR (Gefitinib) & JNK (SP600125), making claudin-2 as a potential therapeutic target to prevent bacterial invasion and inflammation [211].

Interleukin-6 (IL-6) increases TJ permeability of Caco-2 monolayer from the basal side by inducing claudin-2 expression. IL-6 activates the mitogen-activated protein kinases/extracellular signal-regulated kinases (MEK/ERK) pathway by inducing phosphorylation of ERK, and

phosphatidylinositol 3'-kinase (PI3K/Akt), by phosphorylating Akt, which in turn enhances cdx-2 expression. In the claudin-2 promoter region (-1067 to -1), four cdx-2 (cdx-A, B, C, D), STAT and nuclear factor kappa-light-chain-enhancer of activated B cells (NF- κ B) putative binding sites are identified. IL-6 induced expression of claudin-2 can be reversed by either using specific inhibitors of MEK/ERK and PI3K/AKT pathways (U0126 (a MEK inhibitor), LY294002 (a PI3K inhibitor) or site directed mutagenesis in the putative cdx-2 binding sites in the promoter region of claudin-2 gene [212].

3.2.3 Claudin-3, Claudin-4, and Claudin-5

Claudin-3 and claudin-4 both are overexpressed in ovarian cancer. A Sp-1 binding site (-112 and -74 bps) in the promoter region of claudin-3 is crucial for its activation. Claudin-3 expression is significantly decreased at mRNA and protein levels, by knocking down the Sp-1 with siRNA, indicating an essential role of Sp-1 in claudin-3 activation [213]. Claudin-4 is mainly expressed in the EM of colon, renal tubules, mammary gland, thyroid gland and considerably raised in their cancers [214]. There are two known Sp-1 binding sites (between -105 to -49 bps) in the promoter region of claudin-4 [215]. Claudin-5 is mostly expressed in the TJs of EM of pancreatic acinar, alveolar lung cells, colon, endothelial cells forming the blood-brain barrier and endoneurial blood-nerve barrier. In colonic regions, its expression is mainly involved in the paracellular sealing of TJs [184;216-218]. Both downregulation and redistribution of claudin-5 can alter TJs structure leading to barrier dysfunction in active Crohn's disease [184]. Forkhead box (foxO) gene family members are potent transcriptional activators with four known members; foxO1 (also known as foxO1a), foxO3 (also known as foxO3a), foxO4, and foxO6 which bind to conserved consensus core recognition motif TTGTTTAC [219-221]. Four pairs of putative binding sites for foxO and tcf- β -catenin (Tcf- β -catenin act as a stabilizer) are identified in the three regions of claudin-5 promoter (region 1, position -2,906/-2,871; region 2, position -2,317/-2,287; region 3, position -1,103/-1,008). Both foxO1 and tcf- β -catenin interact with region 1 of the claudin-5 promoter to repress its transcription [222].

3.2.4 Claudin-7

Claudin-7 is expressed prominently in the biphasic type of synovial sarcoma of adults. E74-like factor 3 (ELF3) belongs to E26 transformation-specific sequence (ETS) family of transcription factors and binds to the Ets binding site in the promoter region (-150 bps) of claudin-7 [223].

Members of ETS family are mainly involved in cell differentiation, proliferation and cell transformation [224]. Regulation of the target genes by ETS factors depend upon their activation by MAPK and their association with other cofactors [225;226]. An essential role of ELF3 is reported in epithelial cell differentiation [227-229] and small interference RNA (siRNA) treatment downregulates the claudin-7 expression validating the central role of ELF3 in claudin-7 activation.

3.2.5 Claudin-15

Claudin-15 is a pore-forming protein expressed in the EM of intestine, liver and kidney tissues. Downregulation of claudin-15 decreases permeability of EM layer and can initiate IBD. Four putative binding sites (BS1-4) of transcription factor hepatocyte nuclear factor 4 alpha (hnf4 α) are present in the (-693 to -47 bps) region of claudin-15 promoter [230]. Hnf4 α is considered as an important regulator of EM barrier integrity and is involved in the regulation of metabolism, cell junction, differentiation and proliferation of liver and intestine epithelial cells [231]. Both animal model and IBD patients' biopsy studies have shown an altered expression of hnf4 α directly influence the expression and distribution of claudin-15 [230].

3.2.6 Claudin 19

The kidney is responsible for the filtration of excretory material from the blood. However, 25–40% of filtered Na⁺ [232], 50–60% of filtered Mg²⁺ [233] and 30–35% of filtered Ca²⁺ [234] are re-absorbed into the body by thick ascending limb, the loop of Henle. Claudin-16 and -19 play a main role in the regulation of Mg²⁺ reabsorption and loss of either claudin-16 or -19 lead to excessive renal waste of Mg²⁺ [235]. Four putative transcription factor (unknown, AP2, NF-E and Sp-1) binding sites are located between -139 and -75 in the promoter region of mouse claudin-19. However, only Sp-1 is described for having an important role in the expression of claudin-19 and a mutation in Sp-1 binding site significantly reduces the claudin-19 expression [236].

Table 3.1 Regulators of claudins

| TJ Proteins | Regulator | Promoter binding region | Expression / Ref. |
|-------------------|---------------|-------------------------|-------------------|
| Claudin-1 | Sp-1 | -138 to -76 bp | ↑[206] |
| | cdx-2 | -1160 to -850bp | ↑ [193] |
| Claudin-2 | cdx-2 | -1067 to -1bp | ↑[212] |
| Claudin-3 | Sp-1 | -112 to -74bp | ↑[213] |
| Claudin-4 | Sp-1 | -105 to -49 bps | ↑ [215] |
| Claudin-5 | FoxO1 | -2,906 to -2,871 bps | ↓ [222] |
| Claudin-7 | ELF-3 | -150 bps | ↑ [223] |
| Claudin-15 | Hnf4 α | -693 to -47 bps | ↑ [230] |
| Claudin-19 | Sp-1 | -139 to -75 bps | ↑ [236] |

Note: arrow (↑) = upregulation, arrow (↓) = downregulation

3.3 Conclusion:

Tight junctions play an important role in the regulation of paracellular movement of molecules across the EM, impart mechanical strength, maintain the polarity of cells and prevent the passage of unwanted molecules and pathogens through the space between the plasma membranes of adjacent cells. The efficiency of the junction in preventing ion passage increases exponentially with the number of strands of claudins family proteins which are having important role in the structure as well as controlling paracellular movement across the tight junctions. Altered expression of claudins family proteins in TJs plays a key role in numerous abnormalities like; cancers, IBDs and leaky diarrhea and a better understanding of their regulatory mechanism could help in designing innovative therapeutic strategies.

3.4 Acknowledgement:

We acknowledge support by the German Research Foundation (DFG) and the Open Access Publication Fund of the University of Göttingen. NK is the recipient of a German Academic Exchange Service (DAAD), Germany and Higher Education Commission (HEC), Pakistan award.

4 Immunosuppressant MPA modulate tight junction through epigenetic activation of MLCK/MLC-2 pathway via p38MAPK.

Niamat Khan^{1,2}, D.V. Krishna Pantakani¹, Lutz Binder¹, Muhammad Qasim^{1,3}, Abdul R. Asif^{1§}

¹Institute for Clinical Chemistry/UMG-Laboratories, University Medical Centre, Robert-Koch-Str. 40, 37075, Goettingen, Germany. ²Department of Biotechnology & Genetic Engineering, ³Department of Microbiology, Kohat University of Science and Technology, Kohat 26000, KPK, Pakistan.

§ Corresponding Author

Accepted in *Frontiers in Physiology*, doi: 10.3389/fphys.2015.00381

4.1 Abstract

Background : Mycophenolic acid (MPA) is an important immunosuppressive drug (ISD) prescribed to prevent graft rejection in the organ transplanted patients, however, its use is also associated with adverse side effects like sporadic gastrointestinal (GI) disturbances. Recently, we reported the MPA induced tight junctions (TJs) deregulation which involves MLCK/MLC-2 pathway. Here, we investigated the global histone acetylation as well as gene-specific chromatin signature of several genes associated with TJs regulation in Caco-2 cells after MPA treatment.

Results: The epigenetic analysis shows that MPA treatment increases the global histone acetylation levels as well as the enrichment for transcriptional active histone modification mark (H3K4me3) at promoter regions of *p38MAPK*, *ATF-2*, *MLCK* and *MLC-2*. In contrast, the promoter region of *occludin* was enriched for transcriptional repressive histone modification mark (H3K27me3) after MPA treatment. In line with the chromatin status, MPA treatment increased the expression of *p38MAPK*, *ATF-2*, *MLCK*, and *MLC-2* both at transcriptional and translational level, while occludin expression was negatively influenced. Interestingly, the MPA induced gene expression changes and functional properties of Caco-2 cells could be blocked by the inhibition of p38MAPK using a chemical inhibitor (SB203580).

Conclusion: Collectively, our results highlight that MPA disrupts the structure of TJs via p38MAPK-dependent activation of MLCK/MLC-2 pathway that results in decreased integrity of Caco-2 monolayer. These results led us to suggest that p38MAPK-mediated loss of integrity of epithelial monolayer could be the possible cause of GI disturbance (barrier dysfunction) in the intestine, leading to leaky style diarrhea observed in the organ-transplanted patients treated with MPA.

Key words: Tight Junction, Permeability, MPA, Epigenetic, Promoter activity

4.2 Introduction

Mycophenolate mofetil (MMF) and enteric-coated mycophenolate-sodium (EC-MPS) are two commercially available formulations of immunosuppressive regimens that contain active agent mycophenolic acid (MPA) [237;238]. MPA inhibits the activity of inosine monophosphate dehydrogenase (IMPDH), a vital enzyme in the *de novo* synthesis of guanine nucleotide, thus preventing the synthesis of DNA and thereby inhibits growth and division of rapidly growing cells such as lymphocytes of the immune system [239]. This property makes MPA as an effective immunosuppressive regime to suppress the immune system in order to prevent graft rejection in organ transplanted patients. Though MPA is vital to suppress the immune system to prevent graft rejection, its use is linked to the gastrointestinal (GI) disturbances in the transplanted patients (for details, see review articles [240;241]). Several studies have shown that defect in the intestinal barrier function due to MMF or EC-MPS treatment results in increased permeability of intestinal mucosa (epithelial monolayer) for the solutes [237], develop leak-flux diarrhea in the rat model [238], and in renal and kidney transplanted patients [239;240].

Gastrointestinal disturbances in inflammatory bowel diseases (IBD) like Crohn's disease and ulcerative colitis, and in graft versus host disease are mainly characterized by epithelial monolayer barrier defects which contribute to enhanced intestinal permeability [242] and subsequent translocation of infectious agents and/or endotoxin from gut [243;244]. Epithelial cells are connected with each other by four different types of junctions called desmosomes, gap-, adheren-, and, tight- junctions (TJs) [245-247]. TJs are complex structure of approximately 35

different proteins including integral membrane proteins (claudins, occludin, junctional adhesion molecules “JAMs”) and peripheral membrane proteins (Zonula Occludens (ZO) such as ZO-1, ZO-2, and ZO-3) [172;173]. TJs assist to seal the paracellular space between the adjacent cells, and is particularly involved in regulating barrier and fence functions [248]. In “barrier function”, TJs regulate the passage of ions, water, and various molecules through paracellular pathways. Thus aberrant barrier function can cause edema, jaundice, diarrhea and blood-borne metastasis, however, the cell polarity is maintained by forming a fence to prevent intermixing of molecules between apical and lateral membrane. It is interesting to note that the altered fence function is involved in cancer progression in terms of loss of cell polarity [249].

In GI tract, TJs opening is considered as a key limiting factor of mucosal paracellular movement of nutrients and solutes. Growing evidences have indicated that TJs opening is modulated by the phosphorylation of myosin light chain 2 (MLC2), which principally depends upon the activation of MLC kinase (MLCK). The MLCK itself is however triggered by different types of stimuli such as IFN-gamma, TNF-alpha, and LIGHT (Lymphotoxin-like inducible protein that competes with glycoprotein D for herpes virus entry on T cells). This stimulation results in contraction of cytoplasmic actin filaments and redistribution of TJs anchoring protein, ZO-1 and structural protein, occludin in IBD (Crohn’s disease, ulcerative disease), leaky flux diarrhea, and cholera (watery diarrhea) [250-254]. . Recently, it has been shown that proinflammatory cytokine (IL-1 β) induces TJs permeability in both *in vitro* and *in vivo* models through *p38MAPK/ATF-2*-dependent regulation of *MLCK* activity [255]. *p38MAPK* is activated by various cellular stress agents (i.e., UV irradiation, heat shock, osmotic stress, lipopolysaccharide, cytokines) [256;257] and is known to play a vital role in apoptosis, cytokines production, transcriptional regulation and cytoskeletal reorganization [258-260]. Previously, we reported that MPA alters TJs assembly in Caco-2 monolayer, similar to GI tract, via MLCK/MLC-2 pathway [253].

The aim of the present study was to investigate whether MPA treatment leads to increased TJs permeability via *p38MAPK* dependent MLCK/MLC-2 pathway in MPA-treated Caco-2 cells monolayer.

4.3 Material and Methods

4.3.1 Experimental Design

We used Caco-2 cells as a model cell line to investigate the MPA-mediated TJs modulation via p38MAPK dependent MLCK/MLC-2 pathway. Towards this, we established three groups: 1. MPA-treated group, 2. SB+MPA-treated group, and 3. DMSO (control)-treated group of differentiated and polarized Caco-2 cells monolayers. Each group was treated with MPA or SB+MPA or DMSO for 72 hrs. Different molecular analyses (epigenetic, mRNA expression, protein expression, and phosphorylation status) and functional analyses (TEER and FITC-Dextran dye flux) were performed to explore the role of p38MAPK-dependent MLCK/MLC-2 pathway in maintaining epithelial monolayer integrity following MPA treatment.

4.3.2 Chemicals/Reagents

Cell culture media Dulbecco's Modified Eagle's medium (DMEM), fetal calf serum (FCS), phosphate buffer saline (PBS), penicillin and streptomycin were purchased from PAA Laboratories, Pasching, Austria. Fluorescein isothiocyanate-conjugated dextran (FITC-dextran), 4 kDa (FD4), Trypsin, MPA, and DMSO were purchased from Sigma-Aldrich, Steiheim, Germany. Protease and phosphatase inhibitor cocktails were purchased from Roche, Mannheim, Germany. Bromophenol blue was obtained from Carl Roth, Karlsruhe, Germany. Sodium dodecyl sulfate (SDS) was obtained from Serva, Heidelberg, Germany. Glycerin, potassium ferricyanide and sodium thiosulfate were purchased from Merck, Darmstadt, Germany. Formic acid was purchased from BASF, Ludwigshafen, Germany. Magnesium chloride ($MgCl_2$), M-MLV RT enzyme, and 5X PCR buffer were from Invitrogen, Karlsruhe, Germany. Deoxynucleotide triphosphates (dNTPs) were from Roche, Mannheim, Germany and PCR primers were synthesized by Eurofins, Ebersberg, Germany. Ribonuclease (RNAase) inhibitor was obtained from Promega, Mannheim, Germany. The cell lysis buffer (10X) was obtained from Cell Signaling Technology, Danvers, MA, USA. All other chemicals used in this work were from the highest available purity from commercial sources unless otherwise stated.

4.3.3 Primer Design

Promoter sequences were retrieved for each gene using Transcriptional Regulatory Element Database (TRED). Primer3 (v. 0.4.0) was used to design primers against promoter region and their specificity was checked by Human BLAT Search.

4.3.4 Cell Culture

All experiments were performed with human colon carcinoma (Caco-2) cells (Passages No. 15-25). Caco-2 cells were purchased from DSMZ (German collection of microorganisms and cell culture, Braunschweig, Germany) and grown in DMEM medium supplemented with 10% FBS, 1% Penicillin/Streptomycin, 1% non-essential amino acids. Confluent monolayers were obtained within 3-5 days after cell seeding (2×10^5 cells/cm²) and grown further for 13 days (d) post-confluency. Medium was changed every other day after formation of confluent monolayer. Three groups were established i.e., MPA-treated, SB203580 (SB)+MPA-treated and DMSO treated (control group). Cells were washed with PBS prior to the 72 h exposure with either MPA (10 μ M) or DMSO. In case of SB (10 μ M) treatment, cells were incubated with SB one hour prior to the addition of MPA.

4.3.5 Caco-2 monolayer integrity assays

4.3.5.1 Determination of trans-epithelial electrical resistance (TEER)

The intactness of paracellular pathways that control small molecules movement across Caco-2 monolayer was examined by TEER as previously described [189;261]. Briefly, Caco-2 cells were seeded on polyester transwell inserts (6.5mm diameter, 0.33 cm² grow surface area, 0.4 μ m pore size; Corning Costar corporation, USA) at a density of 2×10^5 cells/well. Stable TEER of confluent monolayer was achieved at days 13-15 after seeding. Caco-2 plated filter having constant TEER ($\geq 400 \Omega \cdot \text{cm}^2$) were included in experiments. Post-confluence monolayers having stable TEER were treated with MPA or SB plus MPA or DMSO (control) for 72 h. TEER was measured at 0, 12, 24, 48 and 72 h time period using an epithelial voltammeter (EVOM2, World Precision Instruments) with a STX2 electrode (World Precision Instruments, FL, USA). The TEER values were normalized by against background resistance of a blank insert that contained only medium. TEER was measured as ohms \times cm² ($\Omega \cdot \text{cm}^2$) using the following formula: Resistance ($TEER$) = $[RC-RE] \times A$, where RC is resistance of the cells (Ω); RE is resistance of the blank (Ω); A is surface area of the membrane insert (cm²). The results were expressed as the

change in TEER with respect to time-matched controls [ΔTEER ($\Omega\cdot\text{cm}^2$)]. TEER values were calculated in three independent biological replicates each performed in duplicates.

4.3.5.2 FITC-dextran assay (FD4)

After 72 h of incubation with MPA or SB plus MPA or DMSO, permeability of Caco-2 monolayers was assessed using a previously reported dye fluxes method [189;262]. Briefly, Caco-2 cells were grown into monolayers and treated as described above. Following MPA treatment, monolayers were rinsed carefully with Hank's balanced salt solution (HBSS). To measure paracellular permeability (apical to basolateral fluxes), HBSS containing 1 mg/mL FD4 solution was added to the apical side for 2 h. Permeability marker flux was assessed by taking 100 μL from the basolateral chamber after 0, 20, 40, 60, 80, 100 and 120 minutes. Fluorescent signal was measured using a Lambda fluoro 320 fluorescence plate reader (MWG Biotech, Ebersberg, Germany) using 492 nm excitation and 520 nm emission filters. Standard curve, generated by serial dilution of FD4, was used to determine the FD4 flux concentrations across the monolayer. The flux concentration, which represents the permeability of monolayer, in the basolateral chamber was calculated by the following formula " $P_{\text{app}} = (\Delta C_A / \Delta t) V_A / A C_L$ ". Where P_{app} is the apparent permeability (cm/s), ΔC_A is the change of FD4 concentration, A is the surface area of the membrane (cm^2), Δt is the change of time, V_A is the volume of the abluminal medium, and C_L is the initial concentration in the luminal chamber. FD4 values were calculated in three consecutive experiments, each performed in duplicates.

4.3.6 RNA expression analysis

Cells were grown for 13 d post-confluence and treated for 72 hours in 6-well plates as described above. Trizol (Trizol reagent; Invitrogen, USA) was used to extract total cellular RNAs from Caco-2 cell monolayers (MPA-treated or SB plus MPA-treated or DMSO-treated) according to the manufacturer's instructions. Briefly, Caco-2 monolayers were rinsed with ice-cold PBS and harvested by scraping with a rubber policeman into Trizol reagent, homogenized by inverting the tube twice, and RNA was extracted using chloroform/isopropanol precipitation. The precipitated RNA was air dried, dissolved in sterile water and stored at -80°C until analysis. RNA was quantified using a NanoDrop 2000C (PeqLab, Thermo Scientific).

Reverse transcription reaction was performed using 1 μg of total RNA in a 30 μL reaction mixture containing 1X RT-PCR buffer (10 mmol/L Tris-HCl [pH 8.3], 15 mmol/L KCl, 0.6

mmol/L MgCl₂), 0.5 μmol/L of each dNTP, 1 U/μL RNase inhibitor and 13.3 U/μL M-MLV RT enzyme. The RT reactions were performed in a thermocycler (Biometra, Goettingen, Germany) at 65°C for 5 min, 37°C for 52 min, and then inactivated by heating at 70°C for 15 min. cDNA was stored at -80°C until use. Online Primer 3 software was used to design primers for the amplification of target genes by real time PCR [263] (For primers used in this study see table 2).

Light Cycler instrument (Roche, Mannheim, Germany) was used to amplify cDNA in a 20 μL reaction mixture containing 1 μL of cDNA solution, 2 μL of 10 X PCR buffer (Invitrogen, Darmstadt, Germany), 2 μL SYBR green, 1 μL DMSO, 0.25 μL of each primer, 2.0 mmol/L MgCl₂, 0.2 mmol/L of each dNTP, and 0.15 U/μL PAN Script DNA polymerase (PAN Biotech, Aidenbach, Germany). The following conditions were set to amplify cDNA; [{denaturation: 95°C for 5 min, one cycle}, {40 cycles, denaturation: 95°C for 30 sec, (annealing: *p38MAPK* (56°C), *ATF-2* (57°C), *MLCK* (56°C), *MLC-2* (57°C), *occludin* (57°C), *ZO-1* (57°C) and *GAPDH* (60°C) for 30 sec), extension (72°C) for 30 sec}].

PCR data was normalized using internal control gene (*GAPDH*) and comparative Ct method ($2^{-\Delta\Delta C_t}$) [264] was used to calculate the alteration of relative mRNA expression as a fold change between MPA treated and control cells. Amplified PCR product specificity was further confirmed by running on 1.5% agarose gel electrophoresis. Three separate experiments were performed with each one in triplicates.

4.3.7 Dot Blot

Dot blot assay was performed as described previously [265] with little modification. Briefly, Caco-2 cells were cultured into differentiated and polarized monolayers and treated with the therapeutic concentration of MPA or DMSO for 72 h. Total cell lysate was prepared by 1X lysis buffer (Cell Signaling) at 0h, 1 h, 12 h, 24 h, 48 h, 72 h. Proteins were quantified by Bio-Rad protein assay kit according to the manufacturer's guidelines. One cm² grid was drawn by pencil on nitrocellulose membrane. Two μl (protein concentration 10μg/μl) of each sample was slowly spotted into the center of grid using narrow-mouth pipette tips. Sample spotted membranes were dried at RT. Non-specific binding sites were blocked by soaking sample spotted membrane in 5% BSA in TBST for one hour at RT on a plate shaker at low speed. Each membrane was incubated with primary antibody (05μg/ml rabbit anti-H3K9ac -Abcam or 1:20,000 rabbit anti-

H4K8ac -Diagenode) dissolved in 5% BSA/TBST for two hours at RT on a plate shaker at low speed. Following incubation with primary antibodies, each membrane was washed three times for 5 min and then incubated with secondary antibodies conjugated with HRP for one hour at RT on a plate shaker at low speed. Then the membrane was washed three times and incubated with ECL reagents for two minutes, covered with saran-wrap and exposed to X-ray film in the dark room for different time, and proceeded for autoradiography using Konica SRX-101A (Konica Minolta).

4.3.8 Western blot

Caco-2 cells were cultured into differentiated and polarized monolayers and treated as described above and were rinsed and collected with ice-cold PBS. Cells were lysed with lysis buffer-CS (50 mM Tris/HCl, pH 7.4, 1.0% Triton X-100, 5 mM EGTA, 10 mM sodium fluoride, 2 µg/mL leupeptin, 10 µg/mL aprotinin, 10 µg/mL bestatin, 10 µg/mL pepstatin A, 1 mM vanadate and 1 mM PMSF). Total proteins (cleared supernatant) were separated by centrifugation from the cell lysate. Protein concentrations were measured using Bio-Rad protein assay kit (Bio-Rad Laboratories) according to the manufacturer's guidelines. Total protein contents were separated by 12.5 % SDS-PAGE and blotted onto PVDF membrane (0.45 µm pore size, Immobilon, Millipore, MA, USA) using Trans-Blot SD cell system (Bio-rad, Munich, Germany) for 30 min at 15V in a blotting buffer (192 mmol/L glycine, 20% methanol, and 25 mmol/L Tris [pH 8.3]). To prevent nonspecific binding sites, each membrane was blocked with 5% milk (w/v) in TBS-T buffer (50 mmol/L Tris-HCl [pH 7.5], 200 mmol/L NaCl, 0.05% Tween 20) for one hour at room temperature. Blocked membranes were washed twice in TBS-T for 5 min, then incubated with following antibodies: 1:10,000 dilution of mouse monoclonal anti-MLCK antibody (Sigma, Mannheim, Germany), 1:500 dilution of a mouse monoclonal anti-MLC-2 antibody (Sigma, Mannheim, Germany), 1:1000 rabbit anti-phospho MLC-2 antibody (Cell Signaling, Beverly, USA), 1 µg/mL rabbit anti-ZO-1, 0.5 µg/mL mouse anti-occludin (Zymed, CA, USA), 1:500 dilution of rabbit anti-H3K9ac (abcam), 1:250 dilution of H4K8ac (diagenode) or 1:5000 anti-β actin (Sigma, Mannheim, Germany) in 5% BSA in TBS-T for overnight at 4°C. Following overnight incubation with primary antibodies, membranes were washed with TBS-T buffer and again incubated with appropriate HRP-conjugated secondary antibodies (Bio-Rad, Munich, Germany), then washed with PBS and arranged for enhanced chemiluminescence detection (GE, Buckinghamshire, UK) according to the manufacturer's recommendation. The

chemiluminescence signal was captured by hyperfilm-ECL (GE, Buckinghamshire, UK) and visualized using Konica SRX-101A (Konica Minolta). The densities of the specified protein bands between MPA-treated, SB plus MPA and control samples were quantified using ImageJ software (v 1.48, NIH, USA).

4.3.9 Chromatin immunoprecipitation (ChIP)

Caco-2 cells were cultured and treated as earlier described in “cell culture”. For ChIP analysis, cells were fixed with formaldehyde at a final concentration of 1.0% for 30 min at room temperature to cross-link DNA binding proteins and DNA [266]. Cells were harvested with ice cold PBS and counted by Advia 120 (Siemens) and equal number of cells were lysed according to the manufacturer’s instructions (Red ChIP Kit™, Diagenode). Cross-linked chromatin was sheared into fragments of 100–1000 bps using Branson Sonifier 250 for 3 minutes using cycles of 30 seconds sonication and one minute on ice. One-tenth of the sample was set aside as an input control, and the rest was pre-cleared with protein A magnetic beads for 30 minutes at 4°C with agitation. Pre-cleaned chromatin was then precipitated with active histone mark antibody (H3K4me3, Abcam, ab8580), as well as with repressive histone mark antibody (H3K27me3, Millipore, 07-449) and normal IgG (One Day ChIP Kit™, Diagenode) from both treated and untreated cells. The Chromatin-antibodies-magnetic beads complexes were washed with 1X ChIP washing buffer (One Day ChIP Kit™, Diagenode). Proteinase K was used to degrade the DNA associated proteins and DNA was isolated by DNA slurry (One Day ChIP Kit™, Diagenode) and quantified by NanoDrop (NanoDrop 2000C, peqlab, Thermo Scientific). ChIP-precipitated genomic DNA was amplified using real time PCR (Roche, Mannheim, Germany) in 20 µL SYBR green based reaction (For promoter based primers see details in table 2). PCR amplification was done under the following conditions; [{denaturation: 95°C for 2 min, one cycle}, {40 cycles, denaturation: 95°C for 30 sec, (annealing: p38MAPK (60°C), ATF-2 (55°C), MLCK (62°C), MLC-2 (62°C), occludin (54°C), ZO-1 (55°C) and GAPDH (59°C) for 30 sec), extension (72°C) for 30 sec}].

4.3.10 Data Analysis

Ct values from real time PCR were analyzed by “input percent method” [267]. Briefly, raw Ct value of the diluted input (1%) was adjusted to 100% by subtracting the dilution factor of 100 or 6.644 cycles (i.e., log₂ of 100). Sample raw Ct values (Δ Ct) were normalized by subtracting

adjusted Input (Ct Input - 6.644) Ct value. And finally the “Input percent” value for each sample was calculated using the following formula. $\text{Input \%} = 100 \cdot 2^{(\text{Adjusted input} - \text{Ct (IP)})}$. The “Input percent” value represents the enrichment of H3K4me3 and/or H3K27me3 at the promoter region of genes studied. Dissociation curve analysis was performed to confirm the specificity of each PCR product. GAPDH was used as an internal control gene.

Table 4.1: Promoter assay and mRNA expression primer list.

| Name | Chromosomal location | Primer types | Direction | Sequences | Product size (bps) |
|----------|----------------------|--------------|--------------------|--|--------------------|
| p38MAPK | 6 | Promoter | Forward Reverse | TTGACTCTTTCCCCGACAC AACTGGAGACCAAAGGCAGA | 187 |
| | | Expression | Forward Reverse | CCAGCTCAGCAGATTATGC TGGTACTGAGCAAAGTAGGCA | 246 |
| ATF-2 | 2 | Promoter | Forward Reverse | CCTCAGCATACTGGTGCATT TGGATGTGCTGACCGAACTA | 159 |
| | | Expression | Forward Reverse | GGCTTCTCCAGCTCACACA TGTTTCAGCTGTGCCACTTC | 326 |
| MLCK | 3 | Promoter | Forward Reverse | TCTGCTGCAGTTCAGAGCAA AGGAGGAATGGTCAACAGCA | 150 |
| | | Expression | Forward Reverse | GATGATGCTCCAGCCAGT GTCCTCAGGGAAGTGGATGA | 177 |
| MLC-2 | 12 | Promoter | Forward Reverse | TCCACCTCCATCTTCTTTGC GCCTTTGCCTTCCTTACACA | 168 |
| | | Expression | Forward Reverse | AGAGACACCTTTGCTGCCCTT CCTTTGCCTTCAGGGTCAAAC | 188 |
| Occludin | 5 | Promoter | Forward Reverse | TGGATGGCAACTAACACCTACA AACGAAAGACTCCTGGGAAAAT | 142 |
| | | Expression | Forward Reverse | TGGGACAGAGGCTATGGAAC ATGCCAGGATAGCACTCAC | 287 |
| ZO-1 | 15 | Promoter | Forward Reverse | GCACATCAGCACGATTTCTG AAACAGTGGGCAAACAGACC | 166 |
| | | Expression | Forward Reverse | TGAGGCAGCTCACATAATGC GGTCTCTGCTGGCTTGTTTC | 224 |
| GAPDH | 12 | Promoter | Forward Reverse | TGAGCAGTCCGGTGTCACTA ACGACTGAGATGGGGAATTG | 152 |
| | | Expression | Forward Reverse | ACCCAGAAGACTGTGGATGG TTCTAGACGGCAGGTCAGGT | 201 |

4.3.11 Statistics

Statistical program GraphPad (GraphPad, San Diego, CA) was used to perform statistical analysis. Data was analyzed by analysis of variance (ANOVA) and comparisons between control and MPA treatment were made using the Bonferroni posttest. Alternatively, statistical significance between control and treatment group were calculated using student’s t-test. Results were expressed as mean \pm standard error of the mean (SEM). Probability of 0.05 or less was deemed statistically significant (* $P < 0.05$, ** $P < 0.01$, *** $P < 0.001$).

4.4 Results

4.4.1 MPA increases global histone (H3K9 and H4K8) acetylation in Caco-2 Cells.

Acetylation of histone proteins plays an important role in the unfolding of chromatin and initiation of transcription. Recently it was reported that MPA treatment increases the histone H3/H4 global acetylation levels in CD4⁺ T cells from systemic lupus erythematosus patients [268]. In order to study whether MPA treatment leads to similar epigenetic changes also in epithelial monolayer, Caco-2 cells monolayers were treated with MPA for various time points and analyzed for global histone acetylation levels using dot- and Western -blot analysis. The dot blot results show that MPA treatment increases global acetylation of H3K9 and H4K8 in Caco-2 cells after 72 h (Fig. 4.1A). Western blot analysis further confirmed that MPA significantly increases the acetylation of H3K9 and H4K8 after 72 h (Fig. 4.1 B-D). These results indicate that MPA treatment significantly alters the epigenetic status of Caco-2 cells.

4.4.2 MPA treatment activates MLCK and MLC-2 while inactivates occludin at epigenetic level in Caco-2 cells.

We and other investigators have reported the involvement of MLCK pathway in the regulation of TJs barrier function [253;269]. In light of the global increase in histone acetylation levels after MPA treatment, we assessed the epigenetic status at the promoter region of *MLCK*, *MLC-2*, *occludin* and *ZO-1* genes, by ChIP assay in MPA treated or untreated Caco-2 monolayer cells. Our ChIP data showed that the transcription permissive histone modification mark (H3K4me3) was increased significantly at the promoter region of *MLCK* and *MLC-2* genes, respectively (Fig. 4.2 A & B). Concomitantly, transcription repressive mark (H3K27me3) was decreased significantly at the promoter region of *MLCK* and *MLC-2* genes, respectively, as compared to controls (Fig. 6A & B). While promoter of *occludin* lost H3K4me3 mark and gained H3K27me3 mark in the MPA treated Caco-2 cells as compared to control cells, indicating the transcriptional silencing of *occludin* after MPA treatment (Fig. 4.2 C). However, the promoter region of *ZO-1* showed no significant changes in H3K4me3 and H3K27me3 levels between MPA-treated cells and control (Fig. 4.2 D).

To confirm the influence of MPA on the epigenetic activation of *MLCK* and *MLC-2* genes, transcriptional and translational expression was analyzed using quantitative PCR and

immunoblotting, respectively. In line with the earlier reports [253;270], MPA treatment significantly increased the expression of MLCK and MLC-2 both at transcriptional and protein level (Fig. 4.2 E-G). Further we analyzed the expression of occludin to confirm the epigenetic data at mRNA and protein level and found significant decrease at protein and mRNA expression (Fig. 4E-G). In contrast, we did not observe any significant difference in ZO-1 RNA or proteins expression in MPA-treated Caco-2 cells as compared to control cells (Fig. 4.2 E-G). Collectively, the gene expression data correlate well with the gene-specific epigenetic changes induced by MPA treatment in Caco-2 monolayer cells.

4.4.3 MPA treatment activates p38MAPK and ATF-2 at epigenetic level in Caco-2 cells.

Recently it was reported that p38MAPK increases TJs permeability in IL-1 β treated Caco-2 through activation of MLCK pathway [255]. In this study we aimed to extend our previous knowledge and explored whether p38MAPK acts upstream of MLCK/MLC-2 pathway in MPA-treated Caco-2 cells. Towards this end, firstly, we assessed the epigenetic status of *p38MAPK* and *ATF-2* genes at their promoter regions by ChIP assay in MPA treated or untreated Caco-2 monolayer cells. Our ChIP results showed that the activation histone modification mark (H3K4me3) was increased significantly at the promoter region of *p38MAPK* and *ATF-2* genes, respectively in MPA treated cells (Fig. 4.3 A & B). Concomitantly, repression mark (H3K27me3) was decreased significantly at the promoter region of *p38MAPK* and *ATF-2* genes, respectively, as compared to controls (Fig. 4.3 A & B). The transcriptionally active epigenetic state of *p38MAPK* and *ATF-2* was confirmed by the mRNA expression analysis that showed significant increase in *p38MAPK* and *ATF-2* expression after MPA (Fig. 4.3 C).

4.4.4 Inhibition of p38MAPK via SB counteracts the altered expression of MLCK, MLC-2, and occludin genes in MPA-treated Caco-2 cells.

In order to test whether MPA indeed regulates p38MAPK-dependent expression of MLCK pathway and thereby the TJs defects, we performed the p38MAPK inhibition and studied its effect at the functional level. The chemical inhibitor SB203580 (SB), a representative of pyridinimidazole, is a specific inhibitor of p38MAPK and is widely used in inhibitory studies to attenuate the activity of p38MAPK and its downstream signaling activities in various physiological processes [271]. Our results showed that p38MAPK inhibition in MPA treated Caco-2 cells prevented any significant change in expression of MLCK, MLC-2, phosphorylated

MLC-2 (pMLC-2) and Occludin protein as compared to DMSO only treated cells (Fig. 4.3 D-G). While the expression of ZO1 was found unaltered by MPA or MPA+SB treated Caco-2 cells (Fig. 4.3 H).

4.4.5 p38MPAK inhibition partially reverses MPA-induced TJs dysfunction

The maintenance of normal protein levels of MLCK, MLC2, and occludin after p38MAPK inhibition prompted us to study the functional properties of Caco-2 monolayer in the presence of SB. The intactness of Caco-2 cells differentiated into polarized confluence monolayer can be measured quantitatively as TEER value and the sum of the resistance indicates the integrity of the monolayer barrier maintained by TJs in the apical surface of the cells. Any damage to the intactness of monolayer results in reduced TEER value. In accordance with the literature, exposure of Caco-2 monolayer to MPA significantly decreased TEER at 24 h after treatment, and the TEER was significantly further decreased by 72 h as compared to the control cells (Fig. 4.3 I). Similarly, FD4 permeability analysis (traditionally used to measure the movement of small molecules across the intestinal epithelium *in vivo*) following 72 h MPA treatment showed a time-dependent increase across (from the apical to the basolateral side) the Caco-2 monolayer, as expected (Fig. 4.3 J).

Interestingly, when MPA-treated Caco-2 cells monolayers were co-incubated with the inhibitor for p38MAPK, very significant preservation of TEER (approximately 50%) was observed as compared to only MPA-treated Caco-2 cells (Fig. 4.3 I-J). Similarly, 50% reduction in the FD4 leak on the basolateral side of the Caco-2 cell monolayer was measured as compared to only MPA-treated monolayer (Fig. 4.3 J). Collectively, these results confirm that the Caco-2 monolayer paracellular permeability is significantly increased after MPA exposure and that can be antagonized by blocking the activity of p38MAPK pathway.

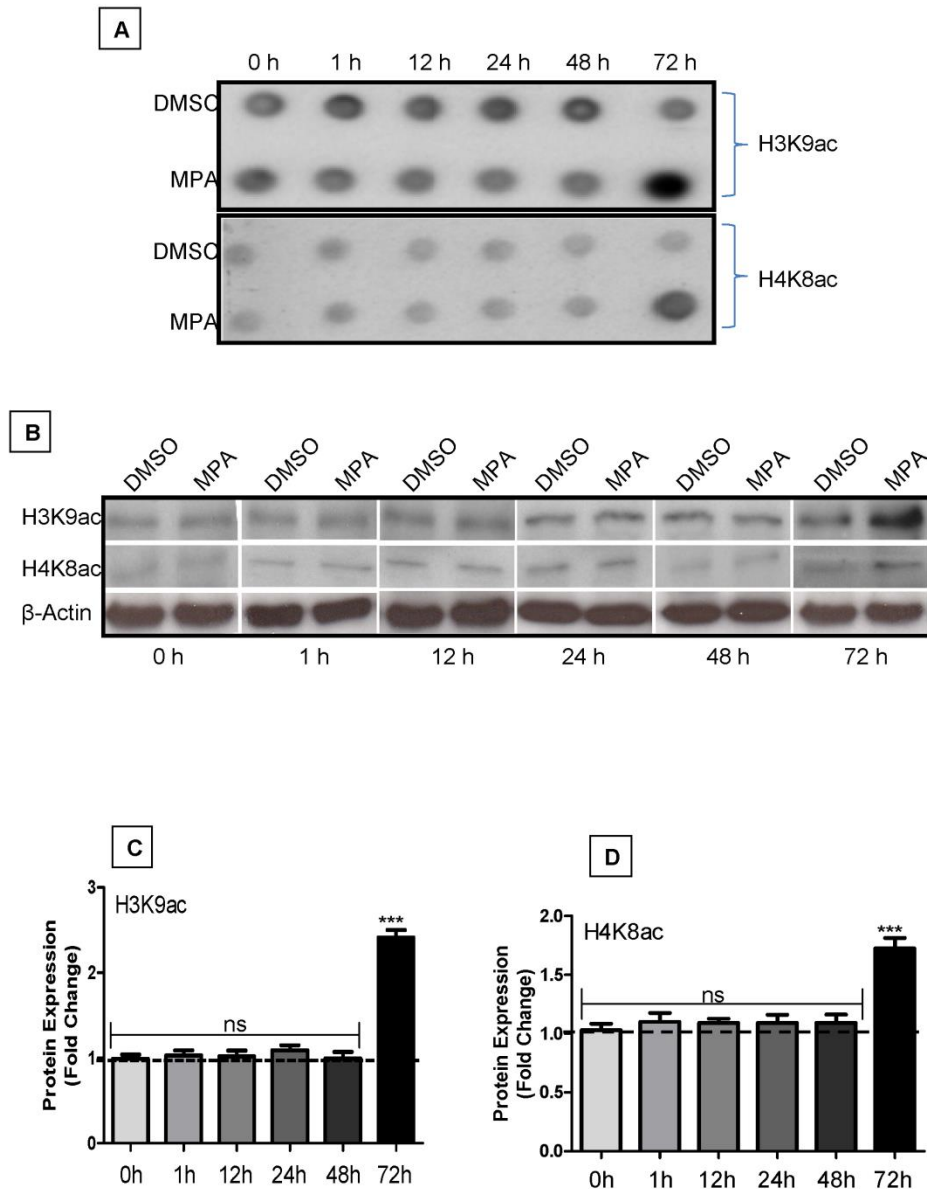


Figure 4.1: MPA treatment increases global histone acetylation in Caco-2 cells. (A) Dot-blot analysis; Caco-2 cells were cultured in 6-well plates and post confluence monolayers were treated either with 10 μ M MPA or DMSO for indicated time points. Total proteins were extracted and a volume of 2 μ l from each time point was spotted on nitrocellulose membrane, dried and then probed with anti-H3K9ac and anti-H4K8ac antibodies. (B) Western blot analysis; Total cell proteins were resolved on 12.5% SDS-PAGE gels and, immunoblotted using anti-H3K9ac & anti-H4K8ac specific antibodies. β -actin was used as a loading control. (C and D). Bar graphs representing the densitometric analysis of three independent experiments from Western blot (B) using the Lab image software. Differences between two groups were analyzed by the two-tailed Student's t-test and of more than two groups by one-way ANOVA with

Bonferroni posttest ($n = 3$) and the values were expressed as means \pm SEM. * $P < 0.05$, ** $P < 0.01$, *** $P < 0.001$ when compared with control cells.

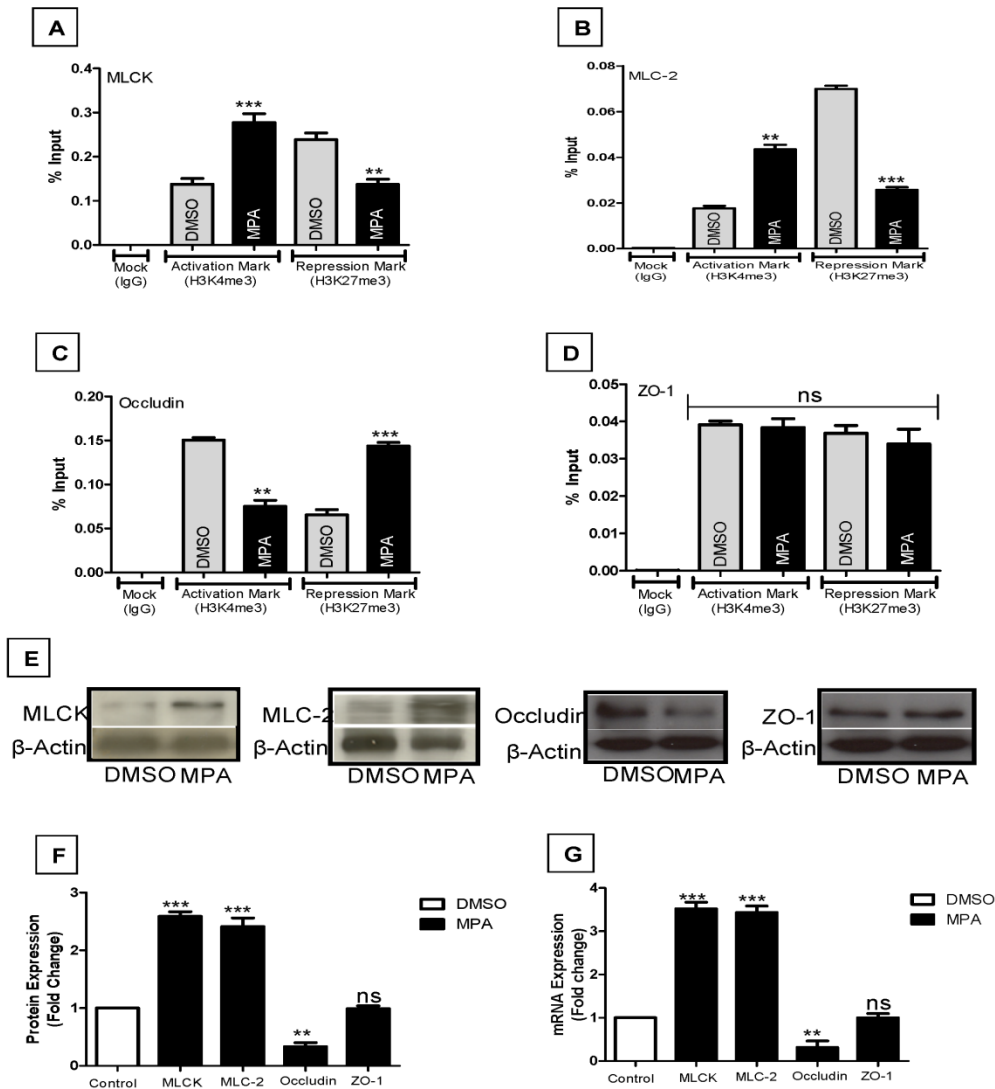


Figure 4.2: causes epigenetic activation of MLCK/MLC-2 pathway and tight junction genes (occludin). (A-D) Caco-2 cells were grown for 13 days post-confluence to form differentiated monolayers and then treated for 72 h with MPA or DMSO. ChIP was performed using anti-H3K4me3 (activation mark) or anti-H3K27me3 (repression mark), followed by real time PCR using promoter-specific primers of the target genes (MLCK, MLC-2, Occludin and ZO-1). Levels of H3K4me3 or H3K27me3 was measured as %age input in the MPA treated as compared to the untreated cells. (E and F) Western blot analyses of MLCK, MLC-2, occludin and ZO-1 after MPA treatment. Whole cell protein lysates were resolved on SDS-PAGE gels and immunoblotted using of anti-MLCK, anti-MLC-2, anti-occludin and anti-ZO-1 specific antibodies. β -actin was used as a loading control for an equal amount of protein.

Densitometric analysis was done using the Lab image software on three independent experiments. Differences between two groups were analyzed by the two-tailed Student's t-test and of more than two groups by one-way ANOVA with Bonferroni posttest. (G) DMSO treated Caco-2 monolayer cells. The values were expressed as means \pm SEM. *P < 0.05, **P < 0.01, ***P < 0.001 when compared with control cells. (n = 3).

4.4.6 Inhibition of p38MAPK through SB demolishes increased promoter activity of downstream targets of p38MPAK in MPA-treated Caco-2 cells.

Next, we analyzed whether the protein expression changes seen after the inhibition of p38MAPK are due to the epigenetic remodeling at the promoter regions of these genes or are due to protein stability. In accordance with the expression data of downstream targets of p38MAPK, the epigenetic signature at the promoter regions of *MLCK*, *MLC-2*, and *Occludin*, but not *ZO1*, was restored to the epigenetic status seen in control cells (Fig. 4.4 A-D) by SB use. Similarly, by use of SB, the promoter region of *ATF2*, but not *p38MAPK*, showed the normal chromatin signature seen in control cells (Fig. 4.4 E & F). These results were further confirmed by mRNA expression analysis, which showed that pretreatment with SB restored the MPA induced gene expression changes in Caco-2 cells while it had no significant inhibitory effects on mRNA expression of the *p38MAPK* gene (Fig. 4.5 A-C).

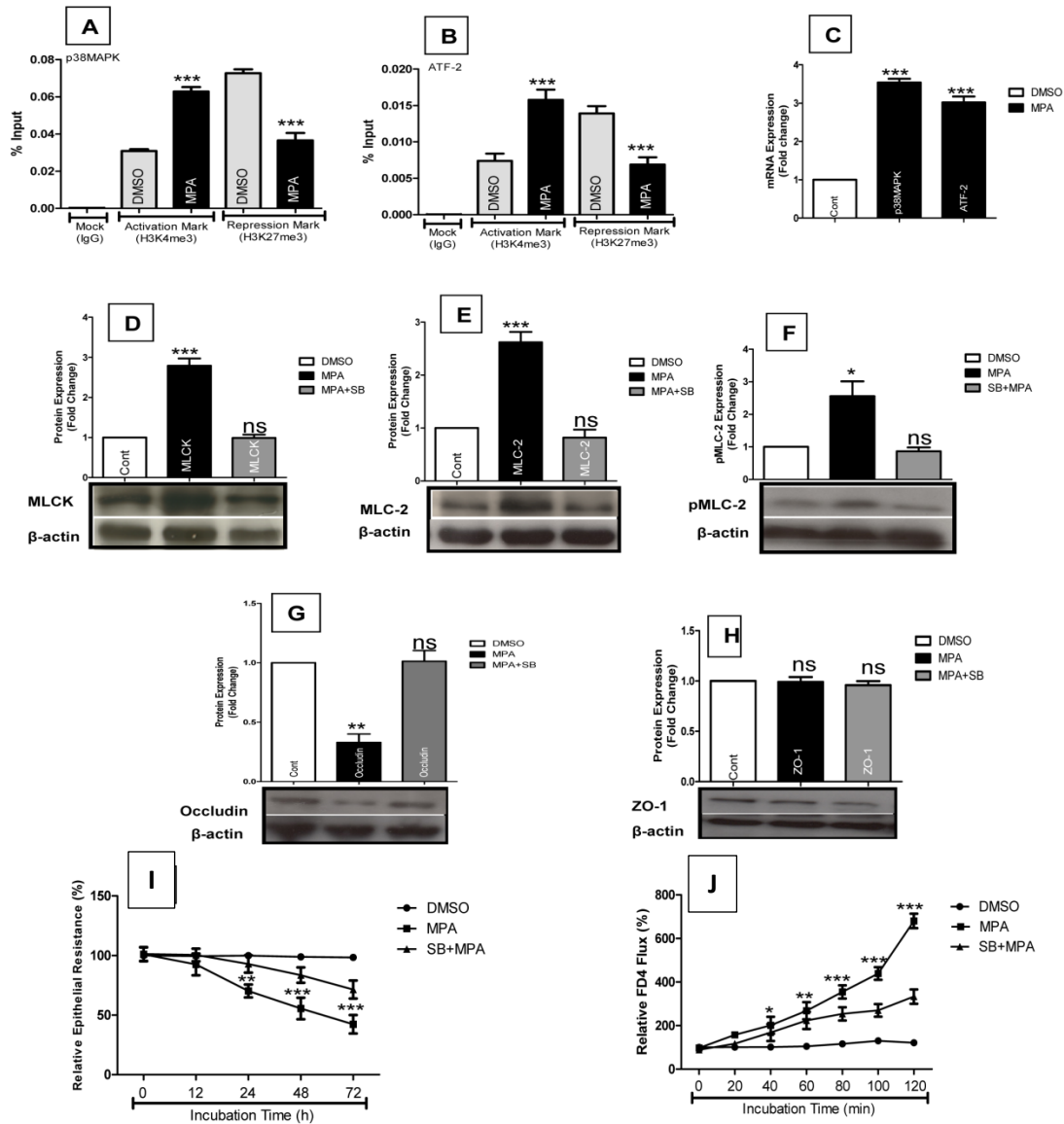


Figure 4.3: p38MAPK regulates MLCK/MLC-2 pathway and its inhibition partially prevents MPA-induced TJs dysfunction. (A-B) Epigenetic status at the promoter regions of p38MAPK & ATF-2 genes MPA or DMSO treated Caco-2 monolayer cells. ChIP was performed with antibodies specific to the activation mark (H3K4me3) or repression mark (H3K27me3), followed by real time PCR analysis. Relative intensity of activation mark (H3K4me3) or repression mark (H3K27me3) were measured as %age input. (C) Bar graph showing the p38MAPK & ATF-2 mRNA expression. (D-H) Western blots and the corresponding densitometric data showing the effect of SB on the expression of MLCK/MLC-2 pathway and tight junction proteins (occludin & ZO-1). (I and J) Line graphs showing the transepithelial electrical resistance (TEER) (I) and paracellular flux (FITC-dextran) (J) assay results obtained either in presence or absence of p38MAPK inhibitor. Error bar indicate means \pm SEM. *P < 0.05, **P < 0.01,

***P < 0.001 compared with the control (DMSO) at that time by ANOVA using a Bonferroni posttest. (n=3)

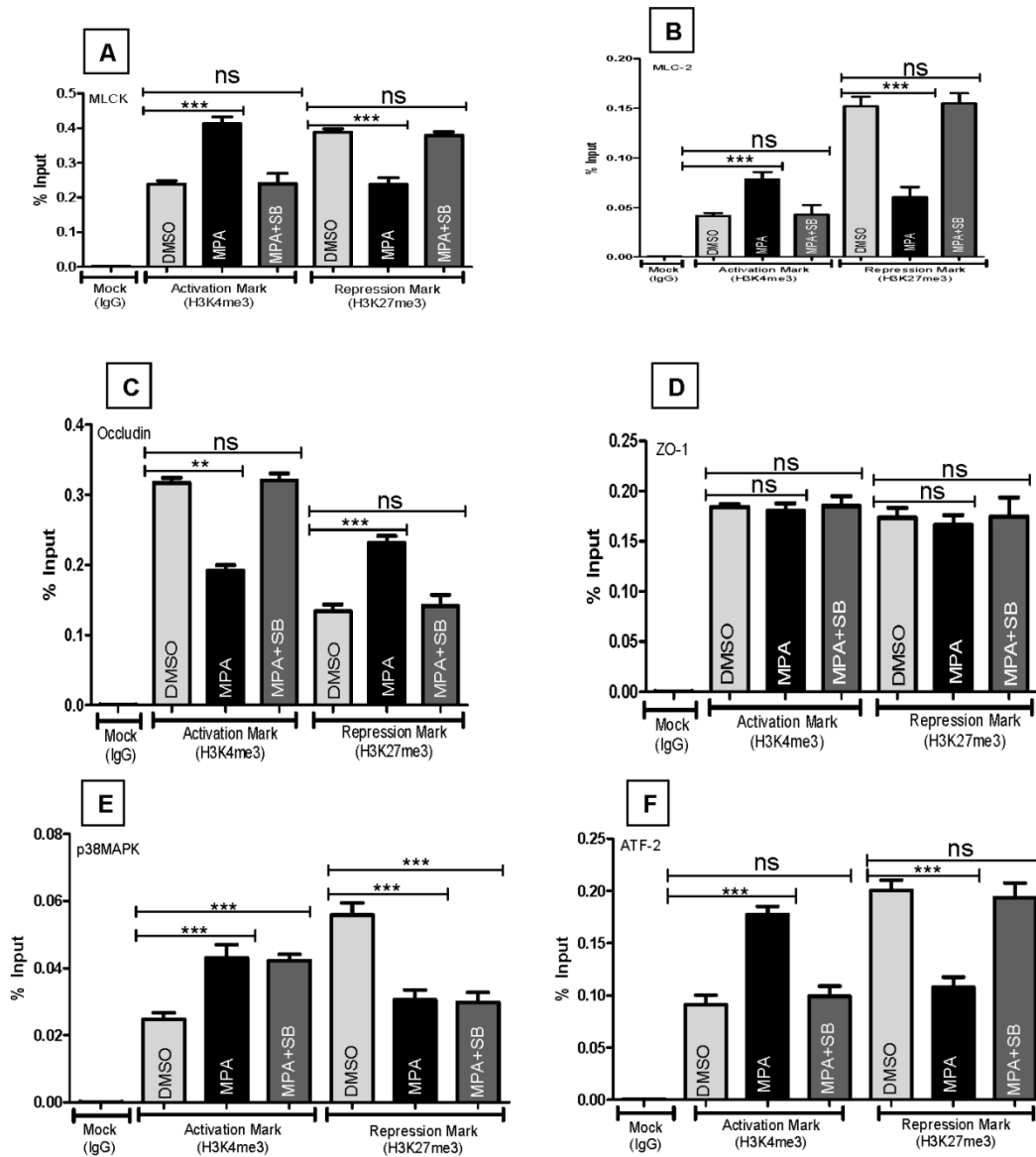


Figure 4.4: Inhibition of p38MAPK counteracts MPA-mediated epigenetic remodeling. Effect of SB203580 on promoter activity of p38MAPK mediated MLCK/MLC-2 pathways and TJs genes in MPA-treated Caco-2 Cells. (A – F) Bar graphs showing the epigenetic status at the promoter regions of MLCK, MLC-2, occludin, ZO-1, p38MAPK and ATF-2 genes in either presence or absence of p38MAPK inhibitor. The ChIP-qPCR data was expressed as means \pm SEM. *P < 0.05, **P < 0.01, ***P < 0.001

when compared with control cells. Differences between two groups were analyzed by the two-tailed Student's t-test and of more than two groups by one-way ANOVA with Bonferroni posttest.

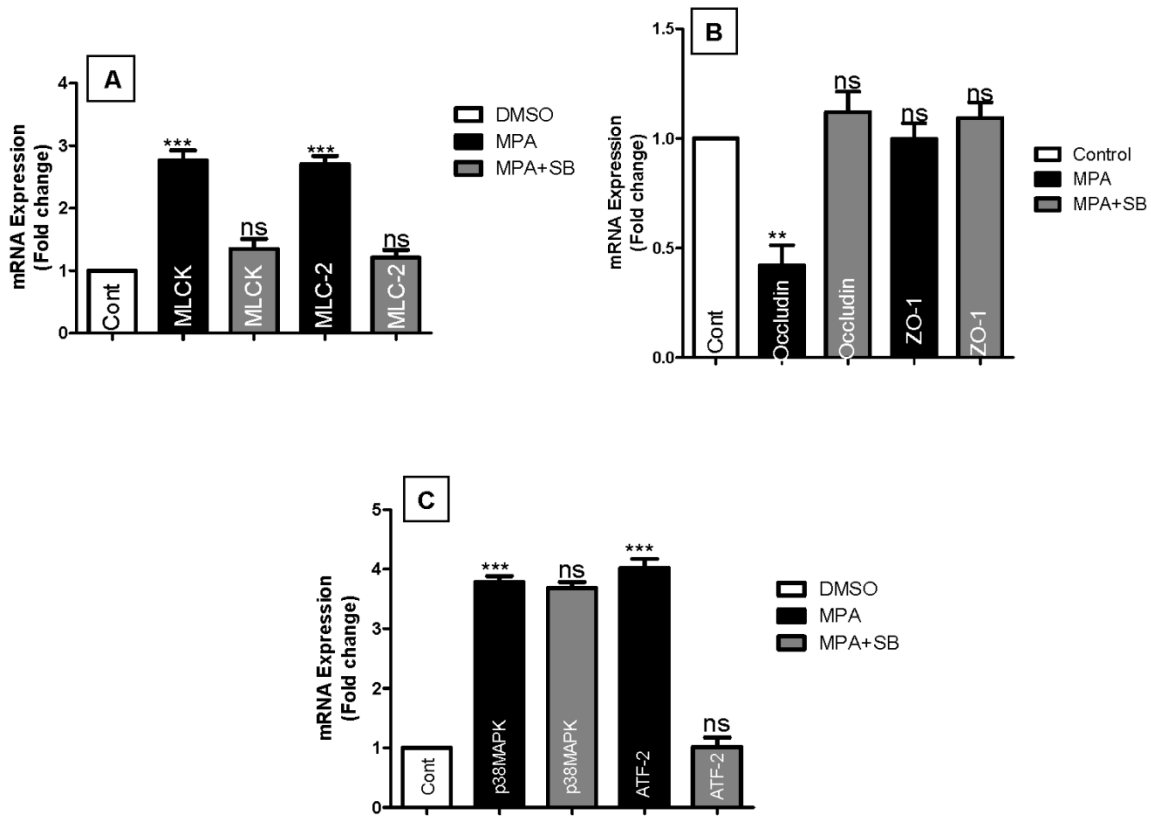


Figure 4.5: p38MAPK inhibition preserves normal MLCK/MLC-2 gene expression in Caco2 cells treated with MPA. Bar graphs showing the mRNA expression levels of MLCK and MLC-2 (A), occludin and ZO-1 (B), and p38MAPK and ATF-2 (C) in either presence or absence of p38MAPK inhibitor. Values are expressed as means \pm SEM. *P < 0.05, **P < 0.01, ***P < 0.001 when compared with control cells. Differences between two groups were analyzed by the two-tailed Student's t-test and of more than two groups by one-way ANOVA with Bonferroni posttest.

4.5 Discussion

Regulation of TJs barrier function, that controls paracellular movement, is a vital and complex process involving complicated intracellular signaling pathways and organization of TJs proteins leading to influence the passage of ions and solutes via paracellular movement across the epithelial monolayer [272;273]. On the basis of initial morphological descriptions, TJs were characterized as a defined structure, both physiologically and morphologically [274]. However, later it was accepted that TJs are a dynamically regulated structure [275;276]. The barrier

function of epithelial monolayer depends upon the continuity of the monolayer and intact TJs [272;277;278]. Intestinal barrier dysfunction through TJs disruption is characterized by increased paracellular permeability along with altered expression and organization of TJs proteins [242;279]. Subsequently, other investigators and we have reported MLCK activation, which directly leads to the phosphorylation of MLC-2, as a common final pathway of acute TJs regulation in response to a broad range of physiological or pathophysiological stimuli [253;280;281]. Phosphorylation of MLC-2 through activated MLCK alone is sufficient to increase TJs permeability, which is associated with redistribution of ZO-1 and occludin [21]. Previously, we have shown that therapeutic dose of MPA caused the increased permeability of Caco-2 monolayer, and this outcome is accompanied by increased activity of *MLCK/MLC-2 pathway* [253]. In this context, it is interesting to note that proinflammatory cytokine (IL-1 β) induced increase in intestinal TJs permeability in both *in vitro* and *in vivo* models is mediated through *p38MAPK/ATF-2*-dependent regulation of *MLCK* activity [255]. In this study, we wanted to extend our previous knowledge of TJs regulation via MLCK pathway in response to MPA. Our data highlight that MPA alters the chromatin structure leading to deregulated expression of genes implicated in TJs function. We identified that p38MAPK and ATF-2 pathway is activated in MPA treated Caco2 monolayer and this pathway was found regulate the MLCK/MLC-2 activity. Interestingly, pharmacological inhibition of p38MAPK counteracted the altered gene expression of MLCK/MLC-2 and thereby maintained the normal function of TJs. Chromatin structure is modulated by the well-known documented posttranslational modification of histone proteins [282]. More than 100 different types of posttranslational modifications that include; acetylation, methylation, phosphorylation and ubiquitination can occur to the amino-terminal tails of histones, which form the nucleosomes of chromatin [283;284]. Majority of these modifications remain poorly understood, however, considerable progress has been made in the understanding of lysine acetylation and methylation of histones in recent years. Lysine acetylation is mostly correlated with nucleosome assembly, chromatin accessibility and transcriptional activity, whereas lysine methylation effects depend upon the modified residue [284]. Acetylated H3K9 [285] and H4K8 are well-known epigenetic markers that are present at the promoter regions of transcriptionally active genes [286]. Their levels are strongly correlated with the gene expression therefore referred as “transcription-linked” histone marks [286;287]. Our global histone acetylation analysis showed significant increase in acetylation at H3K9 and

H4K8. This global chromatin change observed after MPA treatment is in agreement with a recent report showing that MPA treatment induces global H3/H4 acetylation in CD4(+)T cells to exert therapeutic effects in systemic lupus erythematosus patients [268]. In this context, it is interesting to note that hydroxamic acid derivatives of MPA were shown to function as histone deacetylase (HDAC) inhibitors [288]. Owing to these evidences, it is interesting to speculate that MPA might exert its therapeutic effect on immune cells not only by blocking IMPDH, but also by acting as epigenetic modifier. And this epigenetic effect might also occur in non-immune cells such as epithelial cells leading to gene expression changes and unwanted phenotypic changes.

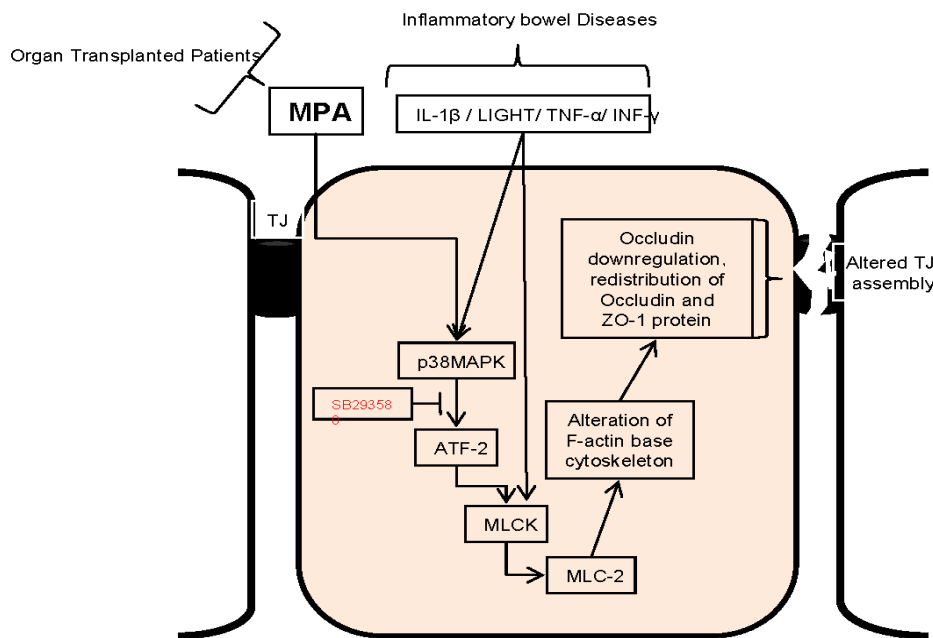
Trimethylation of H3K4 is found at more than 90% of the RNA polymerase II binding regions [289] at the promoter region of protein coding genes and is linked to gene activation, whereas trimethylation of H3K27 is linked to repression of the gene [289;290]. Our ChIP-qPCR data showed significant enrichment of H3K4me3 at the promoter regions of *MLCK* and *MLC-2* genes, enrichment of H3K27me3 at the promoter region of *Occludin*, while no change in H3K4me3 and H3K27me3 levels at *ZO-1* promoter region after MPA treatment. The gene expression analyses at transcriptional and translational level further strengthened the epigenetic activation of *MLCK* and *MLC-2* genes and repression of *occludin* gene. Interestingly, Inhibition of p38MAPK with SB prevented the MPA mediated epigenetic changes as well as the gene expression pattern. Presence of SB together with MPA, significantly but not completely reduced the MPA induced TJs permeability, suggesting role for additional signaling pathways/proteins in TJs deregulation in MPA-treated Caco-2 cells. In view of current data, it would be interesting to check whether p38MAPK conditional knockout mice could alleviate or completely block the MPA-mediated TJs dysfunction. Therefore, a more detailed analysis of TJs proteins regulation as well as their regulating pathway(s) is necessary to understand the mechanism of leak flux diarrhea in *in vitro* model that is comparable to *in vivo* model of MPA therapy.

4.6 Conclusions

In summary, this study provides new insights and an essential understanding into the mechanisms of MPA-mediated decrease in intestinal epithelial barrier function. Our data pointed out epigenetic activation of *p38MAPK*, *ATF-2*, *MLCK* and *MLC-2* genes whereas repression of *occludin* gene at promoter level (Fig. 4.6). To the best of our knowledge, this is the first *in vitro*

experimental study that provides direct evidence to indicate the role of chromatin remodeling in the p38MAPK-dependent MLCK pathway activation in response to MPA exposure. From these results, it can be hypothesized that comparable barrier function modulations may occur in the patients under MPA therapy leading to GI tract complication in some organ transplanted patients.

Figure 4.6: Proposed mechanism of MPA-induced TJs assembly deregulation in Caco-2 cells monolayer. Proinflammatory cytokines (observed in IBD) activates directly or through p38MAPK the MLCK pathway which leads to the altered TJs proteins contents and composition in TJs assembly, resulting compromised epithelial barrier function. This compromised barrier function contributes to leaky style



diarrhea in IBD patients.

Identification of altered chromatin structure at p38MAPK, ATF-2, MLCK and MLC-2 promoter regions after MPA treatment allow us to assume that MPA either directly or through unknown mediators activates the p38MAPK cascade.

Activation of the p38MAPK-dependent MLCK/MLC-2 pathway consequently reorganizes F-actin base cytoskeleton, redistribute ZO-1 and occludin proteins of TJs assembly, resulting in increased permeability of Caco-2 monolayer. Abbreviations: MPA- mycophenolic acid, p38MAPK- p38 mitogen activated protein kinase, ATF-2- activating transcription factor-2, MLCK- myosin light chain kinase, MLC-2- myosin light chain-2, TJs- tight junctions, ZO-1- Zonula Occludins, IL-1β- Interleukin-1 beta, TNF-α- Tumor necrosis factor-alpha, INF-γ- Interferon-γ, IMPDH-2- Inosine-5'-monophosphate dehydrogenase 2.

4.7 Competing Interests

The authors declare that they have no competing interests.

4.8 Author's contribution

NK and ARA conceived the study. NK, QM and DVKP performed and analyze the data. NK, DVKP, LB and ARA participated in interpretation and drafting the manuscript. DVKP and ARA supervised the study. All authors read and approved the final manuscript.

4.9 Acknowledgments

The authors acknowledge the support by the German Research Foundation (DFG) and the Open Access Publication Fund of the University of Göttingen. Niamat Khan is the recipient of a German Academic Exchange Service (DAAD) and Higher Education Commission (HEC) of Pakistan Award.

5 Active and repressive chromatin associated proteome after MPA treatment and the role of midkine in epithelial monolayer permeability

Niamat Khan^{1,2}, Christof Lenz^{1,3}, Lutz Binder¹, D.V. Krishna Pantakani¹, Abdul R. Asif^{1§}

¹Institute for Clinical Chemistry/UMG-Laboratories, University Medical Center, Robert-Koch-Str. 40, 37075, Goettingen, Germany. ²Department of Biotechnology & Genetic Engineering, Kohat University of Science and Technology, Kohat 26000, KPK, Pakistan. ³Bioanalytical Mass Spectrometry, Max Planck Institute for Biophysical Chemistry, Am Fassberg 11, 37077 Göttingen, Germany.

§ Corresponding Author

5.1 Abstract

Mycophenolic acid (MPA) is prescribed to maintain allograft in organ-transplanted patients. However, gastrointestinal (GI) complications, particularly diarrhea, are frequently observed as side effect following MPA therapy. We recently reported that MPA altered tight junctions (TJs) mediated barrier function in a Caco-2 cells monolayer model system. This study investigates whether MPA induces epigenetic changes which lead to GI complications, especially diarrhea? We employed a ChIP-O-Proteomics approach to identify proteins associated with active (H3K4me3) as well as repressive (H3K27me3) chromatin histone modifications in MPA-treated cells, and characterized the role of midkine, a H3K4me3-associated protein, in the context of epithelial monolayer permeability. We identified a total of 333 and 306 proteins associated with active and repressive histone modification marks, respectively. Among them 241 proteins were common both in active and repressive chromatin, 92 proteins were associated exclusively with the active histone modification mark, while 65 proteins remained specific to repressive chromatin. Our results show that 45 proteins which bind to the active and seven proteins which bind to the repressive chromatin region exhibited significantly altered abundance in MPA treated cells as compared to DMSO control cells. A number of novel proteins whose function is not known in bowel barrier regulation were among the identified proteins, including midkine. Our functional integrity assays for Caco-2 cell monolayer showed that inhibition of midkine expression prior to MPA treatment can completely block MPA-mediated increase in barrier

permeability. The ChIP-O-Proteomics approach delivered a number of novel proteins with potential implication in MPA toxicity. In line with this it can be proposed that midkine inhibition could be a potent therapeutic approach to prevent MPA-mediated increase in TJ permeability as well as leak flux diarrhea in organ transplanted patients.

5.2 Introduction

Mycophenolic acid (MPA) is a reversible yet highly selective non-competitive inhibitor of inosine 5'-monophosphate dehydrogenase-2 (IMPDH-2) enzyme. IMPDH-2 is expressed in proliferating immune cells (B & T cells) and is involved in the biosynthesis of guanine nucleotide via *de novo* pathway [1;291]. This inhibitory property led to classify MPA as an immunosuppressant which is prescribed to organ transplant patients to prevent graft rejection [292]. Same as most available immunosuppressants, MPA is associated with gastro intestinal (GI) complications including diarrhea [4]. Hence, more attention is needed either to focus on dose related strategies or to explore mechanisms of action that can help to minimize MPA associated side effects in organ transplant patients.

Drugs may alter the epigenetic status of exposed cells via direct or indirect mechanisms [293]. Hydralazine, which is prescribed to treat hypertension, is known to inhibit DNA methylation in T-cells and to induce autoreactivity as a side effect [294]. While acute exposure of isotretinoin, a drug prescribed to treat severe acne as well as various skin cancers influences the transcriptional activity of transcriptional factor FoxO1. FoxO1 activates the promoter of FoxO1-binding site genes via all-trans-retinoic acid and consequently causes many side effects such as hepatotoxicity, hair loss, bone toxicity, hypertriglyceridemia etc. [293;295]. Recently, it has been reported that MPA downregulates histone deacetylases (HDAC2, HDAC7 & SIRT1) and upregulates histone acetyltransferases (CREBBP & PCAF) in CD4+ T cells isolated from systemic lupus erythematosus patients [296]. Therefore, we hypothesized that epigenetic changes may be involved in the etiology of GI complications observed in organ transplant patients after MPA therapy.

The main objective of this study was to correlate the pathophysiology of GI complications, especially MPA-induced diarrhea in organ transplanted patients, with the altered expression of Chromatin immunoprecipitation-O-Proteomics (ChIP-O-Proteomics) precipitated protein(s). Our ChIP-O-Proteomics results indicate that MPA treatment increases the expression of midkine as

well as its association with H3K4me3-marked chromatin. Functional analysis of differentiated and polarized Caco-2 cells monolayer revealed that midkine inhibitor (iMDK) can significantly inhibit the MPA mediated increase in monolayer permeability.

5.3 Material and Methods

5.3.1 ChIP-O-Proteomics

Caco-2 cells were grown for 13 days post-confluence to establish a monolayer of differentiated and polarized cells resembling enterocytes. Monolayers were incubated with MPA (10 μ M) or DMSO (as a control) for 72 h. ChIP assay was performed as following; Caco-2 cells were fixed with 37% formaldehyde at a final concentration of 1% for 30 min at room temperature (RT) followed by quenching with glycine (0.125M) for an additional 5 min at RT. Cells were collected in ice-cold PBS and equal numbers of cells from each treatment group were lysed with lysis buffer (Red ChIP KitTM, Diagenode). Chromatin was sheared using a Branson Sonifier 250 in shearing buffer according to the manufacturer's instructions (Red ChIP KitTM, Diagenode). After pre-clearing, chromatin from each treatment was divided into three aliquots. An aliquot from each sample was either incubated with active histone mark antibody (anti-H3K4me3; abcam) or repressive histone mark antibody (anti-H3K27me3; Milipore), or with IgG (One Day KitTM, Diagenode) for overnight at 4°C. Antibody-chromatin complexes were further incubated with pre-activated Protein-A magnetic beads, washed and sample was divided into two portions. One portion was treated with proteinase-K to use for a promoter study at DNA level and the other portion was used for the identification of chromatin binding proteins using mass spectrometry.

5.3.1.1 Promoter assay:

DNA-protein cross-linking was reversed by degrading DNA binding proteins with proteinase K. DNA was purified with DNA slurry (One Day KitTM, Diagenode) and quantified by NanoDrop (NanoDrop 2000C, peqlab, Thermo Scientific). ChIP-precipitated genomic DNA was used as a template in a SYBR green (Roche, Mannheim, Germany) based real time PCR reaction. Comparative threshold cycle (CT) method ($2^{-\Delta\Delta CT}$) [297] was used to analyze the real time PCR data and described as fold change. Data was normalized to GAPDH, a housekeeping internal control gene.

5.3.1.2 Proteins purification from chromatin-antibody complexes

Glycine elution method was used to isolate proteins from chromatin-antibody complexes. Briefly, glycine buffer (pH 2.5) was added to each sample for 5 min with agitation at RT. Supernatant was neutralized by adding Tris (pH 8.0). To eliminate interfering substances such as detergents, salts, phenolic acid and nucleic acid, proteins were precipitated overnight by acetone precipitation and the pellets was dried in a SpeedVac concentrator (UNIVAPO 150 H, Germany). Proteins were then reduced with 25 mM Dithiothreitol (DTT), alkylated by adding 100 mM Iodoacetamide (IAA) and subject to in solution trypsin digestion. To stop the trypsin activity each sample was acidified by incubating with 5% Trifluoroacetic acid (TFA) and the supernatant was collected, dried using a SpeedVac, reconstituted in 2% acetonitrile/0.1% formic acid (v:v) and prepared for nanoLC-MS/MS analysis.

5.3.1.3 nanoLC-MS/MS analysis

For mass spectrometric analysis, samples were enriched on a self-packed reversed phase-C18 precolumn (0.15 mm ID x 20 mm, Reprosil-Pur120 C18-AQ 5 μm , Dr. Maisch, Ammerbuch-Entringen, Germany) and separated on an analytical reversed phase-C18 column (0.075 mm ID x 200 mm, Reprosil-Pur 120 C18-AQ, 3 μm , Dr. Maisch) using a 30 min linear gradient of 5-35 % acetonitrile/0.1% formic acid (v:v) at 300 nl min^{-1} . The eluent was analyzed on a Q Exactive hybrid quadrupole/orbitrap mass spectrometer (ThermoFisher Scientific, Dreieich, Germany) equipped with a FlexIon nanoSpray source and operated under Excalibur 2.4 software using a data-dependent acquisition method. Each experimental cycle was of the following form: one full MS scan across the 350-1600 m/z range was acquired at a resolution setting of 70,000 FWHM, and automatic gain control (AGC) target of $1 \cdot 10^6$ and a maximum fill time of 60 ms. Up to the 12 most abundant peptide precursors of charge states 2 to 5 above a $2 \cdot 10^4$ intensity threshold were then sequentially isolated at 2.0 FWHM isolation width, fragmented with nitrogen at a normalized collision energy setting of 25%, and the resulting product ion spectra recorded at a resolution setting of 17,500 FWHM, and AGC target of $2 \cdot 10^5$ and a maximum fill time of 60 ms. Selected precursor m/z values were then excluded for the following 15 s. Two technical replicates per sample were acquired.

5.3.1.4 Data processing

Peak lists were extracted from the raw data using Raw2MSMS software v1.17 (Max Planck Institute for Biochemistry, Martinsried, Germany). Protein identification was achieved using

MASCOT 2.4 software (Matrixscience, London, United Kingdom). Proteins were identified against the UniProtKB *Homo sapiens* reference proteome v2015.02 (20268 protein entries along with a set of 51 contaminants commonly identified in our laboratory). The search was performed with trypsin as enzyme and iodoacetamide as cysteine blocking agent. Up to two missed tryptic cleavages and methionine oxidation as a variable modification were allowed for. Search tolerances were set to 10 ppm for the precursor mass and 0.05 Da for fragment masses, and ESI-QUAD-TOF specified as the instrument type.

Scaffold software version 4.4.1.1 (Proteome Software Inc., Portland, OR) was used to validate MS/MS based peptide and protein identifications. Peptide identifications were accepted if they could be established at greater than 95.0% probability by the Percolator algorithm. Protein probabilities were assigned by the Protein Prophet algorithm [298]. Protein identifications were accepted if they could be established at greater than 99% by the Percolator algorithm and contained at least 2 identified peptides. Protein hits that contained similar peptides and could not be differentiated based on MS/MS analysis alone were grouped to satisfy the principles of parsimony. Proteins sharing significant peptide evidence were grouped into clusters. Proteins were annotated with GO terms from NCBI downloaded on Feb 23, 2015. [299]. Relative quantification of proteins in the samples was achieved by Analysis of Variance (ANOVA) of normalized Spectral Counts using a Benjamini-Hochberg-corrected p value of 0.1 to judge significance. To allow for the calculation of low abundance protein ratios, a value of 3 spectral counts was introduced as a plausible minimum where necessary to avoid division by zero issues.

5.3.2 mRNA Expression Assay:

Caco-2 cells were grown and treated as previously described [64;300]. Briefly, differentiated and polarized Caco-2 cells monolayers were treated with MPA or iMDK+MPA or MPA+iMDK or DMSO (control) for 72 h. Cells were harvested and the total RNA was isolated using the Trizol method. Total RNA was reverse transcribed and the expression of the *midkine* gene was quantified by real time PCR using cyberGreen as the detecting dye.

5.3.3 Cell cytotoxicity assays

Differentiated and polarized monolayers of Caco-2 cells were treated with MPA or iMDK (0-100nM) +MPA or DMSO for 72 h. Following 72 h of treatment, supernatants were collected to

measure the lactate dehydrogenase (LDH) marker using cytotoxicity detection kit (LDH FS, Diagnostics) according to the manufacturer's guidelines. Cells were collected and the trypan blue exclusion test performed to assess cell viability as previously described [64;301;302]

5.3.4 Caco-2 monolayer integrity

Trans epithelial electrical resistance (TEER) and FITC-dextran (FD4) assays were performed as described previously [300] to assess the intactness of the paracellular pathway in the monolayer between adjacent cells. Briefly, differentiated and polarized monolayers of Caco-2 cells were established on transwell insert membranes. Each monolayer was treated with MPA or iMDK+MPA or MPA+iMDK or DMSO (control) for 72 h. TEER values were recorded at several indicated time points. Following 72 h treatment and TEER reading, each monolayer was washed and FD4 dye was added to the apical chamber for 2 h. Samples were collected from basolateral chamber and dye concentrations were measured using a Lambda fluoro 320 fluorescence plate reader (MWG Biotech, Ebersberg, Germany).

5.4 Results and discussion:

We recently reported that MPA treatment increases the expression of the MLCK-MLC2 pathway in Caco-2 cell monolayers [64]. Our subsequent results showed that MPA treatment alters the expression of MLCK-MLC2 by modulating the epigenetic status at their respective promoter regions [300]. To identify the proteins that participate or associate with epigenetic changes occurring at chromatin level during MPA treatment, we undertook a ChIP-O-Proteomics approach (Fig. 5.1 A). Towards this, we first performed ChIP, and the immunoprecipitated sample was aliquoted into two parts prior to separation of DNA and protein complex. One part was analyzed for MLCK promoter epigenetic status (for quality control), while the other part was used for ChIP-O-Proteomics analysis. Traditional ChIP-qPCR revealed that the promoter region of MLCK, in MPA-treated Caco-2 cells, is enriched for H3K4me3 (Fig. 5.1 B & C), further confirming our gene expression data and allowing us to proceed with the ChIP-O-Proteomics approach. Our promoter assay results of MLCK are consistent with these findings [303;304].

We used label free, quantitative spectral counting based ChIP-O-Proteomics approach to identify and quantify the proteins associated with either H3K4me3 (active) or H3K27me3 (repressive)

histone marks. Proteins associated with chromatin regions that represent either active or repressive promoters of protein coding genes were identified by mass spec using the following criteria {protein threshold = 99%, minimum number of peptide = 2, peptide threshold = 95%, false discovery rate = 1% } for protein selection. Analysis of variance (ANOVA) was performed with multiple testing correction (Hochberg-Benjamini-Correction) using Scaffold software to obtain a quantitative profile of proteins identified at $\geq 99\%$ confidence using label free spectral counting. Proteins precipitated by an IgG control were subtracted from the results list. Our ChIP-O-Proteomics approach identified a catalog of proteins at both the active and/or repressive promoter regions. We identified a total of 333 proteins associated with anti-H3K4me3, and 306 proteins associated with anti-H3K27me3 antibodies in MPA-treated cells as well as in DMSO (control) treated cells. Among these proteins, 241 were commonly found at both active and repressive chromatin (Fig. 5.1 D). 92 proteins were found to associate specifically with the active histone modification mark, while 65 proteins remained specific to repressive chromatin (Fig. 5.1 D). A number of proteins (i.e., Cdx-1, TOP2-A, H2AFX, RCC1 & RBBP4 etc.) were previously identified as H3K4me3-associated in mouse embryonic stem cells [305]. Similarly, IL3, HNRPM, 40S ribosomal proteins, 60S ribosomal proteins and LAP2B were identified as H3K4me3-associated proteins in HeLa cells [306]. In addition, however, we report here sets of protein candidates (Supplementary data file 1) that have not been previously associated with active or repressive chromatin marks. This discrepancy with other studies may be due to the specific cell system and enrichment scheme used here. Unlike genomics which is rather constant, proteomics is dynamic in nature [307] differing from cell type to cell type and even within same cells under different environmental conditions.

Next, we analyzed the differential protein complements associated with active and repressive chromatin regions of MPA-treated Caco-2 cells (Fig. 5.1 E & F). Our mass spec data revealed altered enrichment of 45 candidates at active chromatin region and seven candidates at repressive chromatin region in MPA treated Caco-2 cells as compared to DMSO (control) treated cells. (Table 5.1). These differentially enriched proteins are known to be involved in the regulation of transcription, cell cycle, chromatin structure, chromosome segregation and condensation, while their altered expression results in the etiology of certain diseases.

Interestingly, our nanoLC-MS/MS results showed significant increases in spectral counts for midkine protein in MPA-treated cells. This result was further confirmed at the epigenetic and mRNA levels (Fig 5.2 A-D). Midkine is a multifunctional cytokine or growth factor that provokes various biological processes including growth, migration, survival, repair and gene expression [308]. Apart from its normal function, overexpression of midkine is considered to play an important role in the etiology of various diseases such as cancer and inflammatory diseases [309]. Elevated concentrations of circulating midkine have been observed in the serum of Crohn's disease (CD) [310] and ulcerative colitis (UC) [311] patients. Increased TJ permeability via different cytokines is also associated with CD and UC diseases [312]. However, the role of midkine in the regulation of the TJ assembly has not been reported in the context of GI tract complications. To understand whether MPA increases midkine mediated monolayer permeability, we performed midkine inhibitor (iMDK) studies. In order to check any possible cytotoxic effect of iMDK on Caco-2 cell monolayer, the cells were incubated with either MPA alone or in combination with varying concentrations of iMDK and tested for cell viability. These results showed that MPA treatment alone, as well as co-treatment with iMDK (5-25 nM), had no significant cytotoxic effect as compared to control cells (Fig. 5.3 A & B) which were further confirmed by measuring cytotoxicity biomarker, lactate dehydrogenase (LDH). However, higher concentrations of iMDK (≥ 50 nM) caused significant cytotoxicity (Fig. 5.3 A & B). We further evaluated the inhibitory concentration of iMDK to prevent midkine expression in MPA-treated Caco-2 cells. Our results show that MPA mediated increased expression of midkine was prevented in Caco-2 cell monolayers by pretreatment with non-cytotoxic concentration of iMDK (25nM) (Fig. 5.3 C). We assessed the Caco-2 cell monolayer integrity using TEER and FD4-flux assays in different treatment groups; (1) MPA-treated group, (2) iMDK+MPA treated group (iMDK was added 1 h prior to co-incubation with MPA for next 72 h), (3) MPA+iMDK (MPA treatment for 60 h and then followed by co-incubation with iMDK for 12 h) (Fig. 5.2 E). TEER and FD4flux assays are well established parameters which are traditionally used to assess epithelial monolayer integrity [313]. Epithelial monolayer integrity is lost either to cell death or compromised TJ assembly. TJ is a complex but dynamic structure; different types of stimuli increase TJ permeability via different types of cellular signaling pathways in various disease models [312]. In agreement with our previous results, TEER values of MPA-treated confluent Caco-2 cell monolayers significantly dropped in a time-dependent manner as compared to

control monolayer and concomitantly FD4 dye flux concentration increased across the Caco-2 cell monolayer. However, pretreatment with midkine inhibitor (iMDK) significantly blocked MPA mediated decrease TEER values, and increased FD4 dye flux across Caco-2 monolayer (Fig. 5.2 E & F). On the other hand, when iMDK was added at the later stage of MPA treatment, no significant differences were observed compared to MPA treatment alone (Fig. 5.2 E & F). In this study we found midkine in the chromatin fraction; in earlier studies, midkine was found to localize to the nucleus and nucleolus in HepG2 cells and to be involved in the transcription of 45SrRNA gene [314;315].

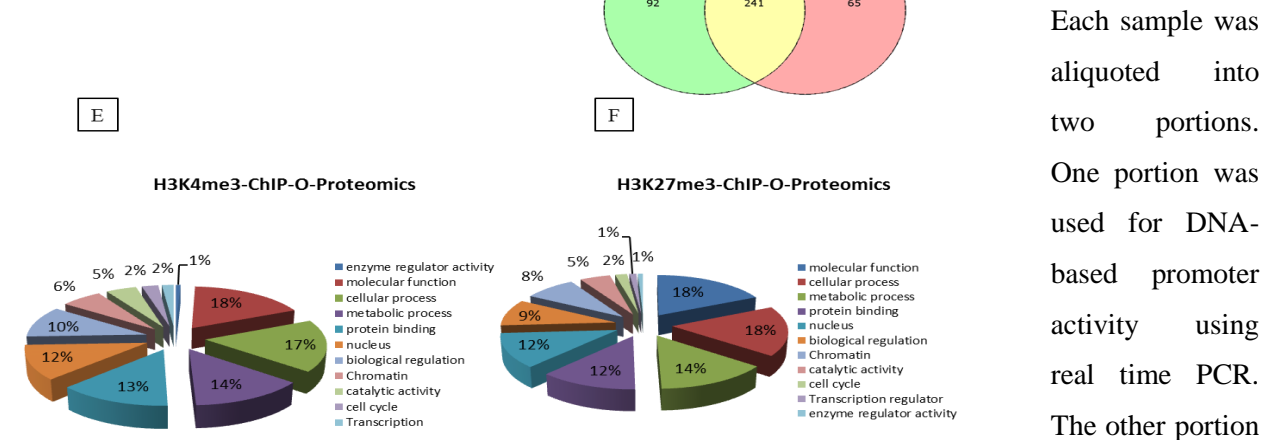
ChIP-o-Proteomics approach is relatively new but effective technique to identify novel chromatin associated targets [316;317]. Using our modified protocol, we could identify number of new proteins associated with the active and repressive chromatin marks. Furthermore, semiquantitative spectral counting approach yielded differential enrichment of 45 candidates at active chromatin region and seven candidates at repressive chromatin region in MPA treated cells as compared to controls. MPA at the used concentration showed no significant cytotoxic effects alone or in combination with midkine inhibitor (iMDK). Inhibition of midkine significantly blocked the MPA mediated epithelial monolayer permeability. These results indicate that combination of immunosuppressive drugs with additional substance like Midkine inhibitor (iMDK) may be helpful to avoid the unwanted effects of immunosuppressive regime. However, further detailed *in vivo* and *in vitro* studies are required to make the immunosuppressive regime safer for the transplanted patients.

Figure 5.1: Schematic overview of ChIP-O-Proteomics experimental steps. (A) Schematic overview of ChIP-O-Proteomics experimental steps. Differentiated and polarized Caco-2 cell monolayers were incubated with MPA or DMSO for 72 hrs. Sheared chromatin having active (H3K4me3) or repressive

histone modification mark (H3K27me3) was precipitated using antibodies, anti-H3K4me3 or anti-H3K27me3 respectively. IgG was used as a background.

Each sample was aliquoted into two portions. One portion was used for DNA-based promoter activity using real time PCR. The other portion

was used to identify and quantify promoter binding proteins using mass spectrometry. Three biological replicates each one with at least two technical replicates were performed for each group. (B & C) ChIP-DNA was subjected to real time PCR with specific primer pair of MLCK promoter region. Each bar represents abundance or depletion of activation mark (H3K4me3) and/or repressive promoter following subtraction of IgG precipitated proteins as background. (E & F). Scaffold analysis of gene ontology (GO) for the ChIP-O-Proteomics identified proteins. (E). H3K4me3 associated proteins and (F) H3K27me3 associated proteins. Pie charts represent the percentages of the identified proteins belong to different function groups.



was used to identify and quantify promoter binding proteins using mass spectrometry. Three biological replicates each one with at least two technical replicates were performed for each group. (B & C) ChIP-DNA was subjected to real time PCR with specific primer pair of MLCK promoter region. Each bar represents abundance or depletion of activation mark (H3K4me3) and/or repressive promoter following subtraction of IgG precipitated proteins as background. (E & F). Scaffold analysis of gene ontology (GO) for the ChIP-O-Proteomics identified proteins. (E). H3K4me3 associated proteins and (F) H3K27me3 associated proteins. Pie charts represent the percentages of the identified proteins belong to different function groups.

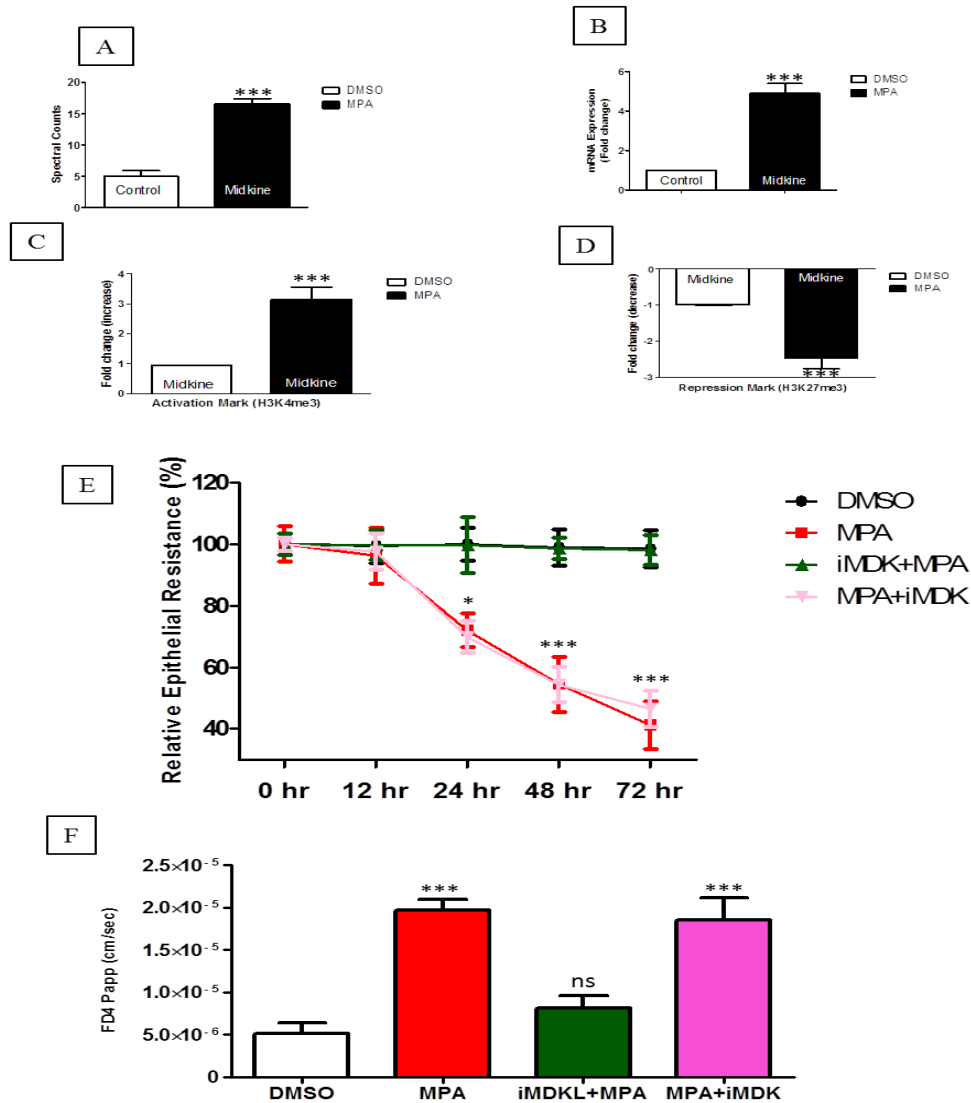


Figure 5.2: Influence of MPA on the expression and activation of midkine gene and Caco-2 cells monolayer integrity. (A-D) Influence of MPA on the expression and activation of midkine gene. (A) Quantification of midkine protein by spectral count after MPA treatment as compared to DMSO (control) cells. Asterisks indicate that the midkine protein was significantly up-regulated after MPA treatment. (B) Expression (mRNA) of midkine gene after MPA-treatment. Expression of mRNA of midkine was investigated using quantitative real time PCR. (C & D) Influence of MPA treatment on the enrichment or depletion of histone active modification mark (H3K4me3) and repressive histone modification mark (H3K27me3) in the promoter of the midkine gene. (E & F) Caco-2 cells monolayer integrity. Caco-2 cells were seeded on the transwell insert membrane. Differentiated and polarized Caco-2 cells were treated as described in material and method. (E) TEER was measured at the indicated times in the graph. (G) Following 72 hrs incubation, FITC-dextran dye (1mg/ml) was added to the apical chamber and dye concentration was measured in the sample collected from basal chamber. TEER and FITC-dextran assay results obtained either in presence or absence of midkine inhibitor (iMDK). Error bars indicate means \pm SEM. *P < 0.05, **P < 0.01, ***P < 0.001. Differences between two groups were analyzed by the two-tailed student's t-test and for more than two groups ANOVA was applied with Bonferroni posttest. (n=3).

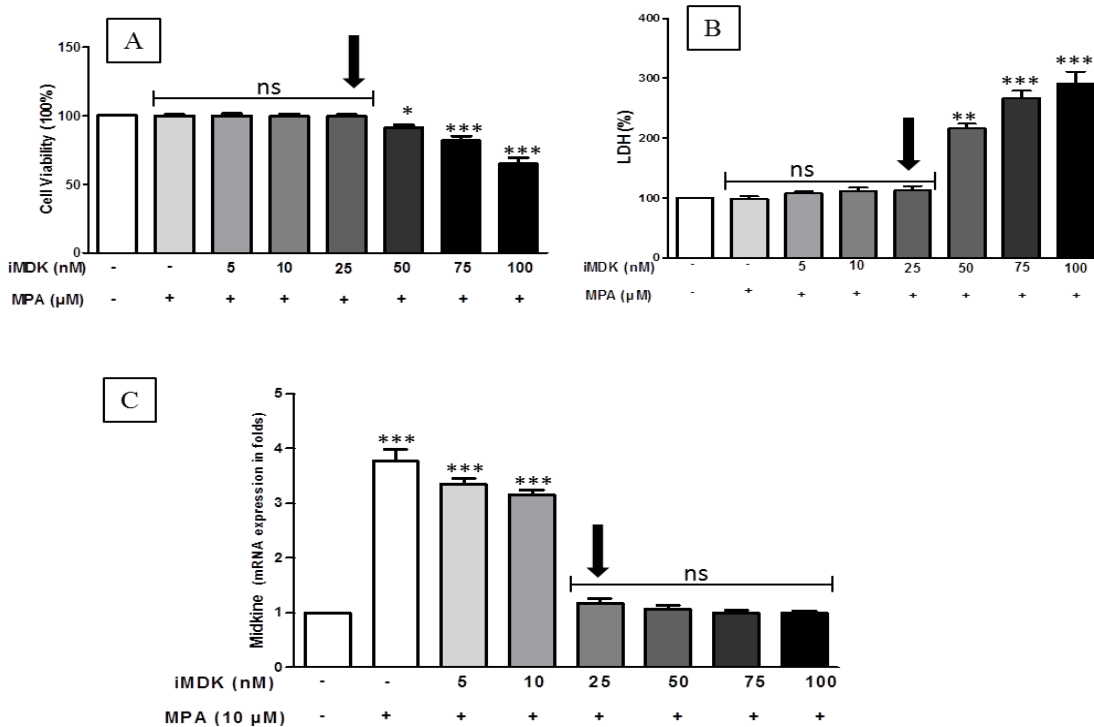


Figure 5.3: Influence of midkine inhibitor (iMDK) on midkine expression and cell viability of MPA-treated Caco-2. (A) Viability of Caco-2 cells {trypan blue dye exclusion assay} after 72 hrs treatment with DMSO (control) and MPA (10μM) alone or in combination with different concentration of iMDK inhibitor (0-100nM). Cell viability was markedly decreased when Caco-2 cells were co-incubated with iMDK (≥ 50 nM) plus MPA (10μM). (B) Cytotoxic effects of midkine inhibitor were assessed by performing LDH leakage assay. Significant leakage of cytotoxic marker (LDH) was found after iMDK (≥ 50 nM) plus MPA (10μM) treatment. (C) Expression of midkine after 72 hrs treatment with DMSO (control), MPA (10μM) alone or in combination with midkine inhibitor (iMDK). iMDK significantly inhibits the expression of midkine gene at the concentration of ≥ 25 nM. Each bar represents separated experiment. Data are presented as means \pm SEM. *P < 0.05, **P < 0.01, ***P < 0.001 compared with the control (DMSO) at that time by ANOVA using a Bonferroni posttest. (n=3)

Table 5.1: Differential proteomic after MPA treatment at histone modifications (H3K4me3 & H3K27me3)

| Supplementary Table | | | | | |
|--|-----------------------------|--|-------------|-------------------------------|---|
| ChIP | Accession No. | Protein Name | Fold change | p-value | Functions (Uniprot) |
| Histone Modification Active Mark (H3K4me3) | Q9UN86 | Ras GTPase-activating protein-binding protein 2 OS | 2.5 ↓ | 0.0067 | mRNA transportation |
| | P63104 | 14-3-3 protein zeta/delta | 1.1 ↑ | 0.0031 | Adaptor protein |
| | P61978 | Heterogeneous nuclear ribonucleoprotein K | 1.4 ↑ | 0.0032 | Transcription activation/repression, hnRNAs metabolism. |
| | P07355 | Annexin A2 | 1.2 ↑ | 0.0011 | Heat response |
| | P68104 | Elongation factor 1-alpha 1 | 1.1 ↑ | 0.0011 | Transcription activity, protein synthesis |
| | Q8IUE6 | Histone H2A type 2-B | 1.2 ↑ | 0.0087 | Chromatin structure |
| | P62258 | 14-3-3 protein epsilon | 1 ↑ | 0.005 | Adaptor protein |
| | P61254 | 60S ribosomal protein L26 | 1 ↑ | 0.0078 | |
| | Q01844 | RNA-binding protein EWS | 1.1 ↑ | 0.003 | Repressor |
| | P68431 | Histone H3.1 | 1.4 ↑ | 0.0011 | Chromatin structure |
| | P16402 | Histone H1.3 | 1.1 ↑ | 0.00019 | Chromatin structure, regulator of individual gene transcription. |
| | P62249 | 40S ribosomal protein S16 | 1.25 ↓ | 0.0042 | |
| | Q15691 | Microtubule-associated protein RP/EB family member 1 | 1.1 ↓ | 0.0046 | Microtubule base cytoskeleton |
| | Q13242 | Serine/arginine-rich splicing factor 9 | 1.1 ↑ | 0.00038 | Splicing activity |
| | P37108 | Signal recognition particle 14 kDa protein | 1.0 ↑ | 0.0039 | |
| | Q96AE4 | Far upstream element-binding protein 1 | 1.4 ↑ | 0.0063 | Transcriptional activity |
| | P24534 | Elongation factor 1-beta | 1.3 ↑ | 0.0015 | Exchanging EF-1alpha bound GDP to GTP |
| | Q12906 | Interleukin enhancer-binding factor 3 | 1.5 ↑ | 0.00042 | Gene regulation, protein synthesis |
| | P10599 | Thioredoxin | 1.1 ↑ | 0.00048 | Transcription activity, redox reaction |
| | P62081 | 40S ribosomal protein S7 | 1.3 ↑ | 0.0071 | rRNA maturation |
| | P62851 | 40S ribosomal protein S25 | 0.9 ↓ | 0.0006 | |
| | Q12874 | Splicing factor 3A subunit 3 | 1.3 ↑ | 0.0058 | Subunit of A & E complex |
| | P62857 | 40S ribosomal protein S28 | 1.1 ↓ | 0.0043 | |
| | P09234 | U1 small nuclear ribonucleoprotein C | 1.1 ↑ | 0.0054 | Splicing activity |
| | Q14157 | Ubiquitin-associated protein 2-like | 1.3 ↑ | 0.00014 | ubiquitin-proteasome pathway, growth and migration of prostate cancer cells |
| | P25398 | 40S ribosomal protein S12 | 1.25 ↓ | 0.0082 | |
| | Q99459 | Cell division cycle 5-like protein | 1.6 ↑ | 0.0032 | Cell cycle regulator, transcription activity |
| | Q95793 | Double-stranded RNA-binding protein Staufien homolog 1 | 1.5 ↑ | 0.0028 | Cross linking cytoskeleton, RNA component, translation |
| | P62424 | 60S ribosomal protein L7a | 1.3 ↑ | 0.0074 | |
| | Q92522 | Histone H1x | 1.7 ↑ | 0.008 | Chromatin condensation |
| | Q71U19 | Histone H2A.V | 1.2 ↑ | 0.0017 | Chromosome segregation, cell division |
| | Q9NYL4 | Peptidyl-prolyl cis-trans isomerase FKBP11 | 1.11 ↓ | 0.0065 | Protein folding |
| | P12277 | Creatine kinase B-type | 1.4 ↑ | 0.00220.0096 | Energy transduction |
| | P14866 | Heterogeneous nuclear ribonucleoprotein L | 1.8 ↑ | 0.0022 | Splicing activity, regulator of exon inclusion. |
| | P02545 | Prelamin-A/C | 1.7 ↑ | 0.0022 | Nuclear lamina, chromatin organization, telomere dynamics |
| | P20700 | Lamin-B1 | 1.8 ↑ | 0.002 | Nuclear lamina, chromatin organization, telomere dynamics |
| | P23528 | Cofilin-1 | 1.4 ↑ | 0.0016 | Cell morphology, cytoskeletal organization. |
| | Q13813 | Spectrin alpha chain, non-erythrocytic 1 | 5.5 ↑ | 0.0038 | Cytoskeleton |
| | P21796 | Voltage-dependent anion-selective channel protein 1 | 1.9 ↑ | 0.0046 | Cell volume, apoptosis |
| | Q15365 | Poly(rC)-binding protein 1 | 1.8 ↑ | 0.0029 | Nucleic acid binding protein |
| P53999 | Activated RNA polymerase II | 2.1 ↑ | 0.006 | Stabilizing the multiproteins | |

| | | | | | |
|--|---------------|--|--------------|----------------|---|
| | | transcriptional coactivator p15 | | | transcription complex |
| | P09327 | Villin-1 | 2.5 ↑ | 0.005 | Cell morphology, division, migration and apoptosis |
| | P21741 | Midkine | 3.8 ↑ | 0.00010 | Growth factor, activator of PI3K, MAPK pathways |
| | Q15366 | Poly(rC)-binding protein 2 | 2.2 ↑ | 0.0093 | Nucleic acid binding protein, adaptor & regulator protein, |
| | P61586 | Transforming protein RhoA | 3 ↑ | 0.0071 | Signal transduction pathway, activator, cell migration |
| Histone Modification Repressive Mark (H3K27me3) | Q06830 | Peroxiredoxin-1 | 1.67 ↓ | 0.00094 | Redox regulation |
| | P13639 | Elongation factor 2 | 1.67 ↓ | 0.00010 | ribosomal translocation |
| | P12956 | X-ray repair cross-complementing protein 6 | 5 ↓ | 0.00098 | Helicase activity, chromosome translocation, negative transcription regulators, |
| | Q9ULV4 | Coronin-1C | 3.33 ↓ | 0.00044 | cytokinesis, motility, and signal transduction |
| | P14174 | Macrophage migration inhibitory factor | 1.25 ↓ | .00058 | Pro inflammatory cytokines |
| | P10599 | Thioredoxin | 1.1 ↑ | 0.00010 | Redox reactions, DNA binding activity |
| | Q9NX24 | H/ACA ribonucleoprotein complex subunit 2 | 4.3 ↑ | 0.00010 | Ribosome biogenesis, telomere maintenance |

Note: Arrows indicate "↑" upregulation and "↓" downregulation of the respective proteins after MPA treatment as compared with DMSO (control in fold change).

5.5 Conflict of Interest

The authors declare that they have no competing interests.

5.6 Acknowledgement

The authors acknowledge the support by the German Research Foundation (DFG) and the Open Access Publication Fund of the University of Göttingen. Niamat Khan is the recipient of PhD scholarship from German Academic Exchange Service (DAAD) and Higher Education Commission (HEC) of Pakistan. The authors would like to thank Susane Goldmann and Lisa Neuenroth for their expert technical assistance with the nanoLC-MS/MS analysis.

6 MPA modulates tight junctions' permeability via midkine/PI3K pathway in Caco-2 cells: A possible mechanism of leak-flux diarrhea in organ transplanted patients

Niamat Khan^{1,2}, , Lutz Binder¹, D.V. Krishna Pantakani¹, Abdul R. Asif^{1§}

¹Institute for Clinical Chemistry/UMG-Laboratories, University Medical Center, Robert-Koch-Str. 40, 37075, Goettingen, Germany. ²Department of Biotechnology & Genetic Engineering, Kohat University of Science and Technology, Kohat 26000, KPK, Pakistan.

§ Corresponding Author

6.1 Abstract

Immunosuppressant mycophenolic acid (MPA) is prescribed to prevent allograft rejection in organ transplanted patients. However, its use is sporadically linked to the leak flux diarrhea and other gastrointestinal (GI) disturbances in around 75% of patients through yet unknown mechanism(s). Recently, we identified midkine as the modulator of tight junctions (TJs) permeability in MPA treated Caco-2 monolayer. In the present study, we explored the possible involvement of midkine dependent PI3K pathway in alteration of TJs under MPA treatment. Caco-2 cells were grown as monolayer to develop the TJs and were treated for 72 hours with MPA alone or midkine inhibitor (iMDK) + MPA or PI3K inhibitors (LY/AMG) + MPA or DMSO as control. Caco-2 monolayer integrity was assessed by trans epithelial electrical resistance (TEER) and FITC-dextran assays. The epigenetic status, mRNA and protein expression of selected genes involved in PI3K pathway and TJs regulation were assessed by chromatin immunoprecipitation (ChIP), qRT-PCR, and western blot, respectively. Our functional assays showed that PI3K inhibitors (LY/AMG) can significantly inhibit the compromised TJs integrity of MPA-treated Caco-2 cells monolayer. ChIP analyses showed a significant epigenetic activation of *midkine*, *PI3K*, *Cdx-2*, and *claudin-2* genes and epigenetic repression of *claudin-1* gene after MPA treatment. The MPA-induced epigenetic alterations were further confirmed by mRNA and protein expression assays after MPA treatment. Collectively, our data show that PI3K pathway as the downstream target of midkine which in turn modulates p38MAPK and pAkt signaling to alter TJs permeability in Caco-2 cell monolayers treated with MPA. These

results highlight the possible use of either midkine or PI3K inhibitors as therapeutic agents to prevent MPA induced GI disturbances.

Key words: Epigenetics, Promoter assay, MPA, PI3K, midkine, Akt, inhibition

6.2 Introduction

Organ transplantation is accepted as the end stage treatment of the failure organ. In case of organ transplantation, immunosuppressive drugs (ISDs) are prescribed to lower the body's ability to reduce the rejection of transplanted graft [318]. MPA is an immunosuppressant agent available as mycophenolate mofetil (MMF) and enteric-coated mycophenolate sodium (EC-MPS), which selectively decreases the *de novo* synthesis of guanine nucleotide pool by inhibiting the enzymatic activity of inosine-5'-monophosphate dehydrogenase-2 (IMPDH-2) [319] and halt the proliferation of lymphocytes [320] at S phase.

Almost all available ISDs including MPA are associated with some forms of GI tract complications. These GI complications in organ transplanted patients are initiated by several factors that can be categorized as infection (viral, bacterial, fungal and parasitic infections), biliary tract diseases, diverticular diseases, perforations, pancreatitis, malignancy and mucosal injury and ulceration (prominent diarrhea) (reviewed in [4]). Clinical data show the occurrence of a significant number of drug-induced diarrhea incidences in liver and kidney organ transplanted patients receiving MPA therapy [24;321]. Diarrhea can result dehydration and discomfort in transplanted patients. Although dose reduction may decrease the chance of diarrhea but it might increase the rate of acute graft rejection. To overcome this problem, two possibilities were proposed, in which either to quantitatively assess and compare the overall diarrheogenic potential [13] or to explore the cellular mechanism(s) of diarrhea of MPA. Earlier task is very difficult or impossible because of specific toxic effects of any ISD cannot be dissociated from the potential contribution of other factors such as drug-drug interactions [13]. While later possibility of understanding cellular mechanism(s) is feasible and is also important to completely describe the pathophysiology of ISD-induced diarrhea and to explore potential anti-diarrheal inhibitor(s).

TJs are complex structures at the apical region of adjacent cells of epithelial monolayer that lines GI tract [16]. TJs control paracellular movement of molecules and ions across the monolayer.

Different types of physiological and pathophysiological stimuli deregulate several pathways such as; PKC [322;323], PI3K [17], MLCK [18], Rho/ROCK [19] and p38MAPK [313;323], which are involved in TJs regulation. Altered regulation of these pathways can lead to the alteration in TJs proteins expression and/or distribution resulting in altered TJ assembly and/or increased permeability [20] and consequently causes diarrhea [21]. Previously, we have reported that the inhibition of p38MAPK pathway in MPA treated Caco-2 cells results in partial prevention of increased TJ permeability [324]. Subsequently, we identified the increased expression of midkine protein in MPA-treated Caco-2 cells and that the inhibition of midkine could completely prevent MPA-mediated TJ permeability [325]. Midkine is a growth factor implicated in the etiology of inflammatory background diseases [326]. In HepG2 cells, midkine was found to exclusively localized to the nucleus as well as nucleolus [327] and involved in the transcription of 45 rRNA gene [314]. In disease model study, midkine was observed to drive lung cancer through activation of PI3K pathway [328]. Midkine also promotes growth, proliferation and self-renewal of embryonic stems (ESCs) via PI3K pathway that show relationship between ESCs and cancer [329]. Interleukin-6 (IL-6) is known to increase TJ permeability via PI3K pathway in inflammatory bowel diseases [17]. Based on above evidences, we hypothesized that MPA may alter the TJ assembly leading to increased permeability of epithelial cells via midkine mediated PI3K pathway, that in turn leads to diarrhea in organ transplanted patients.

To test the above hypothesis, we analyzed the PI3K pathway in MPA treated Caco-2 cell monolayer and found PI3K as the missing link between midkine and MLCK/MLC-2 and p38MAPK pathways in deregulation of TJs in MPA treated cells.

6.3 Material and Methods

6.3.1 Cell Culture

Human colon adenocarcinoma (Caco-2) cells were purchased from DSMZ (German collection of microorganisms and cell culture, Braunschweig, Germany) and grown in culture flasks at 37°C with 5% CO₂ and 95% humidity in DMEM medium supplemented with 10% FBS, 1% Penicillin/Streptomycin and 1% non-essential amino acids. All experiments were performed with Caco-2 cells (Passages No. 15-25). Caco-2 cells are intestinal epithelial cells line that form differentiated and polarized confluent monolayer. This cells line has been regularly used to study the barrier function, drugs transportation across the monolayer and pathophysiology of

epithelium [330]. Confluent monolayer were obtained within 3-5 days (d) when cultured with cell seeding density (2×10^5 cells/cm²). Post-confluent Caco-2 monolayers were further grown for 13 d prior treatment and medium was changed every other day. In our previous studies, we found that therapeutic concentration of MPA alter TJ assembly in Caco-2 cell monolayer, but did not activate apoptotic pathway to compromise cell viability [331]. Therefore we applied therapeutic concentration of MPA in all experiments for TJ study.

6.3.2 Inhibitory Assays

Stock solutions of midkine inhibitor (iMDK, The Netherland), PI3K inhibitors (AMG-511, ChemieTek, USA) and LY294002, InvivoGen, USA) and p38MAPK inhibitor (SB203580, InvivoGen, USA) were prepared in DMSO. Inhibitor experiments were performed using working concentration of midkine inhibitor iMDK (25nM), PI3K inhibitor AMG-511 (5nM), PI3 inhibitor LY294002 (20 μ M) and p38MAPK inhibitor SB203580 (10 μ M) along with MPA (10 μ M) therapeutic concentration.

6.3.3 Experimental design

Six groups of differentiated and polarized Caco-2 cells monolayers were established and treated with MPA or iMDK+MPA or LY+MPA or AMG+MPA or SB+MPA or DMSO (control) for 72 h. Following 72 h of treatment, epigenetic, expression and immuno-fluorescence experiments were performed according established protocols.

6.3.4 Cell cytotoxicity assays

Cell viability assay of each group was performed using trypan blue dye exclusion assay as previously reported [302]. Cell viability results were further confirmed by measuring cytotoxic marker Lactate Dehydrogenase (LDH) using cytotoxicity detection kit (LDH FS, Diaysys) and by following manufacturer's instruction. Results were presented as percentage and all values were normalized to control value of 100%.

6.3.5 Caco-2 cells monolayer integrity

Following 72 h treatments, intactness of Caco-2 cells monolayer of each group was assessed through the commonly available TEER and FITC-dextran assays as previously described [324].

6.3.6 Primer Design:

Transcriptional Regulatory Element Database (TRED) was browsed to retrieve the promoter region sequences of the genes described in this study. Promoter based primers were designed by Primer3 (v. 0.4.0) and their specificity were confirmed by comparing with human genome in Human BLAT Search.

6.3.7 Expression Assay:

Total RNAs were isolated from Caco-2 cells of each group using Trizol method as previously described [324]. For gene expression analysis, one microgram RNA from each group was reversed transcribed into cDNA using cDNA kit (28025-013, Invitrogen, USA) and real time PCR (Light Cycler® 480, Roche, Manheim, Germany).

The mRNA amount of the gene of interests in each sample was normalized to GAPDH serving as housekeeping gene, which were amplified in parallel reaction as an internal control. Data was analyzed by comparative Ct method ($2^{-\Delta\Delta CT}$) and described as fold change between different groups [297;332].

6.3.8 Western blot

Immunoblot analyses were performed as previously described [324]. Briefly, whole cells lysate of each group was prepared using lysis buffer. Twenty microgram of total proteins were separated by 12.5% SDS-PAGE and transferred onto PVDF membrane (Immobilon, Millipore, MA, USA) using Trans-Blot SD cell system (Bio-rad, Munich, Germany). After blocking with 5% milk, membranes were probed with primary antibody (2 µg/ml anti-claudin-1 (mouse monoclonal (Invitrogen, Camarillo, CA, USA)); 3 µg/ml anti-claudin-2 (rabbit polyclonal (Novex, Life Technologies, Frderick, MD, USA)), 1:1000 AKT (Cell Signaling) and 1: 1000 pAKT (p473AKT, Cell Signaling) in 5% BSA in TBS-T overnight at 4°C. β-actin (Sigma, Mannheim, Germany) (1:5000) was used as a loading control. Following overnight incubation with primary antibodies, membranes were washed and again incubated with appropriate HRP-conjugated secondary antibodies (Bio-Rad, Munich, Germany). Immunoreactive bands were visualized with enhanced chemiluminescence (GE, Buckinghamshire, UK) according to the manufacturer's recommendation. The densities of the specified protein bands between different groups were quantified using ImageJ software, version 1.48/Java (NIH, USA).

6.3.9 ChIP Assay:

ChIP assay was performed as previously described [324]. Briefly, Caco-2 cells were fixed with 37% formaldehyde and untreated formaldehyde was quenched with glycine. Equal number of cells from each treatment group was lysed with cell lysis buffer (Red ChIP KitTM, Diagenode). Chromatin shearing was performed by Branson Sonifier 250 in shearing buffer according to the manufacturer's instructions (Red ChIP KitTM, Diagenode). After pre-clearing the sheared chromatin, chromatin of each treatment was immunoprecipitated with active histone mark antibody (H3K4me3, rabbit polyclonal (abcam, Cambridge, UK)) or repressive histone mark antibody (H3K27me3, (MerckMillipore, Billerica, MA, USA)) overnight at 4°C. In parallel, IgG (One Day KitTM, Diagenode) was used as an experimental negative control and input (1%) was used as a positive control. Antibody-chromatin complexes were washed with 1X ChIP washing buffer (One Day KitTM, Diagenode). DNA-protein cross-linking was reversed by degrading DNA binding proteins with proteinase K. DNA was purified with DNA slurry (One Day KitTM, Diagenode). ChIP-precipitated genomic DNA as a template was amplified by real time PCR (Roche, Mannheim, Germany) in 20 µL SYBR green based reaction (For promoter based primers see details in Table 6.1). Real time PCR data was analyzed by input percent method as previously described [324].

6.3.10 Immunofluorescence microscopy of TJs proteins:

Caco-2 monolayers were established on Lab-TekTM eight chamber slides (Nunc, Naperville, IL, USA) and treated for 72 with MPA or iMDK+MPA or DMSO. Monolayers were immunostained as previously reported [331], but with minor modifications. Briefly, monolayers were carefully rinsed with PBS and fixed with 3.7% formaldehyde for 20 min at room temperature (RT). Monolayers were rinsed with PBS and Triton X-100 (0.2%) was used for permeabilization of the cells within the monolayer, then rinsed with PBS and blocked with 1% bovine serum albumin (BSA) for 30 min at RT. Each monolayer was incubated overnight with anti-claudin-1 (3 µg/ml) and anti-claudin-2 (2 µg/ml) at 4°C. After washing with PBS, each monolayer was incubated with secondary antibodies (anti-rabbit IgG conjugated with Alexa 488 and anti-mouse IgG conjugated with Cy3 dye (Molecular Probes, Eugene, OR, USA) in 1% BSA for one hour at RT in dark. Fluorescence images were acquired using Axiovert 200M confocal microscope (Carl Zeiss, Jena, Germany).

6.3.11 Statistics

Data are presented as means \pm standard error of the mean (SEM) of at least three independent experiments, each with at least in duplication. Graphpad prism 5 (GraphPad, San Diego, CA) was used to analyse the data and to present in graphic form. For multiple comparisons, analysis of variance (ANOVA) and Bonferroni posttests were performed. Values of $P \leq 0.05$ were considered statistically significant. In each figure * $P < 0.05$, ** $P < 0.01$, *** $P < 0.001$.

6.4 Results

6.4.1 MPA induces midkine-dependent epigenetic activation of PI3K, Cdx-2 and Cludin-2 (Cldn-2) genes and repression of claudin-1(Cldn-1) gene.

Different types of cellular signaling pathways (such as PI3K, PKCA, JNK, JunD, RhoA etc) are triggered by various types of infectious agents and cytokines and lead to increased TJs permeability in several disease conditions and model systems [333]. We investigated the influence of MPA treatment on the regulation of these pathways through our epigenetic target approach (promoter assays of the selected genes). Our epigenetic analyses showed that MPA treatment leads to epigenetic activation of PI3K, but not other pathways (Fig. 6.1A and Fig. 6.2 A & B). We analyzed the PI3K promoter epigenetic status by ChIP and identified significant enrichment of transcriptional activation mark (H3K4me3) and concomitant decrease in transcriptional repression mark (H3K27me3) after MPA treatment (Fig. 6.1 A). To confirm these results, we analyzed the PI3K mRNA expression and found it to be upregulated (Fig. 6.1 B). Then, we performed midkine-dependency analysis for PI3K epigenetic activation during MPA treatment and found that the inhibition of midkine results in downregulation of PI3K expression and also the epigenetic silencing marked by increased H3K27me3 levels (Fig. 6.1 A, B). These results confirm that midkine indeed regulate PI3K expression during MPA treatment. To test the role of PI3K pathway in TJs regulation, we employed PI3K inhibitor (LY or AMG) studies in Caco-2 monolayers. The LY is known to be effective at 20 μ M in human epithelial cell lines

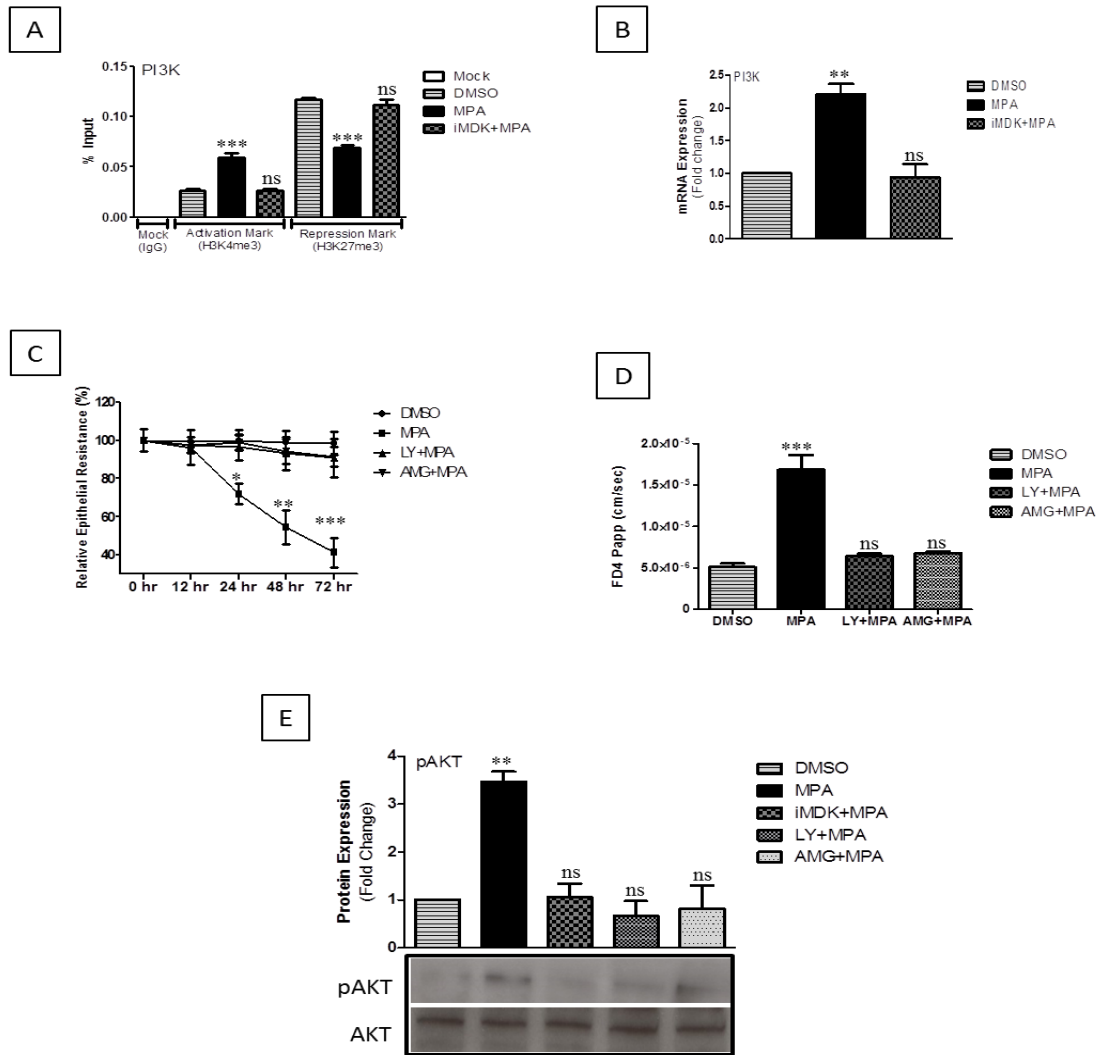


Figure 6.1: Influence of MPA on PI3K/AKT pathway and PI3K/Akt dependent modulation of TJ permeability. (A) Differentiated and polarized monolayer of Caco-2 cells was treated with DMSO, MPA alone or in combination with iMDK for 72 hrs. Following cells fixation and lysis, chromatin was sheared into small fragments and immunoprecipitated with antibodies (anti-H3K4me3, anti-H3K27me3, IgG) followed by real time PCR. The graph represents the ChIP-qPCR data of activation mark (H3K4me3) and repression mark (H3K27me3) at the promoter region of PI3K γ gene in Caco-2 cells monolayer treated with either DMSO or MPA alone or in combination with midkine inhibitor. DMSO treated cells were used as a control. Relative intensity of respective histone modification was measured using % input method. (B) The mRNA expression of *PI3K* gene in Caco-2 cell monolayers treated with either MPA alone or with midkine inhibitor. DMSO treated cells were used as a control. *GAPDH* gene was used as a house keeping gene to normalize the real time PCR data. The data was analyzed by comparative Ct method (Fold Change = $2^{(-\Delta\Delta Ct)}$) and presented as fold change when compared with control (as one fold).

(C) The influence of PI3K pathway inhibition on TJs permeability of confluent Caco-2 monolayer treated with MPA. TEER was measured at various time points (0 h, 12 h, 24 h, 48 h, and 72 h) after MPA addition or in combination with PI3K inhibitors, LY or AMG. Caco-2 monolayers treated with DMSO were used as control. MPA decreases TEER in confluent monolayer of differentiated and polarized Caco-2, while PI3K inhibition (LY or AMG) restores decreased TEER. (D) Paracellular FD4 dye flux assay results of Caco-2 monolayers that were treated with either MPA or in combination with PI3K inhibitors, LY or AMG. (E) Representative Western blot and densitometric analysis of AKT/pAKT in Caco-2 cell monolayers treated with either MPA or midkine inhibitor (iMDK), or PI3K inhibitors (LY or AMG). Inhibition of PI3K pathway attenuates the MPA-induced phosphorylation of AKT rather than total AKT expression in MPA treated cells. Data are shown as means band density of pAKT normalized relative to total AKT expression. (A-D) Statistically significant differences between groups, based on two tailed student's t-test and for more than two groups by one-way ANOVA with Bonferroni posttest for multiple comparisons, are indicated by * $P < 0.05$, ** $P < 0.01$, *** $P < 0.001$. ns = non-significant. Error bars represent \pm SEM (n = 3).

(Caco-2, HT29, MCF10A cells and T84 cells) [334-337], hence used at 20 μ M in this study. Another PI3K inhibitor, AMG, was not tested in Caco-2 cells, hence we firstly established that 5 nM of AMG could be used without compromising the cell viability (Fig. 6.3 A, B). Then we assessed the role of PI3K pathway in TJ integrity using TEER and FD4 dye flux assays. Our results showed that MPA-mediated decreased TEER could be significantly blocked with pre-incubation of both PI3K pathway inhibitors (LY or AMG) in Caco-2 cells monolayers followed by co-incubation with LY+MPA or AMG+MPA (Fig. 6.1 C). Similarly, MPA-mediated FD4 dye flux was significantly blocked across the Caco-2 cell monolayer that was exposed to PI3K inhibitors (LY or AMG) one hour prior to the co-incubation with therapeutic concentration of MPA (Fig. 6.1 D).

Protein kinase B (PKB) or Akt is a serine-threonine kinase that is activated by PI3K transducer and is involved in the regulation of different biological processes including angiogenesis, growth, metabolism, proliferation and cell survival [338]. However cytokines (such as TNF- α , IL-6) increase TJ permeability via PI3K/AKT pathway [17;86]. Hence, we checked for the activated Akt (phosphoAkt/pAkt) by Western blot analysis and found that MPA treatment increases the pAkt levels, which can be counteracted by pre-treatment with either midkine or

PI3K inhibitors (Fig. 6.1 E). Collectively, these results show that midkine activates PI3K/Akt pathway after MPA treatment.

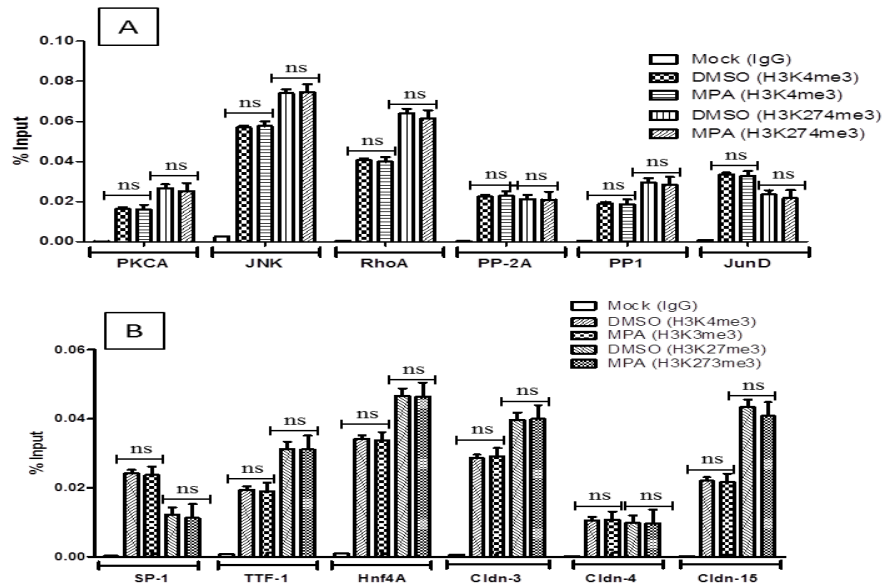


Figure 6.2: Regulatory effect of MPA treatment on the promoter of other genes involved in the regulation of TJ permeability. (A & B) Promoter activity of (*PKCA*, *JNK*, *RhoA*, *PP-2A*, *PP1*, *JunD*, *Sp-1*, *TTF-1*, *Hnf4A*, *Cldn-3*, *-4* & *Cldn-15*) genes: ChIP assay was performed with antibodies specific to the activation mark (H3K4me3) or repression mark (H3K27me3) or IgG, followed by real time PCR analysis. Data was analyzed using % input method to calculate the respective relative intensity of activation or repression mark in the MPA treated cells as compared to control cells. Differences between groups were analyzed by ANOVA with Bonferroni posttest. The values were expressed as means \pm SEM. * $P < 0.05$, ** $P < 0.01$, *** $P < 0.001$ when compared with control cells. ns = non-significant. (n = 3)

6.4.2 MPA activates *Cdx-2* expression via midkine/PI3K pathway.

Cdx-2 is a transcription factor involved in the regulation of early differentiation and maintenance of intestinal epithelial cells [339]. Increased production of IL-6, a cytokine known to increase TJ permeability in IBD [17], is reported to enhance the expression of *Cdx-2* via PI3K pathway that in turn transcriptionally activates *Cldn-2* and consequently increases TJ permeability for cation molecules [17]. Whether MPA modulates *Cdx-2* expression via PI3K pathway in MPA treated Caco-2 cells is not known. To address this question, we performed qRT-PCR analysis and found that *Cdx-2* mRNA levels increase significantly in Caco-2 cells treated with MPA (Fig. 6.4 A). Interestingly, the increased *Cdx-2* expression is prevented by inhibiting either midkine or PI3K

signaling pathways (Fig. 6.4 A). Then, we performed epigenetic analysis of *Cdx-2* promoter region and found that MPA treatment significantly increases H3K4me3 mark and concomitantly decreases H3K27me3 (Fig. 6.4 B), indicating the activation of *Cdx-2* gene. In line with the gene expression data, midkine inhibitor (iMDK) or PI3K inhibitors (LY or AMG) significantly prevented the increased promoter activation of *Cdx-2* gene in MPA-treated cells as compared to control (Fig. 6.4 B). These results can be concluded that *Cdx-2* is epigenetically activated after MPA-treatment via midkine/PI3K pathway.

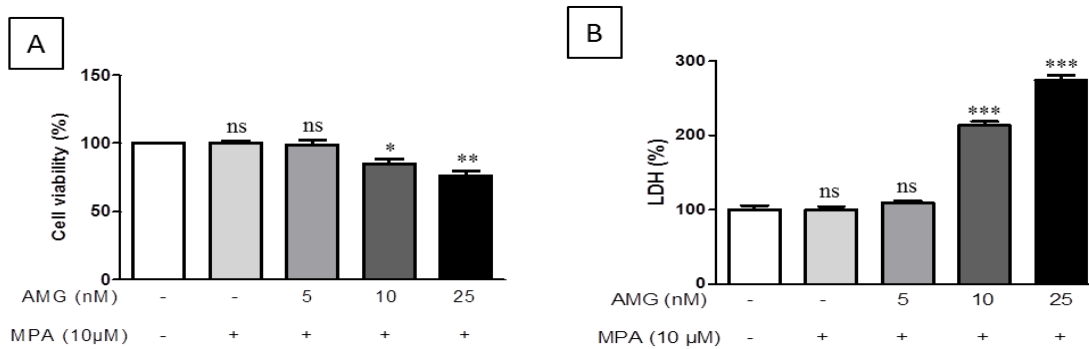


Figure 6.3: Cytotoxic effects of PI3K inhibitor (AMG) in co-treatment with MPA on Caco-2 cells.

(A & B) Caco-2 cells were grown for 13 days post-confluence and treated with MPA or (AMG + MPA) or DMSO for 72 h. Cell viability assay. Cellular viability was measured using trypan blue exclusion assay after 72 h of treatment. Results are expressed as percentage of DMSO control (100%). (A) Cell viability was further confirmed by measuring the LDH release in the culture media in percentage to the DMSO control (100%). (B) Differences between groups were analyzed by ANOVA with Bonferroni posttest. The values were expressed as means \pm SEM. * $P < 0.05$, ** $P < 0.01$, *** $P < 0.001$ when compared with control cells. ns = non-significant. (n = 3)

6.4.3 MPA-mediated altered expression of *Cldn-1* and *Cldn-2* are prevented by midkine or PI3K inhibitors.

Cldn-1 and *Cldn-2* are important components of TJs assembly. *Cldn-1* is also called pore-sealing claudin therefore its expression is inversely proportional to TJs permeability [340;341]. On the other hand, *Cldn-2* is known as pore-forming claudin and its expression is directly proportional to TJs permeability [17;341]. Previous reports showed PI3K dependent downregulation of *Cldn-1* and upregulation of *Cldn-2* that in turn increase TJ permeability in different disease model studies [342-344]. Our expression analysis show that MPA-treatment significantly decreases the

expression of pore-sealing Cldn-1 protein, while increases the expression of Cldn-2 (Fig. 6.5 A, B). However, MPA mediated altered Cldn-1 and Cldn-2 expression was significantly blocked in Caco-2 cells monolayer pre-treated with midkine inhibitor (iMDK) or with PI3K inhibitors (LY or AMG) (Fig. 6.5 A, B). In agreement with the protein expression data, qRT-PCR analysis further confirmed that MPA decreases Cldn-1 mRNA expression while it increases Cldn-2 mRNA expression (Fig. 6.5 C, D). Moreover, the altered claudins expressions could be prevented by pre-treatment of Caco-2 cell monolayers with either midkine or PI3K inhibitors (Fig. 6.5 C). Activation of Cldn-2 and inactivation of Cldn-1 were further confirmed at epigenetic level (Fig. 6.6).

Next, we performed immunostaining to investigate the junctional distribution of Cldn-1 and Cldn-2 in Caco-2 cell monolayer. Immunostaining results showed uniform and continuous pattern of Cldn-1 and Cldn-2 staining at the cell junctions in control cells (Fig. 6.5 E). Intriguingly, MPA-treatment not only resulted in decreased expression of Cldn-1, but also disrupted its distribution (Fig. 6.5 E). On the other hand, MPA treatment increased the expression of Cldn-2 as seen by marked increase in staining however; the pattern of Cldn-2 is disrupted and is accumulated at some regions (Fig. 6.5 E). Caco-2 cell monolayers that were co-treated with midkine inhibitor (iMDK) along with MPA showed restored expression and pattern of distribution that was quite similar to control cells (Fig. 6.5 E).

Taken together, these results indicate that MPA treatment activates midkine/PI3K pathway that in turn alters the expression and distribution of TJs assembly proteins (Cldn-1 and Cldn-2) and consequently increase the permeability.

6.4.4 p38MAPK pathway is activated by Midkine/PI3K signaling in MPA treated Caco-2 cells.

In our previous study, we reported that inhibition of p38MAPK pathway partially prevented MPA mediated increase TJ permeability in Caco-2 cells monolayer [324]. In this study, we investigated at epigenetic level, the cross talk between PI3K and p38MAPK pathways after MPA-treatment. Our results show that MPA significantly activates *p38MAPK* gene at epigenetic level [324]. MPA-mediated epigenetic activation of p38MAPK was significantly blocked in cells that were pre-incubated with midkine inhibitor (iMDK) or PI3K inhibitors (LY or AMG) (Fig. 6.7 A). Similar to epigenetic analysis results, the mRNA expression analysis data confirmed that

inhibition of midkine or PI3K is sufficient to counteract MPA-mediated changes and to restore normal levels of p38MAPK (Fig. 6.7 B).

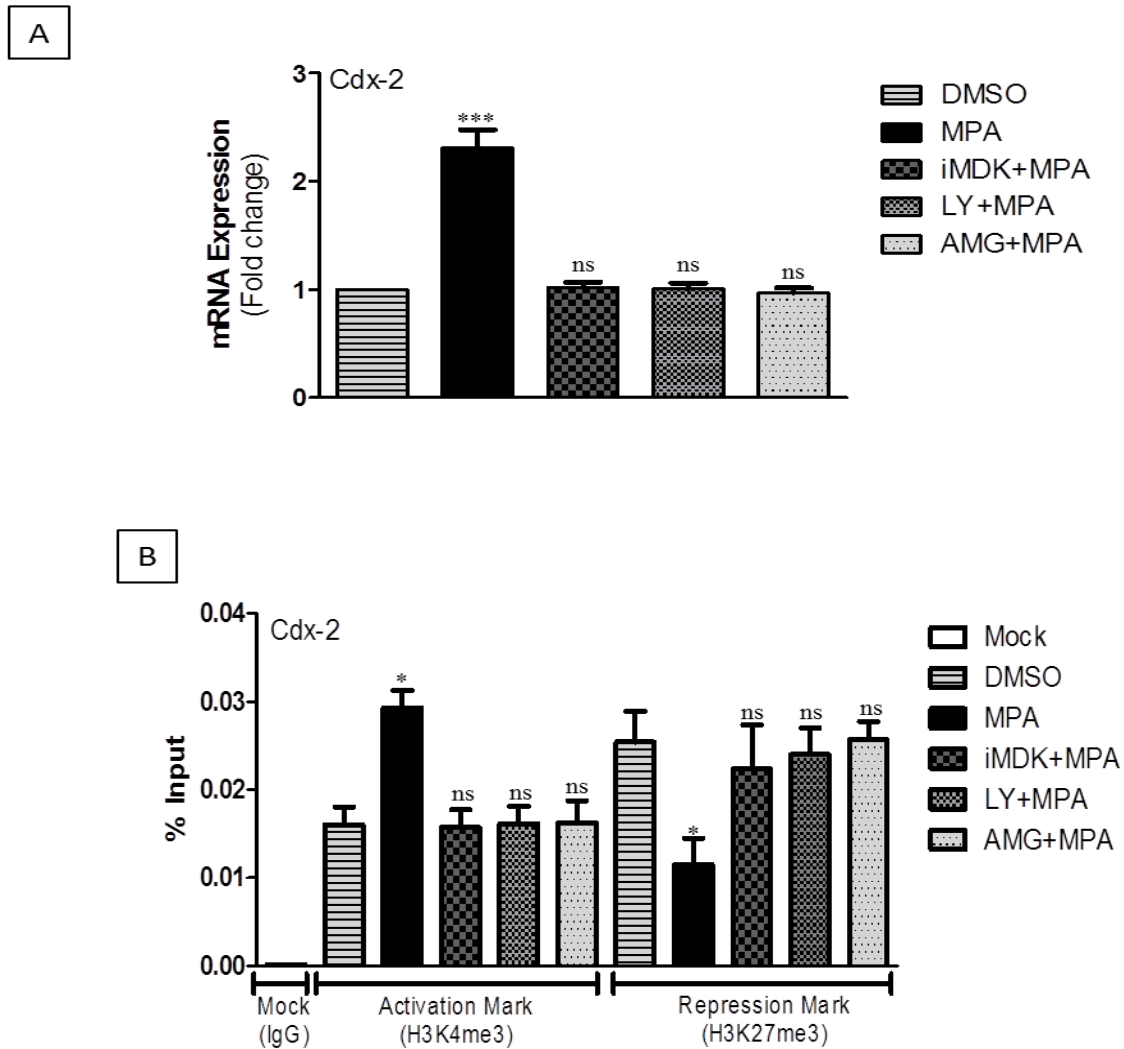


Figure 6.4: Activation of Cdx-2 gene via midkine/PI3K pathway after MPA treatment. (A) qRT-PCR results of Cdx-2 mRNA expression in control (DMSO) and different treatment groups. GAPDH was used as a house keeping gene to normalize the real time PCR data. The data was analyzed by comparative Ct method (Fold Change = $2^{(-\Delta\Delta Ct)}$) and presented as fold change when compared with control (as one fold). (B) The ChIP-qPCR data of activation mark (H3K4me3) and repression mark (H3K27me3) at the promoter region of Cdx-2 in Caco-2 cells monolayer treated with either MPA alone or in different treatment groups. DMSO treated cells were used as a control. Relative intensity of respective histone modifications were measured using % input method. Statistically significant differences between groups, based on two tailed student's t-test and for more than two groups by one-way ANOVA with Bonferroni

posttest for multiple comparisons, are indicated by $*P < 0.05$, $**P < 0.01$, $***P < 0.001$. ns = non-significant. Error bars represent \pm SEM (n = 3).

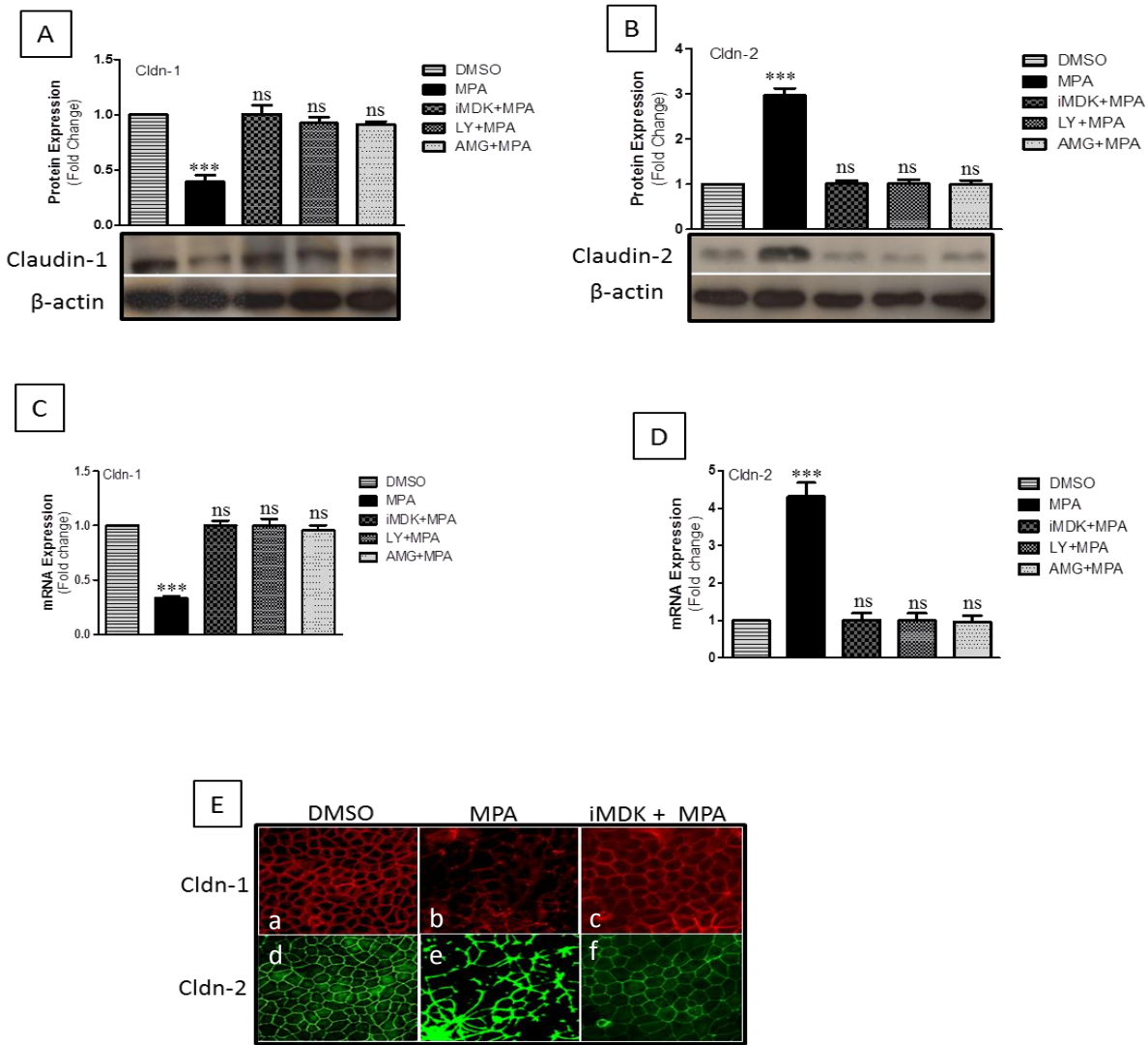


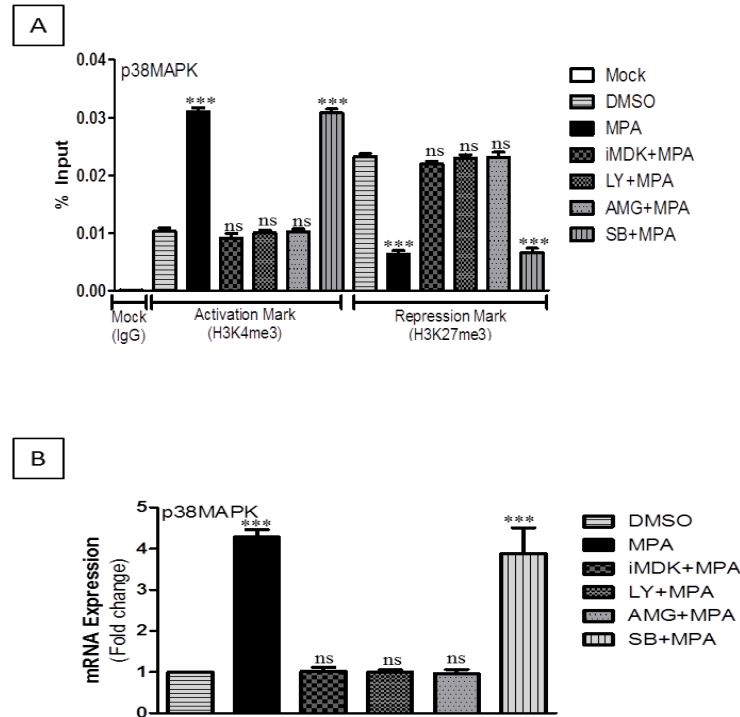
Figure 6.5: Influence of midkine mediated PI3K pathway on TJ structural proteins (claudin-1, -2) in MPA treated Caco-2 cells. (A & B) Western blot analysis of TJ proteins (Claudin-1, -2) in Caco-2 cell monolayers treated with MPA or midkine/PI3K inhibitors (iMDK/LY/AMG). Immunoblots were probed with antibodies against TJ proteins (A) Claudin-1 and (B) Claudin-2. Immunoblotting with β -actin (A & B) was used as a loading control. Densitometric analyses were performed using the Lab image software. (C & D) qRT-PCR analysis of *Claudin-1* and -2 gene expression in Caco-2 cell monolayers treated with MPA or midkine/PI3K inhibitors (iMDK/LY/AMG). GAPDH was used as a house keeping gene to normalize the real time PCR data. The data was analyzed by comparative Ct method (Fold

Change = $2^{(-\Delta\Delta Ct)}$ and presented as fold change when compared with control (as one fold). Differences between groups were analyzed by ANOVA with Bonferroni posttest. The values were expressed as means \pm SEM. * $P < 0.05$, ** $P < 0.01$, *** $P < 0.001$ when compared with control cells. ns = non-significant. (n = 3). (E) Differentiated and polarized monolayer of Caco-2 cells were established eight well chamber slide and treated with either DMSO, MPA alone or in combination with midkine inhibitor iMDK) for 72 hrs. Caco-2 cells monolayers were fixed, permeated and stained for Cldn-1 and Cldn-2. The figure shows the distribution of Cldn-1 and Cldn-2 in cells exposed to DMSO (a & d), or MPA (b & e) or iMDK+MPA (c & f). Secondary antibodies conjugated with either Cy3 (Cldn-1) or Alex Fluor 488 (Cldn-2) were used to stain and detect the corresponding proteins.



Figure 6.6: Promoter activity of claudin-1 and claudin-2 genes. (A & B) ChIP assay was performed with antibodies specific to the activation mark (H3K4me3) or repression mark (H3K27me3) or IgG, followed by real time PCR analysis. Percent input (% Input) method was applied to calculate the respective relative intensity of activation or repression mark in the MPA treated cells alone or in combination [PI3K inhibitors (iMDK/LY/AMG) plus MPA treated cells] as compared to control cells. Differences between two groups were analyzed by the two-tailed Student's t-test and of more than two groups by one-way ANOVA with Bonferroni posttest. The values were expressed as means \pm SEM. * $P < 0.05$, ** $P < 0.01$, *** $P < 0.001$ when compared with control cells. ns = non-significant.

Figure 6.7: Midkine/PI3K dependent activation of p38MAPK pathway after MPA treatment. (A) The ChIP-qPCR data of activation mark (H3K4me3) and repression mark (H3K27me3) at the promoter region of p38MAPK in Caco-2 cell monolayers treated with either MPA alone or in midkine and PI3K



inhibition groups. DMSO treated cells were used as a control. Relative intensity of respective histone modification was measured using % input method. (B) The mRNA expression levels of *p38MAPK* either in presence or absence of PI3K inhibitors in MPA treated Caco-2 cell monolayers as compared to control

cells. Differences between groups were analyzed by ANOVA with Bonferroni posttest. The values were expressed as mean \pm SEM. * $P < 0.05$, ** $P < 0.01$, *** $P < 0.001$ when compared with control cells. ns = non-significant. (n = 3).

6.5 Discussion

Intestinal epithelium is mainly gated by intercellular junctions such as; gap junctions, adheren junctions, desmosome junctions and TJs [341;345]. TJs control paracellular pathway between the adjacent cells [346] and are especially important in preventing translocation of infectious agents and toxins from the lumen into the blood stream [347]. Defects in TJs assembly are key factors associated with IBD and other inflammatory conditions of the gut [348]. In this study, we have characterized the disease-relevant role of midkine dependent PI3K pathway that consequently induces TJs permeability in MPA treated Caco-2 cells monolayer. Midkine, a cytokine or heparin-binding growth factor, plays an important role in the pathogenesis of inflammatory and malignant diseases [349]. The interesting aspect of this study is the midkine dependent activation

of *PI3K*, *Cdx-2*, *Cldn-2*, *p38MAPK* genes and inactivation of *Cldn-1* gene at the epigenetic and at mRNA & protein level in MPA treated Caco-2 cells. Further, we analyzed the effects of midkine or PI3K inhibition in MPA-treated confluent monolayer of Caco-2 cells and found increased TEER and decreased FD4 fluxes, confirming the protective role of PI3K inhibitors (iMDK or LY or AMG) in MPA-treated cells.

To explore the involvement of cell signaling pathway(s), we performed inhibitory assays with PI3K pathway inhibitors (iMDK/LY/AMG) in MPA-treated Caco-2 cells. Recently, we reported that inhibition of midkine significantly blocks MPA-mediated increased TJs permeability in Caco-2 cells (unpublished data, Paper 2 [325]). Midkine is known as the upstream regulator of PI3K pathway [328]. PI3K is a family of enzymes involved in different cellular functions including cell differentiation, growth, proliferation, motility, survival and intracellular trafficking [350]. PI3K is also known to regulate epithelial barrier function via TJs modulation [17]. To confirm whether the PI3K signaling was closely associated with the regulation of TJs in MPA treated Caco-2 cells, we performed epigenetic and gene expression studies. We observed the enrichment of histone activation mark (H3K4me3) and simultaneously depletion of histone repressive mark (H3K27me3) in the promoter of *PI3K* gene in MPA treated Caco-2 cells, which were not shown in the previous studies. A wide range of studies conducted in yeast up to human have shown active and repressive promoter regions are enriched with histone modification H3K4me3 and H3K27me3 respectively. Our results are consistent with the notion that the promoter region of a gene enriched with H3K4me3 is competent for transcription, and promoter region of a gene marked with H3K27me3 is incompetent for transcription [351].

Insulin, cytokines, survival and growth factors are known to phosphorylate AKT through PI3K pathway [17;352;353]. Phosphorylated AKT is able to regulate a large number of downstream targets including transcription factors (reviewed in [354;355]). PI3K/Akt pathway is considered as a target in the therapy of IBDs such as Crohn's Disease [356]. IL-6 induces phosphorylation of AKT through PI3K pathway in Caco-2 cells and increases TJs permeability [17]. To the best of our knowledge this is the first report that shows that midkine up-regulation leads to phosphorylation of AKT via PI3K pathway and consequently alters TJs permeability in MPA-treated Caco-2 cells.

Cdx-2 plays a critical role in the transcriptional regulation of intestinal genes [357]. Cdx-2 increases expression of pore-forming Cldn-2 in TJs assembly resulting elevated cations permeability via IL-6 dependent activation of PI3K/AKT pathway [17]. We observed midkine/PI3K dependent activation of Cdx-2 gene at promoter level and increased expression at mRNA level after MPA treatment.

Dynamic nature of TJs assembly depends upon the claudin family members such as pore-forming and pore-sealing claudins. Altered expression of claudin family members significantly deregulates TJ permeability [358]. Overexpression of pore-sealing claudin was reported to increase the TEER and to strengthen barrier integrity leading to decreased paracellular permeability in epithelial MDCK cells [359]. While on the other hand, down regulation of pore-sealing claudin such as cldn-1 and overexpression of pore-forming claudin such as Cldn-2 decrease TEER [360]. Decreased expression of Cldn-1 is associated with increased intestinal permeability in IBS patients [361]. Patients of IBDs such as ulcerative colitis and Crohn's disease have a mucosal barrier dysfunction, that can be assessed by measuring the intestinal permeability [362]. Moreover, specimens of these patients showed higher expression of Cldn-2. Pro-inflammatory cytokines (TNF-alpha, IL-13, IL-6) are known to induce Cldn-2 expression in *in vitro* intestinal cell models as well as in *in vivo* mouse model [17;363;364]. Such as IL-6 induces Cldn-2 expression via PI3K dependent pathway and increases TJ permeability [17]. In agreement with the earlier studies [17;344;365], we show in this report for the first time midkine /PI3K pathway mediated downregulation of Cldn-1 and upregulation of Cldn-2 protein after MPA-treatment that leads to increase TJs permeability.

Decreased TEER value and increased FD4 fluxes confirmed the modulatory role of MPA on barrier function. As TEER value of monolayer inversely reflects the ion conductance through the TJs-controlled paracellular pathways, the alteration observed after MPA therapeutic concentration exposure highlights FD4 fluxes transportation across the Caco-2 monolayers. We observed significant decrease in TEER and increase in FD4 flux correlated with overexpression of Claudin-2 and downregulation of Claudin-1 in MPA treated Caco-2 cells. These results are consistent with the previous finding of *in vitro* and *in vivo* model studies such as MDCK cells show increase TEER with the overexpression of claudin-1 that in turn decreases paracellular

permeability [366;367] While claudin-1 knockdown mice show loss of TJ barrier to water and macromolecules [368].

TJs assembly proteins such claudins, occludin are connected with F-actin based cytoskeleton through a scaffolding protein ZO-1 [75;369;370]. This anchoring property of ZO-1 protein is due to the PDZ-binding motif in the N-terminal which interacts with PDZ-binding motif in the C-terminal domain of claudins proteins [371;372]. Recently, ZO-1 dependent interaction was observed between C-terminal tail of Cldn-1, Cldn-2 and Occludin proteins. [373]. ZO-1 knock down cells study show disruption of claudins localization and barrier function [374;375]. Previously, our group has reported MPA-mediated modulation of F-actin based cytoskeleton via MLCK/MLC-2 pathway and redistribution of ZO-1 and Occludin from TJs assembly [331]. Recently we have reported decrease expression of Occludin protein via p38MAPK dependent MLCK/MLC-2 pathway after MPA treatment [324]. In this study, we observed irregular pattern of Cldn-1 and Cldn-2 in the TJs assemblies apart from their altered expression. This altered distribution pattern of Cldn-1 and Cldn-2 proteins in TJs assembly can be due to the disruption of F-actin based cytoskeleton, redistribution/downregulation of ZO-1 as well as redistribution/decrease expression of Occludin proteins in TJs assembly. Our results are consistent with previous findings such as; **(1)** where *E. coli* heat stable toxin dissolves and condenses F-actin based cytoskeleton in T84 cells and alterations of F-actin based cytoskeleton were accompanied by redistribution of ZO-1, Cldn-1 and Occludin [376]. In another *in vitro* model study, alteration of F-actin based cytoskeleton and redistribution of Occludin, ZO-1, Cldn-1 and Cldn-2 were observed in the presence of RhoA, Rac1 and Cdc-42 enzymes [377]. **(2)** ZO-1 knock down and/or ZO-1 and ZO-2 double knock down MDCK cells show disruption of the localization of Cldn-2 and Occludin at TJs [378;379]. **(3)** Cldn-1 and Cldn-2 recruit Occludin and reconstitutes TJs strands [380]. In the absence of Occludin, ZO-1 disappears from TJ and Cldn-1 is downregulated [381].

In addition, infection of *Salmonella* significantly increases the expression of Cldn-2 protein both in *in vitro* and *in vivo* model studies and is also known to modulate the localization of junctional Cldn2 protein [360]. Deprivation of glutamine not only decreases the expression of Cldn-1 protein but also alter distribution in TJs assembly via PI3K/Akt pathway in Caco-2 cells [382;383].

IL-1 β increases TJs permeability via p38MAPK/ATF-2 pathway in *in vitro* and *in vivo* model studies [313]. Previously we reported that MPA mediated increased TJs permeability can be partially prevented by blocking p38MAPK pathway [324]. In this study, we observed midkine/PI3K dependent activation of *p38MAPK* gene after MPA treatment. Inhibition of midkine/PI3K pathway completely blocked MPA modulated TJs permeability. These results are consistent with the previous findings that show PI3K dependent activation of p38MAPK pathway [384;385].

Pro-inflammatory cytokines, infections and chemical agents alter TJs-dependent permeability through activation of different types of pathways in different disease model studies. Such as protein kinase C (PKC) and protein phosphatases (PP) regulate TJ assembly via altered activation (phosphorylation and dephosphorylation) of occludin protein [333]. Expression of Thyroid Transcription Factor-1 (TTF-1) induces expression of occludin and Cldn-1 in lung epithelial cell line [386]. *Salmonella* increases expression of Cldn-2 via JNK pathway while *Complyobacter jejuni* down regulates Cldn-4 in turn increases TJ permeability [333]. Depletion of polyamines disrupts TJs permeability via JunD dependent negative regulation of ZO-1 gene [387]. Sodium butyrate and Naringenin enhances barrier functions through increased expression of Cldn-1 and Cldn-4 respectively via transcription factor SP-1 [388;389]. Loss of Hnf4A affects colonic ions transport via down regulation of Cldn-15 and causes IBD type chronic inflammation in mice [230]. Decreased expression of Cldn-3 and Cldn-4 were observed in the colonic biopsies samples of IBD patients [390]. RhoA dependent increased TJs permeability is also reported by different studies [391]. We did not find the activation of these pathways through our epigenetic analyses after MPA treatment. From these findings it can be concluded that MPA alters TJs permeability only through midkine/PI3K dependent pathway.

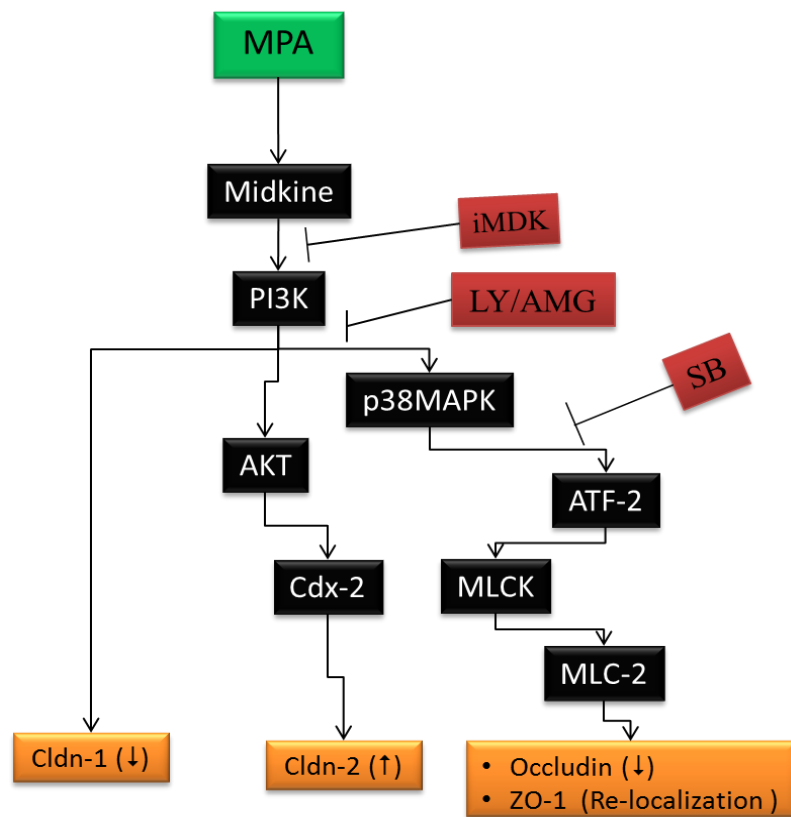


Figure 6.8: Proposed mechanism of MPA-induced TJ assembly deregulation in Caco-2 cells monolayer. Midkine activates PI3K/ p38MAPK dependent MLCK pathway and consequently reorganizes F-actin base cytoskeleton which leads to redistribution of ZO-1 and occludin proteins as well as downregulation of occludin protein. In parallel, midkine protein increases expression of claudin-2 and decreases expression of claudin-1 proteins in TJ assembly via PI3K

pathway in MPA treated Caco-2 cell monolayer. PI3K inhibitors (iMDK/LY/AMG) block MPA-mediated alters TJ assembly in Caco-2 cells monolayers. Abbreviations: MPA- mycophenolic acid, p38MAPK- p38 mitogen activated protein kinase, ATF-2- activating transcription factor-2, MLCK- myosin light chain kinase, MLC-2- myosin light chain-2, TJ- tight junction, ZO-1- Zonula Occludins, PI3K- phosphatidylinositol-4,5-bisphosphate 3-kinase, iMDK- midkine inhibitor, LY – LY294002, AMG – AMG-511, SB - 203580.

The data presented in this study provide a comprehensive view of paracellular permeability regulation and is the first report, according to our knowledge, to demonstrate the role of midkine dependent TJ regulation via PI3K pathway in MPA treated Caco-2 cells. This prospect could contribute to the development of diarrhea in organ transplanted patients with mucosal inflammation, treated with MPA; provide similar effects occur systemically in vivo.

6.6 Conclusion

The outcome of this study, using *in vitro* intestinal model, demonstrates that exposure of confluent Caco-2 cell monolayers to the MPA therapeutic concentrations leads to midkine dependent PI3K pathway activation that ultimately modulates the expression of Cldn-1 and -2 proteins and activates p38MPAK mediated MLCK/MLC-2 pathway and consequently increases monolayer permeability (Fig. 6.8). Our results presented in this study can open new perspectives

in the knowledge of TJs regulation mechanism that can lead to the identification of midkine as a noninvasive permeability-based marker of leak flux diarrhea of MPA therapy in organ transplanted patients. This study also emphasized therapeutic ability of iMDK/LY/AMG that improves the barrier function of Caco-2 cell monolayers under MPA stimulation. Additional studies are required to exclude confined role of midkine in MPA-treated cells and in addition to confirm these findings in other *in vitro* intestinal models as well as *in vivo* models studies.

6.7 Conflict of Interest

The authors declare that they have no competing interests.

6.8 Acknowledgement

The authors acknowledge the support by the German Research Foundation (DFG) and the Open Access Publication Fund of the University of Göttingen. Niamat Khan is the recipient of PhD scholarship from German Academic Exchange Service (DAAD) and Higher Education Commission (HEC) of Pakistan.

Table 6.1: List of primers of midkine/PI3K related genes

| Types | Primer name | Chromosomal location | Direction | Sequence |
|-------------------------------|-------------|----------------------|--------------------|--|
| Promoter Assay Primers | PI3Kgamma | 7 | Forward Reverse | CGGCAATAGTTTTGCAGGTG GGTTTTCTTCATGGTTGAGG |
| | CDX-2 | 13 | Forward Reverse | AAGGTTTACACTGCGGAAGC TCATACCACACCCTGTGCAT |
| | Cldn-1 | 3 | Forward Reverse | GGACAGGATCTGACTCACCA CATCTCCTGGCATCCTCTTC |
| | Cldn-2 | X | Forward Reverse | TCTCTTGGCCTCCAACCTGT CTGTGTGTGGCACATTCCAT |
| | P38MAPK | 6 | Forward Reverse | TTTACTCTTTCCCCGACAC AACTGGAGACCAAAGGCAGA |
| | PKCA | 17 | Forward Reverse | GGACCATGGCTGACGTTTTTC CGGCACCTACCAGATGAAGT |
| | JNK | 10 | Forward Reverse | CTAATCAAGGCTCTGCGGTA ACCAAGAAGCTGCAAGATGC |
| | RhoA | 3 | Forward Reverse | ATGGGTGGCACTCAGTCTCT ATGGGTGGCACTCAGTCTCT |
| | PP-2A | 9 | Forward Reverse | AATCTCCTGCTCTGCCAAAC AGCGAAGATGTTAGCCTTCG |
| | PP-1 | 10 | Forward Reverse | CCCTGAACAATTCCGTCCT CCCTGAACAATTCCGTCCT |
| | JunD | 19 | Forward Reverse | TTTCTCTCCTCCCTCTGTCC GCAGATCAAAGACCCCAAGA |
| | SP-1 | 12 | Forward Reverse | GCCGTTGTTCTGTCAATCCT TGGTGTCCGCCTAAAAAGAC |
| | TTF-1 | 14 | Forward Reverse | TGGGAGGATCTTGTCTTTGG TGGTATTTCCGGTCTCCACT |
| | Hnf4A | 20 | Forward Reverse | CCCAGAACAAGGATCCAGAA CCCCAAGTCAGGCATTCTAA |
| | Cldn-3 | 7 | Forward Reverse | CCCAAAGTGGTGAGGAGAGA CCCAAAGTGGTGAGGAGAGA |
| | Cldn-4 | 7 | Forward Reverse | TGACAAAAACCCCTCCCTCT ACGGACTTAACGTTCCGAGA |
| | Cldn-15 | 7 | Forward Reverse | GTTCAAGCAATCGTCTCAGC CATCCATTCACCAGGGAAC |
| | GAPDH | 12 | Forward Reverse | TGAGCAGTCCGGTGTCACTA ACGACTGAGATGGGGAATTG |
| Expression Primers | PI3Kgamma | 7 | Forward Reverse | CCAAGGAAGCTTCAATGCTGAC TCCTCTGCTGTGAGAGGGTTAA |
| | CDX-2 | 13 | Forward Reverse | GAACCTGTGCGAGTGGATG AAGGGCTCTGGGACACTTCT |
| | Cldn-1 | 3 | Forward Reverse | CAGTGGAGGATTTACTCCTATGC GTGGCAACTAAAATAGCCAGACC |
| | Cldn-2 | X | Forward Reverse | CCAGCATTGTGACAGCAGTT TCATGCCACCACAGAGATA |
| | P38MAPK | 6 | Forward Reverse | CCAGCTTCAGCAGATTATGC TGGTACTGAGCAAAGTAGGCA |
| | GAPDH | 12 | Forward Reverse | ACCCAGAAGACTGTGGATGG TTCTAGACGGCAGGTCAGGT |

7 Summary

MPA is a potent ISD drug due to its ability to suppress the proliferation of lymphocytes by inhibiting the enzymatic activity of IMPDH-2 with relatively high specificity. In rapidly proliferating lymphocytes, IMPDH-2 enzyme is important for the conversion of IMP into GMP, a building block of nucleic acid replication and transcription, via *de novo* pathway. Therefore, MPA is prescribed to organ transplanted patients to prevent allograft destruction by lymphocytes. However, MPA use is linked to sporadic GI complications including the most prominent leak flux diarrhea with unknown etiology. Leak flux diarrhea occurs because of altered regulation of barrier function of gut epithelial monolayer which is controlled by TJs that are present between the apical regions of adjacent cells. Recently, our group has reported that MPA activates the MLCK/MLC-2 pathway and alters TJs permeability via downregulation of occludin and redistribution of ZO-1 proteins. Further, it was shown that inhibition of MLCK/MLC-2 pathway only partially prevented MPA mediated increase in TJs permeability. These observations led us to predict that regulation of TJs permeability by MPA treatment may involve further cellular mechanisms.

The aim of the present study was to extend our previous knowledge of MLCK/MLC-2 pathway to epigenetic level and to explore other cellular signaling pathway(s) that compromise TJs permeability in *in-vitro* model of epithelial monolayer. Histone modifications such as active histone modification mark (H3K4me3) and repressive histone modification mark (H3K27me3) play an important role in the regulation of protein-coding genes at transcription level. During transcription, the promoter region of protein-coding gene is enriched with H3K4me3 and concomitantly depleted for H3K27me3 at the promoter. Taking advantage of these histone modification marks, we performed ChIP-O-Proteomics to immuno-precipitate active and repressive chromatin complexes from MPA and DMSO (control) treated Caco-2 cells (Figure 7.1).

Our promoter based study performed with ChIP-DNA showed a significant activation of *p38MAPK*, *MLCK/MLC-2* pathway genes. We confirmed through epigenetic (promoter activity), expression (mRNA and protein expression) and inhibitory assays that MPA activates MLCK/MLC-2 pathway via p38MAPK. We also observed down regulation of occludin protein after MPA treatment. Further, inhibition of p38MAPK pathway significantly blocked the

downregulation of occludin at expression (mRNA & protein) level as well as at epigenetic level (promoter level). However, our functional assay showed that MPA-mediated increased TJs permeability can only be partially prevented by blocking either MLCK/MLC-2 pathway or p38MAPK pathway.

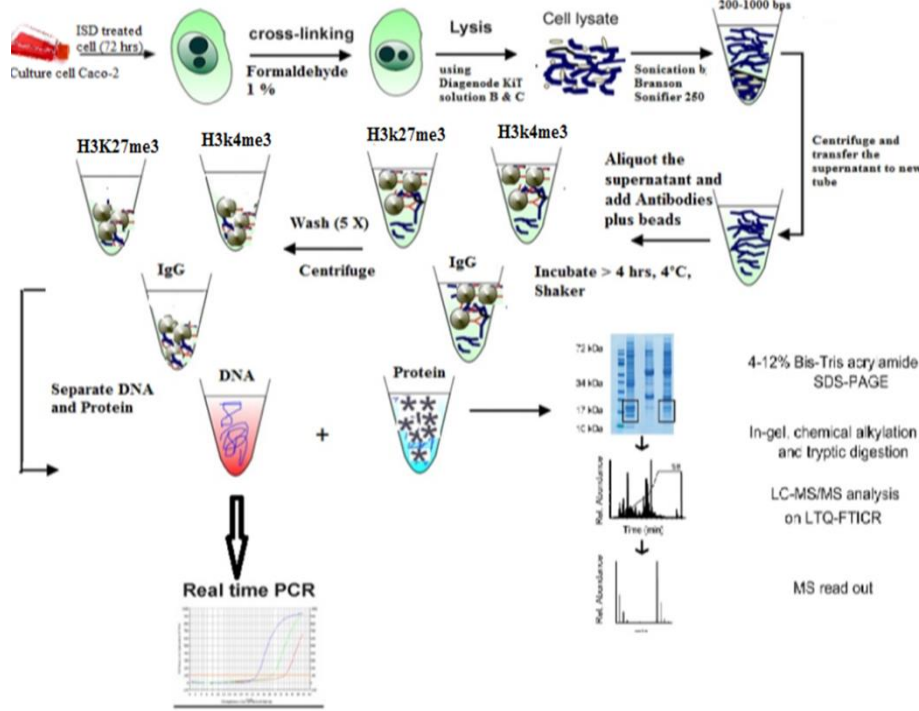


Figure 7.1: Chromatin Immunoprecipitation.

Caco-2 cells were grown for 13 days post-confluency to establish differentiated and polarized monolayer. Monolayers were treated with MPA or PI3K inhibitors (iMDK/LY/AMG) + MPA or DMSO (control). Monolayers were fixed with 1% formaldehyde, lysed and ChIP was performed using H3K4me3, H3K27me3 or IgG antibodies. Each sample was divided into two portions, one portion was analyzed by qPCR with

promoter specific primers to detect and quantify activation/ repression of target genes. While the second portion was used for label free spectral counting based quantitative proteomics to identify the chromatin binding proteins.

In order to identify additional molecules or pathways involved in TJs regulation (Figure 7.2), the proteome part of the ChIP was subjected to label free spectral counting quantitative mass spectrometric analysis. We identified 398 proteins at both active and repressive promoter regions. These identified proteins include 241 commonly associated with both the active and repressive chromatin regions. While 92 and 65 proteins were specific to active or repressive promoter regions, respectively. Differential proteomics analysis showed significant altered expression of 45 proteins at active promoter region and seven proteins at the repressive promoter region of the genes in MPA-treated cells. These proteins are known to be involved in the regulation of certain cellular functions such as chromatin structure, chromosomes segregation, transcription, cell cycles, apoptosis etc and altered expression of these proteins cause different types of abnormalities.

Among these proteins, we identified MPA-mediated increased enrichment of midkine protein in active chromatin precipitates. Altered expression of midkine is previously described to be involved in the regulation of inflammatory-related diseases. Considering the previous reports and our CHIP-O-Proteomics results, we hypothesized that MPA may alter midkine-dependent TJs barrier function of the differentiated and polarized monolayer of Caco-2 cells. To evaluate the possible role of midkine dependent regulation of TJs assembly, Caco-2 cells monolayer integrity was assessed by TEER and FITC-dextran assays after midkine inhibition in MPA treated Caco-2 cells monolayer. We observed MPA mediated increased permeability of Caco-2 cell monolayer was significantly blocked via midkine inhibition. We also observed that midkine inhibitor (iMDK) can only inhibit MPA mediated increased permeability when applying prior to the MPA exposure rather than after the MPA treatment.

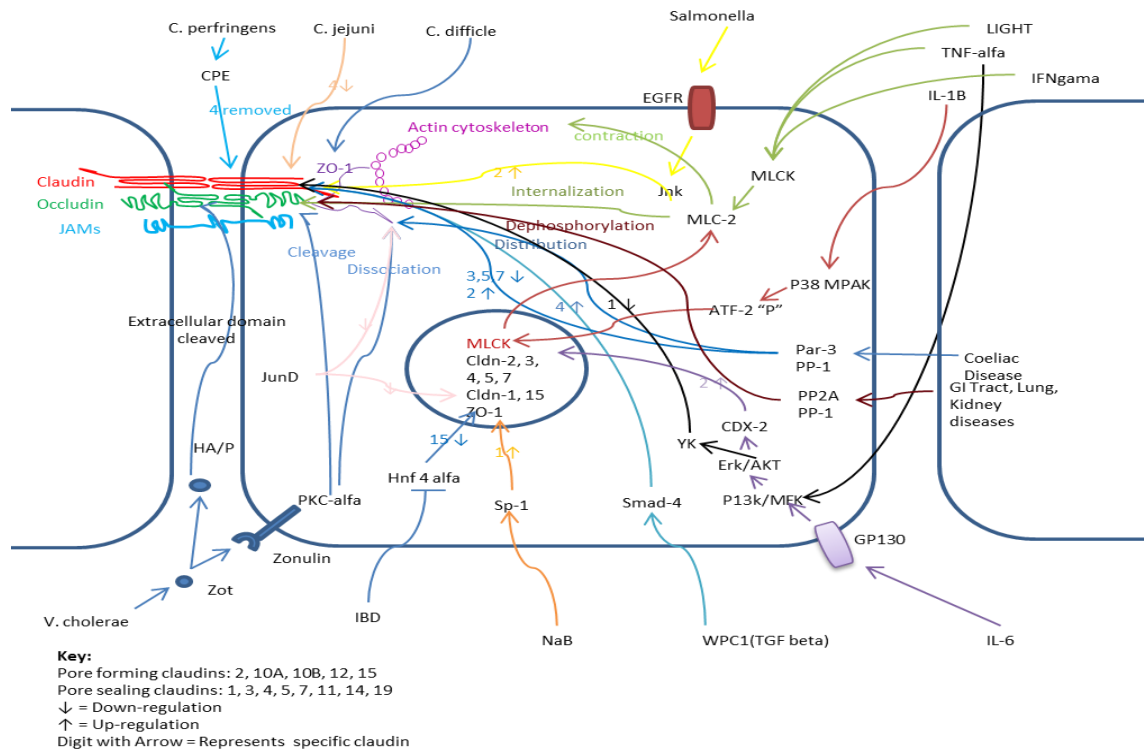


Figure 7.2: TJs regulation. We selected a panel of around 28 genes that belong to different pathways, transcription factors and TJs regulation genes which are already reported in the regulation of TJs assembly in different GI tract diseases. MLCK alters F-actin based cytoskeleton via pMLC-2 and consequently increases TJs permeability. PI3K pathway increases TJs permeability through increased expression of Cldn-2 and redistribution of Cldn-1 via activated Cdx-2 and Src kinase. Protein kinase C

(PKC) and protein phosphatases (PP) regulate TJs assembly via altered activation (phosphorylation and dephosphorylation) of occludin protein. Infectious agents such as *Salmonella* increase the expression of Cldn-2 via JNK pathway, while *Campylobacter jejuni* down-regulates Cldn-4 in order to increase TJ permeability.

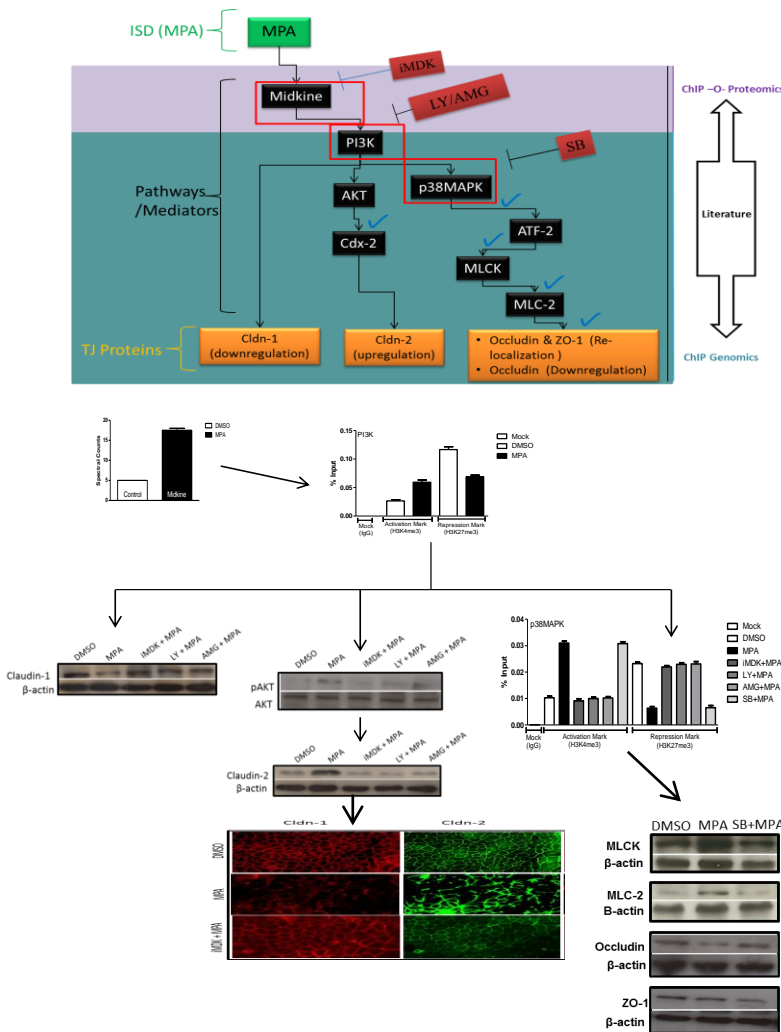


Figure 7.3: Proposed and experimental evidence for MPA mediated TJs disruption:

MPA increased expression of midkine protein leading to increased activation of PI3K pathway. PI3K pathway regulated p38MAPK mediated MLCK/MLC-2 pathway. MLCK/MLC-2 pathway altered the expression and distribution of TJs proteins (occludin & ZO-1). PI3K pathway also regulated increased expression of pore-forming claudin-2 and decreased expression of pore-sealing claudin-1. Pre-treatment with midkine inhibitor (iMDK) or PI3K inhibitors (LY/AMG) significantly prevented midkine mediated PI3K dependent increase TJ permeability.

Midkine protein is known to activate PI3K pathway and to increase TJs permeability. Our promoter based study showed the activation of PI3K gene

after MPA treatment. Based on the previous reports, we hypothesized that midkine may activate PI3K gene and increase TJs permeability via PI3K-dependent pathway in MPA-treated cells. To answer this question, we performed epigenetic, expression, and Caco-2 cells monolayer integrity analyses. Our results showed that MPA treatment increased midkine-mediated activation and expression of PI3K pathway. Our Caco-2 cells monolayer integrity assays further indicated that inhibition of PI3K pathway significantly blocked MPA mediated increase in TJ permeability in Caco-2 cells monolayer. AKT is one of the downstream target of PI3K pathway and regulates a

number of downstream targets including transcription factors such as Cdx-2. We investigated AKT phosphorylation and expression after MPA treatment using immunoblot analysis. Midkine-mediated and PI3K-dependent increased phosphorylation of AKT was observed in MPA treated cells. We further observed that MPA significantly activates *Cdx-2* gene via midkine-mediated PI3K-dependent pathway. Cdx-2 is a transcription factor involved in the regulation of various genes that regulate differentiation and growth of the intestinal cells and its altered expression is previously reported in increased TJs permeability. Next we investigated the molecular makeup of TJs assembly after MPA treatment. We performed immunoblot analysis of pore-sealing Cldn-1 and pore-forming Cldn-2. Our results showed midkine mediated decreased expression of Cldn-1 and increased expression of Cldn-2 via PI3K pathway in MPA-treated Caco-2 cells. We also found midkine mediated PI3K dependent activation of p38MAPK after MPA treatment.

From these findings it can be concluded that MPA increases Caco-2 cell monolayer permeability via midkine/PI3K pathway. Inhibition of either midkine or PI3K pathway is sufficient to prevent a significant part of the MPA-mediated loss of TJs integrity in Caco-2 cells. Midkine/PI3K pathway also activates MLCK/MLC-2 pathway via p38MAPK pathway (Figure 7.3). These observations support the hypothesis that MPA regulates TJs assembly that leads to increase permeability of epithelial monolayer and consequently diarrhea. This model also suggests that early treatment with midkine inhibitor can provide significant benefit to prevent MPA-mediated increased TJs permeability. Therefore, combination of immunosuppressive drug (MPA) with additional substance like midkine inhibitor (iMDK) may be helpful as a preventative strategy to avoid the unwanted effects of immunosuppressive regime. However, to generalize the concept of dual or combination therapy i.e., midkine inhibitor plus MPA, additional evaluation such as, *in vitro* and *in vivo* studies are needed to make the immunosuppressive regime safer for the transplanted patients.

8 Reference List

1. Allison AC, Eugui EM. Mycophenolate mofetil and its mechanisms of action. *Immunopharmacology* 2000; 47(2-3):85-118.
2. Lamba V, Sangkuhl K, Sanghavi K, Fish A, Altman RB, Klein TE. PharmGKB summary: mycophenolic acid pathway. *Pharmacogenet Genomics* 2014; 24(1):73-79.
3. Schanz S, Ulmer A, Rassner G, Fierlbeck G. Successful treatment of subacute cutaneous lupus erythematosus with mycophenolate mofetil. *Br J Dermatol* 2002; 147(1):174-178.
4. Helderman JH, Goral S. Gastrointestinal complications of transplant immunosuppression. *J Am Soc Nephrol* 2002; 13(1):277-287.
5. Bentley R. Mycophenolic Acid: a one hundred year odyssey from antibiotic to immunosuppressant. *Chem Rev* 2000; 100(10):3801-3826.
6. Sebastian L, Madhusudana SN, Ravi V, Desai A. Mycophenolic acid inhibits replication of Japanese encephalitis virus. *Chemotherapy* 2011; 57(1):56-61.
7. Nicoletti R, De SM, De SS, Trincone A, Marziano F. Antagonism against *Rhizoctonia solani* and fungitoxic metabolite production by some *Penicillium* isolates. *Mycopathologia* 2004; 158(4):465-474.
8. Staatz CE, Tett SE. Clinical pharmacokinetics and pharmacodynamics of mycophenolate in solid organ transplant recipients. *Clin Pharmacokinet* 2007; 46(1):13-58.
9. Tredger JM, Brown NW, Adams J, Gonde CE, Dhawan A, Rela M et al. Monitoring mycophenolate in liver transplant recipients: toward a therapeutic range. *Liver Transpl* 2004; 10(4):492-502.
10. Shaw LM, Korecka M, DeNofrio D, Brayman KL. Pharmacokinetic, pharmacodynamic, and outcome investigations as the basis for mycophenolic acid therapeutic drug monitoring in renal and heart transplant patients. *Clin Biochem* 2001; 34(1):17-22.
11. Manitpisitkul W, McCann E, Lee S, Weir MR. Drug interactions in transplant patients: what everyone should know. *Curr Opin Nephrol Hypertens* 2009; 18(5):404-411.
12. Rangel EB, Melaragno CS, Sa JR, Gonzalez AM, Linhares MM, Salzedas A et al. Mycophenolate mofetil versus enteric-coated mycophenolate sodium after simultaneous pancreas-kidney transplantation. *Transplant Proc* 2009; 41(10):4265-4269.
13. Pescovitz MD, Navarro MT. Immunosuppressive therapy and post-transplantation diarrhea. *Clin Transplant* 2001; 15 Suppl 4:23-28.
14. Bushra R, Aslam N, Khan AY. Food-drug interactions. *Oman Med J* 2011; 26(2):77-83.
15. Malinowski M, Martus P, Lock JF, Neuhaus P, Stockmann M. Systemic influence of immunosuppressive drugs on small and large bowel transport and barrier function. *Transpl Int* 2011; 24(2):184-193.
16. Tsukita S, Furuse M, Itoh M. Multifunctional strands in tight junctions. *Nat Rev Mol Cell Biol* 2001; 2(4):285-293.
17. Suzuki T, Yoshinaga N, Tanabe S. Interleukin-6 (IL-6) regulates claudin-2 expression and tight junction permeability in intestinal epithelium. *J Biol Chem* 2011; 286(36):31263-31271.

18. Marchiando AM, Shen L, Graham WV, Weber CR, Schwarz BT, Austin JR et al. Caveolin-1-dependent occludin endocytosis is required for TNF-induced tight junction regulation in vivo. *J Cell Biol* 2010; 189(1):111-126.
19. Le DG, Haure-Mirande V, Ferrier L, Bonnet C, Hulin P, de CP et al. Visceral adipose tissue and leptin increase colonic epithelial tight junction permeability via a RhoA-ROCK-dependent pathway. *FASEB J* 2014; 28(3):1059-1070.
20. Catalioto RM, Maggi CA, Giuliani S. Intestinal epithelial barrier dysfunction in disease and possible therapeutical interventions. *Curr Med Chem* 2011; 18(3):398-426.
21. Hodges K, Gill R. Infectious diarrhea: Cellular and molecular mechanisms. *Gut Microbes* 2010; 1(1):4-21.
22. Krajewska J, Handkiewicz-Junak D, Jarzab B. Sorafenib for the treatment of thyroid cancer: an updated review. *Expert Opin Pharmacother* 2015;1-11.
23. Schiller LR, Pardi DS, Spiller R, Semrad CE, Surawicz CM, Giannella RA et al. Gastro 2013 APDW/WCOG Shanghai working party report: chronic diarrhea: definition, classification, diagnosis. *J Gastroenterol Hepatol* 2014; 29(1):6-25.
24. Malinowski M, Martus P, Lock JF, Neuhaus P, Stockmann M. Systemic influence of immunosuppressive drugs on small and large bowel transport and barrier function. *Transpl Int* 2011; 24(2):184-193.
25. Gorkiewicz G, Thallinger GG, Trajanoski S, Lackner S, Stocker G, Hinterleitner T et al. Alterations in the colonic microbiota in response to osmotic diarrhea. *PLoS One* 2013; 8(2):e55817.
26. Woods TA. Diarrhea. 1990.
27. Lam JT, Martin MG, Turk E, Hirayama BA, Bosshard NU, Steinmann B et al. Missense mutations in SGLT1 cause glucose-galactose malabsorption by trafficking defects. *Biochim Biophys Acta* 1999; 1453(2):297-303.
28. Buret AG. Mechanisms of epithelial dysfunction in giardiasis. *Gut* 2007; 56(3):316-317.
29. Schiller LR. Secretory diarrhea. *Curr Gastroenterol Rep* 1999; 1(5):389-397.
30. Bjarnason I, Macpherson A, Hollander D. Intestinal permeability: an overview. *Gastroenterology* 1995; 108(5):1566-1581.
31. Guttman JA, Finlay BB. Subcellular alterations that lead to diarrhea during bacterial pathogenesis. *Trends Microbiol* 2008; 16(11):535-542.
32. Cunningham KE, Turner JR. Myosin light chain kinase: pulling the strings of epithelial tight junction function. *Ann N Y Acad Sci* 2012; 1258:34-42.
33. Hering NA, Fromm M, Schulzke JD. Determinants of colonic barrier function in inflammatory bowel disease and potential therapeutics. *J Physiol* 2012; 590(Pt 5):1035-1044.
34. Schulzke JD, Ploeger S, Amasheh M, Fromm A, Zeissig S, Troeger H et al. Epithelial tight junctions in intestinal inflammation. *Ann N Y Acad Sci* 2009; 1165:294-300.
35. Tsukita S, Furuse M, Itoh M. Multifunctional strands in tight junctions. *Nat Rev Mol Cell Biol* 2001; 2(4):285-293.

36. Groschwitz KR, Hogan SP. Intestinal barrier function: molecular regulation and disease pathogenesis. *J Allergy Clin Immunol* 2009; 124(1):3-20.
37. Furuse M, Hirase T, Itoh M, Nagafuchi A, Yonemura S, Tsukita S et al. Occludin: a novel integral membrane protein localizing at tight junctions. *J Cell Biol* 1993; 123(6 Pt 2):1777-1788.
38. Martin-Padura I, Lostaglio S, Schneemann M, Williams L, Romano M, Fruscella P et al. Junctional adhesion molecule, a novel member of the immunoglobulin superfamily that distributes at intercellular junctions and modulates monocyte transmigration. *J Cell Biol* 1998; 142(1):117-127.
39. Ikenouchi J, Furuse M, Furuse K, Sasaki H, Tsukita S, Tsukita S. Tricellulin constitutes a novel barrier at tricellular contacts of epithelial cells. *J Cell Biol* 2005; 171(6):939-945.
40. Goldblum SE, Rai U, Tripathi A, Thakar M, De LL, Di TN et al. The active Zot domain (aa 288-293) increases ZO-1 and myosin 1C serine/threonine phosphorylation, alters interaction between ZO-1 and its binding partners, and induces tight junction disassembly through proteinase activated receptor 2 activation. *FASEB J* 2011; 25(1):144-158.
41. Yamaguchi H, Kojima T, Ito T, Kimura Y, Imamura M, Son S et al. Transcriptional control of tight junction proteins via a protein kinase C signal pathway in human telomerase reverse transcriptase-transfected human pancreatic duct epithelial cells. *Am J Pathol* 2010; 177(2):698-712.
42. Al-Sadi R, Guo S, Ye D, Dokladny K, Alhmod T, Ereifej L et al. Mechanism of IL-1beta modulation of intestinal epithelial barrier involves p38 kinase and activating transcription factor-2 activation. *J Immunol* 2013; 190(12):6596-6606.
43. Sheth P, Samak G, Shull JA, Seth A, Rao R. Protein phosphatase 2A plays a role in hydrogen peroxide-induced disruption of tight junctions in Caco-2 cell monolayers. *Biochem J* 2009; 421(1):59-70.
44. Schumann M, Gunzel D, Buergel N, Richter JF, Troeger H, May C et al. Cell polarity-determining proteins Par-3 and PP-1 are involved in epithelial tight junction defects in coeliac disease. *Gut* 2012; 61(2):220-228.
45. Press B. Optimization of the Caco-2 permeability assay to screen drug compounds for intestinal absorption and efflux. *Methods Mol Biol* 2011; 763:139-154.
46. Clarke LL. A guide to Ussing chamber studies of mouse intestine. *Am J Physiol Gastrointest Liver Physiol* 2009; 296(6):G1151-G1166.
47. Berkes J, Viswanathan VK, Savkovic SD, Hecht G. Intestinal epithelial responses to enteric pathogens: effects on the tight junction barrier, ion transport, and inflammation. *Gut* 2003; 52(3):439-451.
48. Tan JL, Ravid S, Spudich JA. Control of nonmuscle myosins by phosphorylation. *Annu Rev Biochem* 1992; 61:721-759.
49. Verin AD, Patterson CE, Day MA, Garcia JG. Regulation of endothelial cell gap formation and barrier function by myosin-associated phosphatase activities. *Am J Physiol* 1995; 269(1 Pt 1):L99-108.
50. Blair SA, Kane SV, Clayburgh DR, Turner JR. Epithelial myosin light chain kinase expression and activity are upregulated in inflammatory bowel disease. *Lab Invest* 2006; 86(2):191-201.
51. Murch SH, Lamkin VA, Savage MO, Walker-Smith JA, MacDonald TT. Serum concentrations of tumour necrosis factor alpha in childhood chronic inflammatory bowel disease. *Gut* 1991; 32(8):913-917.
52. Taylor CT, Dzus AL, Colgan SP. Autocrine regulation of epithelial permeability by hypoxia: role for polarized release of tumor necrosis factor alpha. *Gastroenterology* 1998; 114(4):657-668.

53. Shen L, Black ED, Witkowski ED, Lencer WI, Guerriero V, Schneeberger EE et al. Myosin light chain phosphorylation regulates barrier function by remodeling tight junction structure. *J Cell Sci* 2006; 119(Pt 10):2095-2106.
54. Wong V, Gumbiner BM. A synthetic peptide corresponding to the extracellular domain of occludin perturbs the tight junction permeability barrier. *J Cell Biol* 1997; 136(2):399-409.
55. Balda MS, Whitney JA, Flores C, Gonzalez S, Cerejido M, Matter K. Functional dissociation of paracellular permeability and transepithelial electrical resistance and disruption of the apical-basolateral intramembrane diffusion barrier by expression of a mutant tight junction membrane protein. *J Cell Biol* 1996; 134(4):1031-1049.
56. Stamatovic SM, Keep RF, Wang MM, Jankovic I, Andjelkovic AV. Caveolae-mediated internalization of occludin and claudin-5 during CCL2-induced tight junction remodeling in brain endothelial cells. *J Biol Chem* 2009; 284(28):19053-19066.
57. Schwarz BT, Wang F, Shen L, Clayburgh DR, Su L, Wang Y et al. LIGHT signals directly to intestinal epithelia to cause barrier dysfunction via cytoskeletal and endocytic mechanisms. *Gastroenterology* 2007; 132(7):2383-2394.
58. Ferran C, Dy M, Sheehan K, Merite S, Schreiber R, Landais P et al. Inter-mouse strain differences in the in vivo anti-CD3 induced cytokine release. *Clin Exp Immunol* 1991; 86(3):537-543.
59. Musch MW, Clarke LL, Mamah D, Gawenis LR, Zhang Z, Ellsworth W et al. T cell activation causes diarrhea by increasing intestinal permeability and inhibiting epithelial Na⁺/K⁺-ATPase. *J Clin Invest* 2002; 110(11):1739-1747.
60. Clayburgh DR, Barrett TA, Tang Y, Meddings JB, Van Eldik LJ, Watterson DM et al. Epithelial myosin light chain kinase-dependent barrier dysfunction mediates T cell activation-induced diarrhea in vivo. *J Clin Invest* 2005; 115(10):2702-2715.
61. Wang J, Anders RA, Wang Y, Turner JR, Abraham C, Pfeffer K et al. The critical role of LIGHT in promoting intestinal inflammation and Crohn's disease. *J Immunol* 2005; 174(12):8173-8182.
62. Zolotarevsky Y, Hecht G, Koutsouris A, Gonzalez DE, Quan C, Tom J et al. A membrane-permeant peptide that inhibits MLC kinase restores barrier function in in vitro models of intestinal disease. *Gastroenterology* 2002; 123(1):163-172.
63. Clayburgh DR, Barrett TA, Tang Y, Meddings JB, Van Eldik LJ, Watterson DM et al. Epithelial myosin light chain kinase-dependent barrier dysfunction mediates T cell activation-induced diarrhea in vivo. *J Clin Invest* 2005; 115(10):2702-2715.
64. Qasim M, Rahman H, Ahmed R, Oellerich M, Asif AR. Mycophenolic acid mediated disruption of the intestinal epithelial tight junctions. *Exp Cell Res* 2014; 322(2):277-289.
65. Nataro JP, Kaper JB. Diarrheagenic *Escherichia coli*. *Clin Microbiol Rev* 1998; 11(1):142-201.
66. Wolff C, Nisan I, Hanski E, Frankel G, Rosenshine I. Protein translocation into host epithelial cells by infecting enteropathogenic *Escherichia coli*. *Mol Microbiol* 1998; 28(1):143-155.
67. Matsuzawa T, Kuwae A, Yoshida S, Sasakawa C, Abe A. Enteropathogenic *Escherichia coli* activates the RhoA signaling pathway via the stimulation of GEF-H1. *EMBO J* 2004; 23(17):3570-3582.
68. Chang YC, Nalbant P, Birkenfeld J, Chang ZF, Bokoch GM. GEF-H1 couples nocodazole-induced microtubule disassembly to cell contractility via RhoA. *Mol Biol Cell* 2008; 19(5):2147-2153.

69. Feng J, Ito M, Ichikawa K, Isaka N, Nishikawa M, Hartshorne DJ et al. Inhibitory phosphorylation site for Rho-associated kinase on smooth muscle myosin phosphatase. *J Biol Chem* 1999; 274(52):37385-37390.
70. Kawano Y, Fukata Y, Oshiro N, Amano M, Nakamura T, Ito M et al. Phosphorylation of myosin-binding subunit (MBS) of myosin phosphatase by Rho-kinase in vivo. *J Cell Biol* 1999; 147(5):1023-1038.
71. Glotfelty LG, Zahs A, Hodges K, Shan K, Alto NM, Hecht GA. Enteropathogenic *E. coli* effectors EspG1/G2 disrupt microtubules, contribute to tight junction perturbation and inhibit restoration. *Cell Microbiol* 2014; 16(12):1767-1783.
72. Atisook K, Carlson S, Madara JL. Effects of phlorizin and sodium on glucose-elicited alterations of cell junctions in intestinal epithelia. *Am J Physiol* 1990; 258(1 Pt 1):C77-C85.
73. Turner JR, Rill BK, Carlson SL, Carnes D, Kerner R, Mrsny RJ et al. Physiological regulation of epithelial tight junctions is associated with myosin light-chain phosphorylation. *Am J Physiol* 1997; 273(4 Pt 1):C1378-C1385.
74. Musch MW, Walsh-Reitz MM, Chang EB. Roles of ZO-1, occludin, and actin in oxidant-induced barrier disruption. *Am J Physiol Gastrointest Liver Physiol* 2006; 290(2):G222-G231.
75. Muza-Moons MM, Schneeberger EE, Hecht GA. Enteropathogenic *Escherichia coli* infection leads to appearance of aberrant tight junction strands in the lateral membrane of intestinal epithelial cells. *Cell Microbiol* 2004; 6(8):783-793.
76. Shifflett DE, Clayburgh DR, Koutsouris A, Turner JR, Hecht GA. Enteropathogenic *E. coli* disrupts tight junction barrier function and structure in vivo. *Lab Invest* 2005; 85(10):1308-1324.
77. Philpott DJ, McKay DM, Mak W, Perdue MH, Sherman PM. Signal transduction pathways involved in enterohemorrhagic *Escherichia coli*-induced alterations in T84 epithelial permeability. *Infect Immun* 1998; 66(4):1680-1687.
78. Yuhan R, Koutsouris A, Savkovic SD, Hecht G. Enteropathogenic *Escherichia coli*-induced myosin light chain phosphorylation alters intestinal epithelial permeability. *Gastroenterology* 1997; 113(6):1873-1882.
79. Simonovic I, Rosenberg J, Koutsouris A, Hecht G. Enteropathogenic *Escherichia coli* dephosphorylates and dissociates occludin from intestinal epithelial tight junctions. *Cell Microbiol* 2000; 2(4):305-315.
80. McNamara BP, Koutsouris A, O'Connell CB, Nougayrede JP, Donnenberg MS, Hecht G. Translocated EspF protein from enteropathogenic *Escherichia coli* disrupts host intestinal barrier function. *J Clin Invest* 2001; 107(5):621-629.
81. Farshori P, Kachar B. Redistribution and phosphorylation of occludin during opening and resealing of tight junctions in cultured epithelial cells. *J Membr Biol* 1999; 170(2):147-156.
82. Kusugami K, Fukatsu A, Tanimoto M, Shinoda M, Haruta J, Kuroiwa A et al. Elevation of interleukin-6 in inflammatory bowel disease is macrophage- and epithelial cell-dependent. *Dig Dis Sci* 1995; 40(5):949-959.
83. Reinisch W, Gasche C, Tillinger W, Wyatt J, Lichtenberger C, Willheim M et al. Clinical relevance of serum interleukin-6 in Crohn's disease: single point measurements, therapy monitoring, and prediction of clinical relapse. *Am J Gastroenterol* 1999; 94(8):2156-2164.
84. Louis E, Belaiche J, Van KC, Franchimont D, de GD, Gueenen V et al. A high serum concentration of interleukin-6 is predictive of relapse in quiescent Crohn's disease. *Eur J Gastroenterol Hepatol* 1997; 9(10):939-944.

85. Suzuki T, Yoshinaga N, Tanabe S. Interleukin-6 (IL-6) regulates claudin-2 expression and tight junction permeability in intestinal epithelium. *J Biol Chem* 2011; 286(36):31263-31271.
86. Amasheh M, Fromm A, Krug SM, Amasheh S, Andres S, Zeitz M et al. TNF α -induced and berberine-antagonized tight junction barrier impairment via tyrosine kinase, Akt and NF κ B signaling. *J Cell Sci* 2010; 123(Pt 23):4145-4155.
87. Heller F, Fuss IJ, Nieuwenhuis EE, Blumberg RS, Strober W. Oxazolone colitis, a Th2 colitis model resembling ulcerative colitis, is mediated by IL-13-producing NK-T cells. *Immunity* 2002; 17(5):629-638.
88. Heller F, Florian P, Bojarski C, Richter J, Christ M, Hillenbrand B et al. Interleukin-13 is the key effector Th2 cytokine in ulcerative colitis that affects epithelial tight junctions, apoptosis, and cell restitution. *Gastroenterology* 2005; 129(2):550-564.
89. Rosen MJ, Chaturvedi R, Washington MK, Kuhnhein LA, Moore PD, Coggeshall SS et al. STAT6 deficiency ameliorates severity of oxazolone colitis by decreasing expression of claudin-2 and Th2-inducing cytokines. *J Immunol* 2013; 190(4):1849-1858.
90. Hershey GK. IL-13 receptors and signaling pathways: an evolving web. *J Allergy Clin Immunol* 2003; 111(4):677-690.
91. Al-Sadi RM, Ma TY. IL-1 β causes an increase in intestinal epithelial tight junction permeability. *J Immunol* 2007; 178(7):4641-4649.
92. Cominelli F, Pizarro TT. Interleukin-1 and interleukin-1 receptor antagonist in inflammatory bowel disease. *Aliment Pharmacol Ther* 1996; 10 Suppl 2:49-53.
93. Bouwman LI, Niewold P, van Putten JP. Basolateral invasion and trafficking of *Campylobacter jejuni* in polarized epithelial cells. *PLoS One* 2013; 8(1):e54759.
94. Lamb-Rosteski JM, Kalischuk LD, Inglis GD, Buret AG. Epidermal growth factor inhibits *Campylobacter jejuni*-induced claudin-4 disruption, loss of epithelial barrier function, and *Escherichia coli* translocation. *Infect Immun* 2008; 76(8):3390-3398.
95. Chen ML, Ge Z, Fox JG, Schauer DB. Disruption of tight junctions and induction of proinflammatory cytokine responses in colonic epithelial cells by *Campylobacter jejuni*. *Infect Immun* 2006; 74(12):6581-6589.
96. Wine E, Chan VL, Sherman PM. *Campylobacter jejuni* mediated disruption of polarized epithelial monolayers is cell-type specific, time dependent, and correlates with bacterial invasion. *Pediatr Res* 2008; 64(6):599-604.
97. Lei S, Cheng T, Guo Y, Li C, Zhang W, Zhi F. Somatostatin ameliorates lipopolysaccharide-induced tight junction damage via the ERK-MAPK pathway in Caco2 cells. *Eur J Cell Biol* 2014; 93(7):299-307.
98. Gonzalez-Mariscal L, Tapia R, Chamorro D. Crosstalk of tight junction components with signaling pathways. *Biochim Biophys Acta* 2008; 1778(3):729-756.
99. Wong V. Phosphorylation of occludin correlates with occludin localization and function at the tight junction. *Am J Physiol* 1997; 273(6 Pt 1):C1859-C1867.
100. Andreeva AY, Krause E, Muller EC, Blasig IE, Utepbergenov DI. Protein kinase C regulates the phosphorylation and cellular localization of occludin. *J Biol Chem* 2001; 276(42):38480-38486.

101. Sakakibara A, Furuse M, Saitou M, Ando-Akatsuka Y, Tsukita S. Possible involvement of phosphorylation of occludin in tight junction formation. *J Cell Biol* 1997; 137(6):1393-1401.
102. Hirase T, Kawashima S, Wong EY, Ueyama T, Rikitake Y, Tsukita S et al. Regulation of tight junction permeability and occludin phosphorylation by Rho-p160ROCK-dependent and -independent mechanisms. *J Biol Chem* 2001; 276(13):10423-10431.
103. Stuart RO, Nigam SK. Regulated assembly of tight junctions by protein kinase C. *Proc Natl Acad Sci U S A* 1995; 92(13):6072-6076.
104. Kale G, Naren AP, Sheth P, Rao RK. Tyrosine phosphorylation of occludin attenuates its interactions with ZO-1, ZO-2, and ZO-3. *Biochem Biophys Res Commun* 2003; 302(2):324-329.
105. Clarke H, Soler AP, Mullin JM. Protein kinase C activation leads to dephosphorylation of occludin and tight junction permeability increase in LLC-PK1 epithelial cell sheets. *J Cell Sci* 2000; 113 (Pt 18):3187-3196.
106. Rao R. Occludin phosphorylation in regulation of epithelial tight junctions. *Ann N Y Acad Sci* 2009; 1165:62-68.
107. Seth A, Sheth P, Elias BC, Rao R. Protein phosphatases 2A and 1 interact with occludin and negatively regulate the assembly of tight junctions in the CACO-2 cell monolayer. *J Biol Chem* 2007; 282(15):11487-11498.
108. Rao RK, Basuroy S, Rao VU, Karnaky Jr KJ, Gupta A. Tyrosine phosphorylation and dissociation of occludin-ZO-1 and E-cadherin-beta-catenin complexes from the cytoskeleton by oxidative stress. *Biochem J* 2002; 368(Pt 2):471-481.
109. Sheth P, Basuroy S, Li C, Naren AP, Rao RK. Role of phosphatidylinositol 3-kinase in oxidative stress-induced disruption of tight junctions. *J Biol Chem* 2003; 278(49):49239-49245.
110. Basuroy S, Sheth P, Kuppaswamy D, Balasubramanian S, Ray RM, Rao RK. Expression of kinase-inactive c-Src delays oxidative stress-induced disassembly and accelerates calcium-mediated reassembly of tight junctions in the Caco-2 cell monolayer. *J Biol Chem* 2003; 278(14):11916-11924.
111. Sollid LM, Lundin KE. Diagnosis and treatment of celiac disease. *Mucosal Immunol* 2009; 2(1):3-7.
112. Suzuki A, Ohno S. The PAR-aPKC system: lessons in polarity. *J Cell Sci* 2006; 119(Pt 6):979-987.
113. Perelle S, Gibert M, Bourlioux P, Corthier G, Popoff MR. Production of a complete binary toxin (actin-specific ADP-ribosyltransferase) by *Clostridium difficile* CD196. *Infect Immun* 1997; 65(4):1402-1407.
114. Voth DE, Ballard JD. *Clostridium difficile* toxins: mechanism of action and role in disease. *Clin Microbiol Rev* 2005; 18(2):247-263.
115. Yuan P, Zhang H, Cai C, Zhu S, Zhou Y, Yang X et al. Chondroitin sulfate proteoglycan 4 functions as the cellular receptor for *Clostridium difficile* toxin B. *Cell Res* 2014.
116. Chen ML, Pothoulakis C, LaMont JT. Protein kinase C signaling regulates ZO-1 translocation and increased paracellular flux of T84 colonocytes exposed to *Clostridium difficile* toxin A. *J Biol Chem* 2002; 277(6):4247-4254.
117. Leibovici-Weissman Y, Neuberger A, Bitterman R, Sinclair D, Salam MA, Paul M. Antimicrobial drugs for treating cholera. *Cochrane Database Syst Rev* 2014; 6:CD008625.

118. Wu Z, Nybom P, Magnusson KE. Distinct effects of *Vibrio cholerae* haemagglutinin/protease on the structure and localization of the tight junction-associated proteins occludin and ZO-1. *Cell Microbiol* 2000; 2(1):11-17.
119. Fullner KJ, Lencer WI, Mekalanos JJ. *Vibrio cholerae*-induced cellular responses of polarized T84 intestinal epithelial cells are dependent on production of cholera toxin and the RTX toxin. *Infect Immun* 2001; 69(10):6310-6317.
120. Uzzau S, Cappuccinelli P, Fasano A. Expression of *Vibrio cholerae* zonula occludens toxin and analysis of its subcellular localization. *Microb Pathog* 1999; 27(6):377-385.
121. Di PM, Lu R, Uzzau S, Wang W, Margaretten K, Pazzani C et al. Zonula occludens toxin structure-function analysis. Identification of the fragment biologically active on tight junctions and of the zonulin receptor binding domain. *J Biol Chem* 2001; 276(22):19160-19165.
122. Wang W, Uzzau S, Goldblum SE, Fasano A. Human zonulin, a potential modulator of intestinal tight junctions. *J Cell Sci* 2000; 113 Pt 24:4435-4440.
123. Fasano A. Innovative strategies for the oral delivery of drugs and peptides. *Trends Biotechnol* 1998; 16(4):152-157.
124. Songyang Z, Fanning AS, Fu C, Xu J, Marfatia SM, Chishti AH et al. Recognition of unique carboxyl-terminal motifs by distinct PDZ domains. *Science* 1997; 275(5296):73-77.
125. Itoh M, Furuse M, Morita K, Kubota K, Saitou M, Tsukita S. Direct binding of three tight junction-associated MAGUKs, ZO-1, ZO-2, and ZO-3, with the COOH termini of claudins. *J Cell Biol* 1999; 147(6):1351-1363.
126. Fanning AS, Ma TY, Anderson JM. Isolation and functional characterization of the actin binding region in the tight junction protein ZO-1. *FASEB J* 2002; 16(13):1835-1837.
127. Van Itallie CM, Anderson JM. Occludin confers adhesiveness when expressed in fibroblasts. *J Cell Sci* 1997; 110 (Pt 9):1113-1121.
128. Pierdomenico M, Stronati L, Costanzo M, Vitali R, Di NG, Nuti F et al. New insights into the pathogenesis of inflammatory bowel disease: transcription factors analysis in bioptic tissues from pediatric patients. *J Pediatr Gastroenterol Nutr* 2011; 52(3):271-279.
129. Chen J, Xiao L, Rao JN, Zou T, Liu L, Bellavance E et al. JunD represses transcription and translation of the tight junction protein zona occludens-1 modulating intestinal epithelial barrier function. *Mol Biol Cell* 2008; 19(9):3701-3712.
130. Mazan-Mamczarz K, Lal A, Martindale JL, Kawai T, Gorospe M. Translational repression by RNA-binding protein TIAR. *Mol Cell Biol* 2006; 26(7):2716-2727.
131. Boyle EC, Brown NF, Finlay BB. *Salmonella enterica* serovar Typhimurium effectors SopB, SopE, SopE2 and SipA disrupt tight junction structure and function. *Cell Microbiol* 2006; 8(12):1946-1957.
132. Liao AP, Petrof EO, Kuppireddi S, Zhao Y, Xia Y, Claud EC et al. *Salmonella* type III effector AvrA stabilizes cell tight junctions to inhibit inflammation in intestinal epithelial cells. *PLoS One* 2008; 3(6):e2369.
133. Wang HB, Wang PY, Wang X, Wan YL, Liu YC. Butyrate enhances intestinal epithelial barrier function via up-regulation of tight junction protein Claudin-1 transcription. *Dig Dis Sci* 2012; 57(12):3126-3135.

134. Mills DM, Bajaj V, Lee CA. A 40 kb chromosomal fragment encoding *Salmonella typhimurium* invasion genes is absent from the corresponding region of the *Escherichia coli* K-12 chromosome. *Mol Microbiol* 1995; 15(4):749-759.
135. Galan JE. Interaction of *Salmonella* with host cells through the centisome 63 type III secretion system. *Curr Opin Microbiol* 1999; 2(1):46-50.
136. Galan JE. *Salmonella* interactions with host cells: type III secretion at work. *Annu Rev Cell Dev Biol* 2001; 17:53-86.
137. Ehrbar K, Miroid S, Friebel A, Stender S, Hardt WD. Characterization of effector proteins translocated via the SPI1 type III secretion system of *Salmonella typhimurium*. *Int J Med Microbiol* 2002; 291(6-7):479-485.
138. Boyle EC, Brown NF, Finlay BB. *Salmonella enterica* serovar Typhimurium effectors SopB, SopE, SopE2 and SipA disrupt tight junction structure and function. *Cell Microbiol* 2006; 8(12):1946-1957.
139. Watanabe M, Fiji HD, Guo L, Chan L, Kinderman SS, Slamon DJ et al. Inhibitors of protein geranylgeranyltransferase I and Rab geranylgeranyltransferase identified from a library of allenoate-derived compounds. *J Biol Chem* 2008; 283(15):9571-9579.
140. Braga VM. Cell-cell adhesion and signalling. *Curr Opin Cell Biol* 2002; 14(5):546-556.
141. Friebel A, Ilchmann H, Aepfelbacher M, Ehrbar K, Machleidt W, Hardt WD. SopE and SopE2 from *Salmonella typhimurium* activate different sets of RhoGTPases of the host cell. *J Biol Chem* 2001; 276(36):34035-34040.
142. Stender S, Friebel A, Linder S, Rohde M, Miroid S, Hardt WD. Identification of SopE2 from *Salmonella typhimurium*, a conserved guanine nucleotide exchange factor for Cdc42 of the host cell. *Mol Microbiol* 2000; 36(6):1206-1221.
143. Zhou D, Chen LM, Hernandez L, Shears SB, Galan JE. A *Salmonella* inositol polyphosphatase acts in conjunction with other bacterial effectors to promote host cell actin cytoskeleton rearrangements and bacterial internalization. *Mol Microbiol* 2001; 39(2):248-259.
144. Zhou D, Mooseker MS, Galan JE. Role of the *S. typhimurium* actin-binding protein SipA in bacterial internalization. *Science* 1999; 283(5410):2092-2095.
145. Zhang YG, Wu S, Xia Y, Sun J. *Salmonella* infection upregulates the leaky protein claudin-2 in intestinal epithelial cells. *PLoS One* 2013; 8(3):e58606.
146. Uzal FA, Vidal JE, McClane BA, Gurjar AA. Toxins Involved in Mammalian Veterinary Diseases. *Open Toxicology J* 2010; 2:24-42.
147. Hanna PC, Mietzner TA, Schoolnik GK, McClane BA. Localization of the receptor-binding region of *Clostridium perfringens* enterotoxin utilizing cloned toxin fragments and synthetic peptides. The 30 C-terminal amino acids define a functional binding region. *J Biol Chem* 1991; 266(17):11037-11043.
148. Hanna PC, Wieckowski EU, Mietzner TA, McClane BA. Mapping of functional regions of *Clostridium perfringens* type A enterotoxin. *Infect Immun* 1992; 60(5):2110-2114.
149. McClane BA. *Clostridium perfringens* enterotoxin acts by producing small molecule permeability alterations in plasma membranes. *Toxicology* 1994; 87(1-3):43-67.

150. Chakrabarti G, Zhou X, McClane BA. Death pathways activated in CaCo-2 cells by Clostridium perfringens enterotoxin. *Infect Immun* 2003; 71(8):4260-4270.
151. Chakrabarti G, McClane BA. The importance of calcium influx, calpain and calmodulin for the activation of CaCo-2 cell death pathways by Clostridium perfringens enterotoxin. *Cell Microbiol* 2005; 7(1):129-146.
152. Sonoda N, Furuse M, Sasaki H, Yonemura S, Katahira J, Horiguchi Y et al. Clostridium perfringens enterotoxin fragment removes specific claudins from tight junction strands: Evidence for direct involvement of claudins in tight junction barrier. *J Cell Biol* 1999; 147(1):195-204.
153. Shrestha A, McClane BA. Human claudin-8 and -14 are receptors capable of conveying the cytotoxic effects of Clostridium perfringens enterotoxin. *MBio* 2013; 4(1).
154. Robertson SL, Smedley JG, III, McClane BA. Identification of a claudin-4 residue important for mediating the host cell binding and action of Clostridium perfringens enterotoxin. *Infect Immun* 2010; 78(1):505-517.
155. Veshnyakova A, Piontek J, Protze J, Waziri N, Heise I, Krause G. Mechanism of Clostridium perfringens enterotoxin interaction with claudin-3/-4 protein suggests structural modifications of the toxin to target specific claudins. *J Biol Chem* 2012; 287(3):1698-1708.
156. Sonoda N, Furuse M, Sasaki H, Yonemura S, Katahira J, Horiguchi Y et al. Clostridium perfringens enterotoxin fragment removes specific claudins from tight junction strands: Evidence for direct involvement of claudins in tight junction barrier. *J Cell Biol* 1999; 147(1):195-204.
157. Berkes J, Viswanathan VK, Savkovic SD, Hecht G. Intestinal epithelial responses to enteric pathogens: effects on the tight junction barrier, ion transport, and inflammation. *Gut* 2003; 52(3):439-451.
158. Burgel N, Bojarski C, Mankertz J, Zeitz M, Fromm M, Schulzke JD. Mechanisms of diarrhea in collagenous colitis. *Gastroenterology* 2002; 123(2):433-443.
159. Hering NA, Andres S, Fromm A, van Tol EA, Amasheh M, Mankertz J et al. Transforming growth factor-beta, a whey protein component, strengthens the intestinal barrier by upregulating claudin-4 in HT-29/B6 cells. *J Nutr* 2011; 141(5):783-789.
160. Marchiando AM, Graham WV, Turner JR. Epithelial barriers in homeostasis and disease. *Annu Rev Pathol* 2010; 5:119-144.
161. Siljamaki E, Raiko L, Toriseva M, Nissinen L, Nareoja T, Peltonen J et al. p38delta mitogen-activated protein kinase regulates the expression of tight junction protein ZO-1 in differentiating human epidermal keratinocytes. *Arch Dermatol Res* 2014; 306(2):131-141.
162. Costa AM, Leite M, Seruca R, Figueiredo C. Adherens junctions as targets of microorganisms: a focus on Helicobacter pylori. *FEBS Lett* 2013; 587(3):259-265.
163. Hong SH, Kim GY, Chang YC, Moon SK, Kim WJ, Choi YH. Bufalin prevents the migration and invasion of T24 bladder carcinoma cells through the inactivation of matrix metalloproteinases and modulation of tight junctions. *Int J Oncol* 2013; 42(1):277-286.
164. van MG, Simons K. The function of tight junctions in maintaining differences in lipid composition between the apical and the basolateral cell surface domains of MDCK cells. *EMBO J* 1986; 5(7):1455-1464.
165. Cerejido M, Valdes J, Shoshani L, Contreras RG. Role of tight junctions in establishing and maintaining cell polarity. *Annu Rev Physiol* 1998; 60:161-177.

166. Schneeberger EE, Lynch RD. Structure, function, and regulation of cellular tight junctions. *Am J Physiol* 1992; 262(6 Pt 1):L647-L661.
167. Gumbiner BM. Breaking through the tight junction barrier. *J Cell Biol* 1993; 123(6 Pt 2):1631-1633.
168. Tsukita S, Yamazaki Y, Katsuno T, Tamura A, Tsukita S. Tight junction-based epithelial microenvironment and cell proliferation. *Oncogene* 2008; 27(55):6930-6938.
169. Matter K, Balda MS. Signalling to and from tight junctions. *Nat Rev Mol Cell Biol* 2003; 4(3):225-236.
170. Kojima T, Murata M, Yamamoto T, Lan M, Imamura M, Son S et al. Tight junction proteins and signal transduction pathways in hepatocytes. *Histol Histopathol* 2009; 24(11):1463-1472.
171. Schmitz H, Barmeyer C, Fromm M, Runkel N, Foss HD, Bentzel CJ et al. Altered tight junction structure contributes to the impaired epithelial barrier function in ulcerative colitis. *Gastroenterology* 1999; 116(2):301-309.
172. Tsukita S, Furuse M, Itoh M. Multifunctional strands in tight junctions. *Nat Rev Mol Cell Biol* 2001; 2(4):285-293.
173. Schneeberger EE, Lynch RD. The tight junction: a multifunctional complex. *Am J Physiol Cell Physiol* 2004; 286(6):C1213-C1228.
174. Ikenouchi J, Furuse M, Furuse K, Sasaki H, Tsukita S, Tsukita S. Tricellulin constitutes a novel barrier at tricellular contacts of epithelial cells. *J Cell Biol* 2005; 171(6):939-945.
175. Loh YH, Christoffels A, Brenner S, Hunziker W, Venkatesh B. Extensive expansion of the claudin gene family in the teleost fish, *Fugu rubripes*. *Genome Res* 2004; 14(7):1248-1257.
176. Tsukita S, Furuse M, Itoh M. Multifunctional strands in tight junctions. *Nat Rev Mol Cell Biol* 2001; 2(4):285-293.
177. Furuse M, Hata M, Furuse K, Yoshida Y, Haratake A, Sugitani Y et al. Claudin-based tight junctions are crucial for the mammalian epidermal barrier: a lesson from claudin-1-deficient mice. *J Cell Biol* 2002; 156(6):1099-1111.
178. Krause G, Winkler L, Piehl C, Blasig I, Piontek J, Muller SL. Structure and function of extracellular claudin domains. *Ann N Y Acad Sci* 2009; 1165:34-43.
179. Oliveira SS, Morgado-Diaz JA. Claudins: multifunctional players in epithelial tight junctions and their role in cancer. *Cell Mol Life Sci* 2007; 64(1):17-28.
180. Hou J, Gomes AS, Paul DL, Goodenough DA. Study of claudin function by RNA interference. *J Biol Chem* 2006; 281(47):36117-36123.
181. Alexandre MD, Jeansonne BG, Renegar RH, Tatum R, Chen YH. The first extracellular domain of claudin-7 affects paracellular Cl⁻ permeability. *Biochem Biophys Res Commun* 2007; 357(1):87-91.
182. Tatum R, Zhang Y, Salleng K, Lu Z, Lin JJ, Lu Q et al. Renal salt wasting and chronic dehydration in claudin-7-deficient mice. *Am J Physiol Renal Physiol* 2010; 298(1):F24-F34.
183. Rosenthal R, Milatz S, Krug SM, Oelrich B, Schulzke JD, Amasheh S et al. Claudin-2, a component of the tight junction, forms a paracellular water channel. *J Cell Sci* 2010; 123(Pt 11):1913-1921.

184. Zeissig S, Burgel N, Gunzel D, Richter J, Mankertz J, Wahnschaffe U et al. Changes in expression and distribution of claudin 2, 5 and 8 lead to discontinuous tight junctions and barrier dysfunction in active Crohn's disease. *Gut* 2007; 56(1):61-72.
185. Das P, Goswami P, Das TK, Nag T, Sreenivas V, Ahuja V et al. Comparative tight junction protein expressions in colonic Crohn's disease, ulcerative colitis, and tuberculosis: a new perspective. *Virchows Arch* 2012; 460(3):261-270.
186. Darji P, Vijayaraghavan R, Thiagarajan CM, Sharma RK, Subbarao B, Pishardy R et al. Conversion from mycophenolate mofetil to enteric-coated mycophenolate sodium in renal transplant recipients with gastrointestinal tract disorders. *Transplant Proc* 2008; 40(7):2262-2267.
187. Moro JA, Almenar L, Martinez-Dolz L, Sanchez-Lazaro I, Agüero J, Salvador A. Tolerance profile of the proliferation signal inhibitors everolimus and sirolimus in heart transplantation. *Transplant Proc* 2008; 40(9):3034-3036.
188. Pirsch JD, Miller J, Deierhoi MH, Vincenti F, Filo RS. A comparison of tacrolimus (FK506) and cyclosporine for immunosuppression after cadaveric renal transplantation. FK506 Kidney Transplant Study Group. *Transplantation* 1997; 63(7):977-983.
189. Qasim M, Rahman H, Ahmed R, Oellerich M, Asif AR. Mycophenolic acid mediated disruption of the intestinal epithelial tight junctions. *Exp Cell Res* 2014; 322(2):277-289.
190. Qasim M, Rahman H, Oellerich M, Asif AR. Differential proteome analysis of human embryonic kidney cell line (HEK-293) following mycophenolic acid treatment. *Proteome Sci* 2011; 9:57.
191. Tsukita S, Furuse M. The structure and function of claudins, cell adhesion molecules at tight junctions. *Ann N Y Acad Sci* 2000; 915:129-135.
192. Dhawan P, Singh AB, Deane NG, No Y, Shiou SR, Schmidt C et al. Claudin-1 regulates cellular transformation and metastatic behavior in colon cancer. *J Clin Invest* 2005; 115(7):1765-1776.
193. Bhat AA, Sharma A, Pope J, Krishnan M, Washington MK, Singh AB et al. Caudal homeobox protein Cdx-2 cooperates with Wnt pathway to regulate claudin-1 expression in colon cancer cells. *PLoS One* 2012; 7(6):e37174.
194. Silberg DG, Swain GP, Suh ER, Traber PG. Cdx1 and cdx2 expression during intestinal development. *Gastroenterology* 2000; 119(4):961-971.
195. van den Akker E, Forlani S, Chawengsaksophak K, de GW, Beck F, Meyer BI et al. Cdx1 and Cdx2 have overlapping functions in anteroposterior patterning and posterior axis elongation. *Development* 2002; 129(9):2181-2193.
196. Chawengsaksophak K, James R, Hammond VE, Kontgen F, Beck F. Homeosis and intestinal tumours in Cdx2 mutant mice. *Nature* 1997; 386(6620):84-87.
197. James R, Kazenwadel J. Homeobox gene expression in the intestinal epithelium of adult mice. *J Biol Chem* 1991; 266(5):3246-3251.
198. Houde M, Laprise P, Jean D, Blais M, Asselin C, Rivard N. Intestinal epithelial cell differentiation involves activation of p38 mitogen-activated protein kinase that regulates the homeobox transcription factor CDX2. *J Biol Chem* 2001; 276(24):21885-21894.

199. Rings EH, Boudreau F, Taylor JK, Moffett J, Suh ER, Traber PG. Phosphorylation of the serine 60 residue within the Cdx2 activation domain mediates its transactivation capacity. *Gastroenterology* 2001; 121(6):1437-1450.
200. Boulanger J, Vezina A, Mongrain S, Boudreau F, Perreault N, Auclair BA et al. Cdk2-dependent phosphorylation of homeobox transcription factor CDX2 regulates its nuclear translocation and proteasome-mediated degradation in human intestinal epithelial cells. *J Biol Chem* 2005; 280(18):18095-18107.
201. Song J, Ugai H, Ogawa K, Wang Y, Sarai A, Obata Y et al. Two consecutive zinc fingers in Sp1 and in MAZ are essential for interactions with cis-elements. *J Biol Chem* 2001; 276(32):30429-30434.
202. Philipsen S, Suske G. A tale of three fingers: the family of mammalian Sp/XKLF transcription factors. *Nucleic Acids Res* 1999; 27(15):2991-3000.
203. Mastrangelo IA, Courey AJ, Wall JS, Jackson SP, Hough PV. DNA looping and Sp1 multimer links: a mechanism for transcriptional synergism and enhancement. *Proc Natl Acad Sci U S A* 1991; 88(13):5670-5674.
204. Li L, He S, Sun JM, Davie JR. Gene regulation by Sp1 and Sp3. *Biochem Cell Biol* 2004; 82(4):460-471.
205. Doetzlhofer A, Rotheneder H, Lagger G, Koranda M, Kurtev V, Brosch G et al. Histone deacetylase 1 can repress transcription by binding to Sp1. *Mol Cell Biol* 1999; 19(8):5504-5511.
206. Wang HB, Wang PY, Wang X, Wan YL, Liu YC. Butyrate enhances intestinal epithelial barrier function via up-regulation of tight junction protein Claudin-1 transcription. *Dig Dis Sci* 2012; 57(12):3126-3135.
207. Christakos S, Dhawan P, Ajibade D, Benn BS, Feng J, Joshi SS. Mechanisms involved in vitamin D mediated intestinal calcium absorption and in non-classical actions of vitamin D. *J Steroid Biochem Mol Biol* 2010; 121(1-2):183-187.
208. Weber CR, Nalle SC, Tretiakova M, Rubin DT, Turner JR. Claudin-1 and claudin-2 expression is elevated in inflammatory bowel disease and may contribute to early neoplastic transformation. *Lab Invest* 2008; 88(10):1110-1120.
209. Dhawan P, Ahmad R, Chaturvedi R, Smith JJ, Midha R, Mittal MK et al. Claudin-2 expression increases tumorigenicity of colon cancer cells: role of epidermal growth factor receptor activation. *Oncogene* 2011; 30(29):3234-3247.
210. Buchert M, Papin M, Bonnans C, Darido C, Raye WS, Garambois V et al. Symplekin promotes tumorigenicity by up-regulating claudin-2 expression. *Proc Natl Acad Sci U S A* 2010; 107(6):2628-2633.
211. Zhang YG, Wu S, Xia Y, Sun J. Salmonella infection upregulates the leaky protein claudin-2 in intestinal epithelial cells. *PLoS One* 2013; 8(3):e58606.
212. Suzuki T, Yoshinaga N, Tanabe S. Interleukin-6 (IL-6) regulates claudin-2 expression and tight junction permeability in intestinal epithelium. *J Biol Chem* 2011; 286(36):31263-31271.
213. Honda H, Pazin MJ, D'Souza T, Ji H, Morin PJ. Regulation of the CLDN3 gene in ovarian cancer cells. *Cancer Biol Ther* 2007; 6(11):1733-1742.
214. Morin PJ. Claudin proteins in human cancer: promising new targets for diagnosis and therapy. *Cancer Res* 2005; 65(21):9603-9606.

215. Honda H, Pazin MJ, Ji H, Wernyj RP, Morin PJ. Crucial roles of Sp1 and epigenetic modifications in the regulation of the CLDN4 promoter in ovarian cancer cells. *J Biol Chem* 2006; 281(30):21433-21444.
216. Wang F, Daugherty B, Keise LL, Wei Z, Foley JP, Savani RC et al. Heterogeneity of claudin expression by alveolar epithelial cells. *Am J Respir Cell Mol Biol* 2003; 29(1):62-70.
217. Amasheh S, Schmidt T, Mahn M, Florian P, Mankertz J, Tavalali S et al. Contribution of claudin-5 to barrier properties in tight junctions of epithelial cells. *Cell Tissue Res* 2005; 321(1):89-96.
218. Rahner C, Mitic LL, Anderson JM. Heterogeneity in expression and subcellular localization of claudins 2, 3, 4, and 5 in the rat liver, pancreas, and gut. *Gastroenterology* 2001; 120(2):411-422.
219. Xuan Z, Zhang MQ. From worm to human: bioinformatics approaches to identify FOXO target genes. *Mech Ageing Dev* 2005; 126(1):209-215.
220. Furuyama T, Nakazawa T, Nakano I, Mori N. Identification of the differential distribution patterns of mRNAs and consensus binding sequences for mouse DAF-16 homologues. *Biochem J* 2000; 349(Pt 2):629-634.
221. Chung SY, Huang WC, Su CW, Lee KW, Chi HC, Lin CT et al. FoxO6 and PGC-1alpha form a regulatory loop in myogenic cells. *Biosci Rep* 2013; 33(3).
222. Taddei A, Giampietro C, Conti A, Orsenigo F, Breviario F, Pirazzoli V et al. Endothelial adherens junctions control tight junctions by VE-cadherin-mediated upregulation of claudin-5. *Nat Cell Biol* 2008; 10(8):923-934.
223. Kohno Y, Okamoto T, Ishibe T, Nagayama S, Shima Y, Nishijo K et al. Expression of claudin7 is tightly associated with epithelial structures in synovial sarcomas and regulated by an Ets family transcription factor, ELF3. *J Biol Chem* 2006; 281(50):38941-38950.
224. Trojanowska M. Ets factors and regulation of the extracellular matrix. *Oncogene* 2000; 19(55):6464-6471.
225. Sharrocks AD. The ETS-domain transcription factor family. *Nat Rev Mol Cell Biol* 2001; 2(11):827-837.
226. Tootle TL, Rebay I. Post-translational modifications influence transcription factor activity: a view from the ETS superfamily. *Bioessays* 2005; 27(3):285-298.
227. Oettgen P, Alani RM, Barcinski MA, Brown L, Akbarali Y, Boltax J et al. Isolation and characterization of a novel epithelium-specific transcription factor, ESE-1, a member of the ets family. *Mol Cell Biol* 1997; 17(8):4419-4433.
228. Cabral A, Fischer DF, Vermeij WP, Backendorf C. Distinct functional interactions of human Skn-1 isoforms with ESE-1 during keratinocyte terminal differentiation. *J Biol Chem* 2003; 278(20):17792-17799.
229. Reddy SP, Vuong H, Adiseshaiah P. Interplay between proximal and distal promoter elements is required for squamous differentiation marker induction in the bronchial epithelium: role for ESE-1, Sp1, and AP-1 proteins. *J Biol Chem* 2003; 278(24):21378-21387.
230. Darsigny M, Babeu JP, Dupuis AA, Furth EE, Seidman EG, Levy E et al. Loss of hepatocyte-nuclear-factor-4alpha affects colonic ion transport and causes chronic inflammation resembling inflammatory bowel disease in mice. *PLoS One* 2009; 4(10):e7609.
231. Babeu JP, Boudreau F. Hepatocyte nuclear factor 4-alpha involvement in liver and intestinal inflammatory networks. *World J Gastroenterol* 2014; 20(1):22-30.

232. Giebisch G, Klose RM, Windhager EE. MICROPUNCTURE STUDY OF HYPERTONIC SODIUM CHLORIDE LOADING IN THE RAT. *Am J Physiol* 1964; 206:687-693.
233. Cole DE, Quamme GA. Inherited disorders of renal magnesium handling. *J Am Soc Nephrol* 2000; 11(10):1937-1947.
234. Hebert SC. Calcium and salinity sensing by the thick ascending limb: a journey from mammals to fish and back again. *Kidney Int Suppl* 2004;(91):S28-S33.
235. Hou J, Goodenough DA. Claudin-16 and claudin-19 function in the thick ascending limb. *Curr Opin Nephrol Hypertens* 2010; 19(5):483-488.
236. Luk JM, Tong MK, Mok BW, Tam PC, Yeung WS, Lee KF. Sp1 site is crucial for the mouse claudin-19 gene expression in the kidney cells. *FEBS Lett* 2004; 578(3):251-256.
237. Bunnapradist S, Sampaio MS, Wilkinson AH, Pham PT, Huang E, Kuo HT et al. Changes in the small bowel of symptomatic kidney transplant recipients converted from mycophenolate mofetil to enteric-coated mycophenolate sodium. *Am J Nephrol* 2014; 40(2):184-190.
238. Xu L, Cai M, Shi BY, Li ZL, Li X, Jin HL. A prospective analysis of the effects of enteric-coated mycophenolate sodium and mycophenolate mofetil co-medicated with a proton pump inhibitor in kidney transplant recipients at a single institute in China. *Transplant Proc* 2014; 46(5):1362-1365.
239. Watts RW. Some regulatory and integrative aspects of purine nucleotide biosynthesis and its control: an overview. *Adv Enzyme Regul* 1983; 21:33-51.
240. Helderman JH, Goral S. Gastrointestinal complications of transplant immunosuppression. *J Am Soc Nephrol* 2002; 13(1):277-287.
241. Malinowski M, Martus P, Lock JF, Neuhaus P, Stockmann M. Systemic influence of immunosuppressive drugs on small and large bowel transport and barrier function. *Transpl Int* 2011; 24(2):184-193.
242. Clayburgh DR, Shen L, Turner JR. A porous defense: the leaky epithelial barrier in intestinal disease. *Lab Invest* 2004; 84(3):282-291.
243. Magnotti LJ, Deitch EA. Burns, bacterial translocation, gut barrier function, and failure. *J Burn Care Rehabil* 2005; 26(5):383-391.
244. Deitch EA. Bacterial translocation or lymphatic drainage of toxic products from the gut: what is important in human beings? *Surgery* 2002; 131(3):241-244.
245. Siljamaki E, Raiko L, Toriseva M, Nissinen L, Nareoja T, Peltonen J et al. p38delta mitogen-activated protein kinase regulates the expression of tight junction protein ZO-1 in differentiating human epidermal keratinocytes. *Arch Dermatol Res* 2014; 306(2):131-141.
246. Hong SH, Kim GY, Chang YC, Moon SK, Kim WJ, Choi YH. Bufalin prevents the migration and invasion of T24 bladder carcinoma cells through the inactivation of matrix metalloproteinases and modulation of tight junctions. *Int J Oncol* 2013; 42(1):277-286.
247. Costa AM, Leite M, Seruca R, Figueiredo C. Adherens junctions as targets of microorganisms: a focus on *Helicobacter pylori*. *FEBS Lett* 2013; 587(3):259-265.
248. Shen L, Weber CR, Raleigh DR, Yu D, Turner JR. Tight junction pore and leak pathways: a dynamic duo. *Annu Rev Physiol* 2011; 73:283-309.

249. Sawada N. Tight junction-related human diseases. *Pathol Int* 2013; 63(1):1-12.
250. Zolotarevsky Y, Hecht G, Koutsouris A, Gonzalez DE, Quan C, Tom J et al. A membrane-permeant peptide that inhibits MLC kinase restores barrier function in in vitro models of intestinal disease. *Gastroenterology* 2002; 123(1):163-172.
251. Utech M, Ivanov AI, Samarin SN, Bruewer M, Turner JR, Mrsny RJ et al. Mechanism of IFN-gamma-induced endocytosis of tight junction proteins: myosin II-dependent vacuolarization of the apical plasma membrane. *Mol Biol Cell* 2005; 16(10):5040-5052.
252. Schwarz BT, Wang F, Shen L, Clayburgh DR, Su L, Wang Y et al. LIGHT signals directly to intestinal epithelia to cause barrier dysfunction via cytoskeletal and endocytic mechanisms. *Gastroenterology* 2007; 132(7):2383-2394.
253. Qasim M, Rahman H, Ahmed R, Oellerich M, Asif AR. Mycophenolic acid mediated disruption of the intestinal epithelial tight junctions. *Exp Cell Res* 2014; 322(2):277-289.
254. Marchiando AM, Shen L, Graham WV, Weber CR, Schwarz BT, Austin JR et al. Caveolin-1-dependent occludin endocytosis is required for TNF-induced tight junction regulation in vivo. *J Cell Biol* 2010; 189(1):111-126.
255. Al-Sadi R, Guo S, Ye D, Dokladny K, Alhmoud T, Ereifej L et al. Mechanism of IL-1beta modulation of intestinal epithelial barrier involves p38 kinase and activating transcription factor-2 activation. *J Immunol* 2013; 190(12):6596-6606.
256. Mittelstadt PR, Salvador JM, Fornace AJ, Jr., Ashwell JD. Activating p38 MAPK: new tricks for an old kinase. *Cell Cycle* 2005; 4(9):1189-1192.
257. Keren A, Tamir Y, Bengal E. The p38 MAPK signaling pathway: a major regulator of skeletal muscle development. *Mol Cell Endocrinol* 2006; 252(1-2):224-230.
258. Baan B, van DH, van der Zon GC, Maassen JA, Ouwens DM. The role of c-Jun N-terminal kinase, p38, and extracellular signal-regulated kinase in insulin-induced Thr69 and Thr71 phosphorylation of activating transcription factor 2. *Mol Endocrinol* 2006; 20(8):1786-1795.
259. Kelkar N, Standen CL, Davis RJ. Role of the JIP4 scaffold protein in the regulation of mitogen-activated protein kinase signaling pathways. *Mol Cell Biol* 2005; 25(7):2733-2743.
260. Lee MR, Dominguez C. MAP kinase p38 inhibitors: clinical results and an intimate look at their interactions with p38alpha protein. *Curr Med Chem* 2005; 12(25):2979-2994.
261. Feldman G, Kiely B, Martin N, Ryan G, McMorrow T, Ryan MP. Role for TGF-beta in cyclosporine-induced modulation of renal epithelial barrier function. *J Am Soc Nephrol* 2007; 18(6):1662-1671.
262. Schlegel N, Meir M, Spindler V, Germer CT, Waschke J. Differential role of Rho GTPases in intestinal epithelial barrier regulation in vitro. *J Cell Physiol* 2011; 226(5):1196-1203.
263. Rozen S, Skaletsky H. Primer3 on the WWW for general users and for biologist programmers. *Methods Mol Biol* 2000; 132:365-386.
264. Schmittgen TD, Livak KJ. Analyzing real-time PCR data by the comparative C(T) method. *Nat Protoc* 2008; 3(6):1101-1108.

265. Bolin I, Lonroth H, Svennerholm AM. Identification of *Helicobacter pylori* by immunological dot blot method based on reaction of a species-specific monoclonal antibody with a surface-exposed protein. *J Clin Microbiol* 1995; 33(2):381-384.
266. Boyd M, Bressendorff S, Moller J, Olsen J, Troelsen JT. Mapping of HNF4alpha target genes in intestinal epithelial cells. *BMC Gastroenterol* 2009; 9:68.
267. Lin X, Tirichine L, Bowler C. Protocol: Chromatin immunoprecipitation (ChIP) methodology to investigate histone modifications in two model diatom species. *Plant Methods* 2012; 8(1):48.
268. Yang Y, Tang Q, Zhao M, Liang G, Wu H, Li D et al. The effect of mycophenolic acid on epigenetic modifications in lupus CD4+T cells. *Clin Immunol* 2015; 158(1):67-76.
269. Cunningham KE, Turner JR. Myosin light chain kinase: pulling the strings of epithelial tight junction function. *Ann N Y Acad Sci* 2012; 1258:34-42.
270. Qasim M, Rahman H, Oellerich M, Asif AR. Differential proteome analysis of human embryonic kidney cell line (HEK-293) following mycophenolic acid treatment. *Proteome Sci* 2011; 9:57.
271. Kumar S, Jiang MS, Adams JL, Lee JC. Pyridinylimidazole compound SB 203580 inhibits the activity but not the activation of p38 mitogen-activated protein kinase. *Biochem Biophys Res Commun* 1999; 263(3):825-831.
272. Anderson JM, Van Itallie CM. Tight junctions and the molecular basis for regulation of paracellular permeability. *Am J Physiol* 1995; 269(4 Pt 1):G467-G475.
273. Gonzalez-Mariscal L, Tapia R, Chamorro D. Crosstalk of tight junction components with signaling pathways. *Biochim Biophys Acta* 2008; 1778(3):729-756.
274. Farquhar MG, Palade GE. Junctional complexes in various epithelia. *J Cell Biol* 1963; 17:375-412.
275. Taylor CT, Dzus AL, Colgan SP. Autocrine regulation of epithelial permeability by hypoxia: role for polarized release of tumor necrosis factor alpha. *Gastroenterology* 1998; 114(4):657-668.
276. Pappenheimer JR. Physiological regulation of transepithelial impedance in the intestinal mucosa of rats and hamsters. *J Membr Biol* 1987; 100(2):137-148.
277. Anderson JM, Van Itallie CM. Physiology and function of the tight junction. *Cold Spring Harb Perspect Biol* 2009; 1(2):a002584.
278. Hering NA, Fromm M, Schulzke JD. Determinants of colonic barrier function in inflammatory bowel disease and potential therapeutics. *J Physiol* 2012; 590(Pt 5):1035-1044.
279. Prasad S, Mingrino R, Kaukinen K, Hayes KL, Powell RM, MacDonald TT et al. Inflammatory processes have differential effects on claudins 2, 3 and 4 in colonic epithelial cells. *Lab Invest* 2005; 85(9):1139-1162.
280. Turner JR. Molecular basis of epithelial barrier regulation: from basic mechanisms to clinical application. *Am J Pathol* 2006; 169(6):1901-1909.
281. Turner JR. Intestinal mucosal barrier function in health and disease. *Nat Rev Immunol* 2009; 9(11):799-809.
282. Strahl BD, Allis CD. The language of covalent histone modifications. *Nature* 2000; 403(6765):41-45.

283. Kouzarides T. Chromatin modifications and their function. *Cell* 2007; 128(4):693-705.
284. Bernstein BE, Meissner A, Lander ES. The mammalian epigenome. *Cell* 2007; 128(4):669-681.
285. Nishida H, Suzuki T, Kondo S, Miura H, Fujimura Y, Hayashizaki Y. Histone H3 acetylated at lysine 9 in promoter is associated with low nucleosome density in the vicinity of transcription start site in human cell. *Chromosome Res* 2006; 14(2):203-211.
286. Gupta AP, Chin WH, Zhu L, Mok S, Luah YH, Lim EH et al. Dynamic epigenetic regulation of gene expression during the life cycle of malaria parasite *Plasmodium falciparum*. *PLoS Pathog* 2013; 9(2):e1003170.
287. Suzuki T, Kondo S, Wakayama T, Cizdziel PE, Hayashizaki Y. Genome-wide analysis of abnormal H3K9 acetylation in cloned mice. *PLoS One* 2008; 3(4):e1905.
288. Batovska DI, Kim DH, Mitsuhashi S, Cho YS, Kwon HJ, Ubukata M. Hydroxamic acid derivatives of mycophenolic acid inhibit histone deacetylase at the cellular level. *Biosci Biotechnol Biochem* 2008; 72(10):2623-2631.
289. Barski A, Cuddapah S, Cui K, Roh TY, Schones DE, Wang Z et al. High-resolution profiling of histone methylations in the human genome. *Cell* 2007; 129(4):823-837.
290. Guenther MG, Levine SS, Boyer LA, Jaenisch R, Young RA. A chromatin landmark and transcription initiation at most promoters in human cells. *Cell* 2007; 130(1):77-88.
291. Ransom JT. Mechanism of action of mycophenolate mofetil. *Ther Drug Monit* 1995; 17(6):681-684.
292. Oremus M, Zeidler J, Ensom MH, Matsuda-Abedini M, Balion C, Booker L et al. Utility of monitoring mycophenolic acid in solid organ transplant patients. *Evid Rep Technol Assess (Full Rep)* 2008;(164):1-131.
293. Csoka AB, Szyf M. Epigenetic side-effects of common pharmaceuticals: a potential new field in medicine and pharmacology. *Med Hypotheses* 2009; 73(5):770-780.
294. Cornacchia E, Golbus J, Maybaum J, Strahler J, Hanash S, Richardson B. Hydralazine and procainamide inhibit T cell DNA methylation and induce autoreactivity. *J Immunol* 1988; 140(7):2197-2200.
295. Melnik BC. Isotretinoin and FoxO1: A scientific hypothesis. *Dermatoendocrinol* 2011; 3(3):141-165.
296. Yang Y, Tang Q, Zhao M, Liang G, Wu H, Li D et al. The effect of mycophenolic acid on epigenetic modifications in lupus CD4+T cells. *Clin Immunol* 2015; 158(1):67-76.
297. Schmittgen TD, Livak KJ. Analyzing real-time PCR data by the comparative C(T) method. *Nat Protoc* 2008; 3(6):1101-1108.
298. Nesvizhskii AI, Keller A, Kolker E, Aebersold R. A statistical model for identifying proteins by tandem mass spectrometry. *Anal Chem* 2003; 75(17):4646-4658.
299. Ashburner M, Ball CA, Blake JA, Botstein D, Butler H, Cherry JM et al. Gene ontology: tool for the unification of biology. The Gene Ontology Consortium. *Nat Genet* 2000; 25(1):25-29.
300. Khan N Qasim M Binder L Pantakani DVK Asif AR . Immunosuppressant MPA modulate tight junction through epigenetic activation of MLCK/MLC-2 pathway via p38MAPK.. *Fonrtiers in Physiology*. In press 2015.

301. Yurdakok B, Kismali G, Ozen D. Ptaquiloside-induced cytotoxicity in Crandall feline kidney and HGC-27 cells. *Oncol Lett* 2014; 8(4):1839-1843.
302. Strober W. Trypan blue exclusion test of cell viability. *Curr Protoc Immunol* 2001; Appendix 3:Appendix.
303. Vermeulen M, Timmers HT. Grasping trimethylation of histone H3 at lysine 4. *Epigenomics* 2010; 2(3):395-406.
304. Arthur RK, Ma L, Slattery M, Spokony RF, Ostapenko A, Negre N et al. Evolution of H3K27me3-marked chromatin is linked to gene expression evolution and to patterns of gene duplication and diversification. *Genome Res* 2014; 24(7):1115-1124.
305. Ji X, Dadon DB, Abraham BJ, Lee TI, Jaenisch R, Bradner JE et al. Chromatin proteomic profiling reveals novel proteins associated with histone-marked genomic regions. *Proc Natl Acad Sci U S A* 2015; 112(12):3841-3846.
306. Soldi M, Bonaldi T. The proteomic investigation of chromatin functional domains reveals novel synergisms among distinct heterochromatin components. *Mol Cell Proteomics* 2013; 12(3):764-780.
307. Tannu NS, Hemby SE. Methods for proteomics in neuroscience. *Prog Brain Res* 2006; 158:41-82.
308. Muramatsu T. Midkine, a heparin-binding cytokine with multiple roles in development, repair and diseases. *Proc Jpn Acad Ser B Phys Biol Sci* 2010; 86(4):410-425.
309. Muramatsu T. Midkine, a heparin-binding cytokine with multiple roles in development, repair and diseases. *Proc Jpn Acad Ser B Phys Biol Sci* 2010; 86(4):410-425.
310. Krzystek-Korpacka M, Neubauer K, Matusiewicz M. Circulating midkine in Crohn's disease: clinical implications. *Inflamm Bowel Dis* 2010; 16(2):208-215.
311. Krzystek-Korpacka M, Neubauer K, Matusiewicz M. Clinical relevance of circulating midkine in ulcerative colitis. *Clin Chem Lab Med* 2009; 47(9):1085-1090.
312. Khan N, Asif AR. Transcriptional regulators of claudins in epithelial tight junctions. *Mediators Inflamm* 2015; 2015:219843.
313. Al-Sadi R, Guo S, Ye D, Dokladny K, Alhmoud T, Ereifej L et al. Mechanism of IL-1beta modulation of intestinal epithelial barrier involves p38 kinase and activating transcription factor-2 activation. *J Immunol* 2013; 190(12):6596-6606.
314. Dai LC, Shao JZ, Min LS, Xiao YT, Xiang LX, Ma ZH. Midkine accumulated in nucleolus of HepG2 cells involved in rRNA transcription. *World J Gastroenterol* 2008; 14(40):6249-6253.
315. Dai L, Xu D, Yao X, Lu Y, Xu Z. Conformational determinants of the intracellular localization of midkine. *Biochem Biophys Res Commun* 2005; 330(1):310-317.
316. Ji X, Dadon DB, Abraham BJ, Lee TI, Jaenisch R, Bradner JE et al. Chromatin proteomic profiling reveals novel proteins associated with histone-marked genomic regions. *Proc Natl Acad Sci U S A* 2015; 112(12):3841-3846.
317. Soldi M, Bonaldi T. The proteomic investigation of chromatin functional domains reveals novel synergisms among distinct heterochromatin components. *Mol Cell Proteomics* 2013; 12(3):764-780.
318. Gummert JF, Ikonen T, Morris RE. Newer immunosuppressive drugs: a review. *J Am Soc Nephrol* 1999; 10(6):1366-1380.

319. Sintchak MD, Nimmegern E. The structure of inosine 5'-monophosphate dehydrogenase and the design of novel inhibitors. *Immunopharmacology* 2000; 47(2-3):163-184.
320. Weigel G, Bertalanffy P, Dubsky P, Griesmacher A, Wolner E. Mycophenolic acid influences T helper 2 (Th2) cytokine induced expression of intercellular cell adhesion molecule-1 (ICAM-1) on human endothelial cells. *Clin Chem Lab Med* 1999; 37(3):253-257.
321. Kronen E, Hogenauer C. Diarrhea in the immunocompromised patient. *Gastroenterol Clin North Am* 2012; 41(3):677-701.
322. Fasano A, Fiorentini C, Donelli G, Uzzau S, Kaper JB, Margaretten K et al. Zonula occludens toxin modulates tight junctions through protein kinase C-dependent actin reorganization, in vitro. *J Clin Invest* 1995; 96(2):710-720.
323. Seth A, Yan F, Polk DB, Rao RK. Probiotics ameliorate the hydrogen peroxide-induced epithelial barrier disruption by a PKC- and MAP kinase-dependent mechanism. *Am J Physiol Gastrointest Liver Physiol* 2008; 294(4):G1060-G1069.
324. Khan N, Pantakani DVK, Qasim M, Binder L, Asif AR. Immunosuppressant MPA modulate tight junction through epigenetic activation of MLCK/MLC-2 pathway via p38MAPK. *Frontiers in Physiology* 2015.
325. Khan N, Lenz C, Pantakani DVK, Binder L, Asif AR. Active and repressive chromatin associated proteins profiling after MPA treatment and the role of midkine in epithelial monolayer permeability (In preparation). 2015.
Unpublished Work
326. Muramatsu T, Kadomatsu K. Midkine: an emerging target of drug development for treatment of multiple diseases. *Br J Pharmacol* 2014; 171(4):811-813.
327. Dai L, Xu D, Yao X, Lu Y, Xu Z. Conformational determinants of the intracellular localization of midkine. *Biochem Biophys Res Commun* 2005; 330(1):310-317.
328. Hao H, Maeda Y, Fukazawa T, Yamatsuji T, Takaoka M, Bao XH et al. Inhibition of the growth factor MDK/midkine by a novel small molecule compound to treat non-small cell lung cancer. *PLoS One* 2013; 8(8):e71093.
329. Yao X, Tan Z, Gu B, Wu RR, Liu YK, Dai LC et al. Promotion of self-renewal of embryonic stem cells by midkine. *Acta Pharmacol Sin* 2010; 31(5):629-637.
330. Sambuy Y, de A, I, Ranaldi G, Scarino ML, Stamatii A, Zucco F. The Caco-2 cell line as a model of the intestinal barrier: influence of cell and culture-related factors on Caco-2 cell functional characteristics. *Cell Biol Toxicol* 2005; 21(1):1-26.
331. Qasim M, Rahman H, Ahmed R, Oellerich M, Asif AR. Mycophenolic acid mediated disruption of the intestinal epithelial tight junctions. *Exp Cell Res* 2014; 322(2):277-289.
332. Hong YJ, Yang SY, Nam MH, Koo YC, Lee KW. Caffeic acid inhibits the uptake of 2-amino-1-methyl-6-phenylimidazo[4,5-b]pyridine (PhIP) by inducing the efflux transporters expression in Caco-2 cells. *Biol Pharm Bull* 2014.
333. Khan N, Zahur M, Asif AR. Mechanism of Tight Junction Regulation in Leak-Flux Diarrhea (Submitted). 2015.
Unpublished Work

334. Laprise P, Chailier P, Houde M, Beaulieu JF, Boucher MJ, Rivard N. Phosphatidylinositol 3-kinase controls human intestinal epithelial cell differentiation by promoting adherens junction assembly and p38 MAPK activation. *J Biol Chem* 2002; 277(10):8226-8234.
335. Elsum IA, Martin C, Humbert PO. Scribble regulates an EMT polarity pathway through modulation of MAPK-ERK signaling to mediate junction formation. *J Cell Sci* 2013; 126(Pt 17):3990-3999.
336. Smyth D, McKay CM, Gulbransen BD, Phan VC, Wang A, McKay DM. Interferon-gamma signals via an ERK1/2-ARF6 pathway to promote bacterial internalization by gut epithelia. *Cell Microbiol* 2012; 14(8):1257-1270.
337. Porquet N, Poirier A, Houle F, Pin AL, Gout S, Tremblay PL et al. Survival advantages conferred to colon cancer cells by E-selectin-induced activation of the PI3K-NFkappaB survival axis downstream of Death receptor-3. *BMC Cancer* 2011; 11:285.
338. Manning BD, Cantley LC. AKT/PKB signaling: navigating downstream. *Cell* 2007; 129(7):1261-1274.
339. Bhat AA, Sharma A, Pope J, Krishnan M, Washington MK, Singh AB et al. Caudal homeobox protein Cdx-2 cooperates with Wnt pathway to regulate claudin-1 expression in colon cancer cells. *PLoS One* 2012; 7(6):e37174.
340. Will C, Fromm M, Muller D. Claudin tight junction proteins: novel aspects in paracellular transport. *Perit Dial Int* 2008; 28(6):577-584.
341. Khan N, Asif AR. Transcriptional regulators of claudins in epithelial tight junctions. *Mediators Inflamm* 2015; 2015:219843.
342. Kojima T, Takano K, Yamamoto T, Murata M, Son S, Imamura M et al. Transforming growth factor-beta induces epithelial to mesenchymal transition by down-regulation of claudin-1 expression and the fence function in adult rat hepatocytes. *Liver Int* 2008; 28(4):534-545.
343. Nomura K, Obata K, Keira T, Miyata R, Hirakawa S, Takano K et al. *Pseudomonas aeruginosa* elastase causes transient disruption of tight junctions and downregulation of PAR-2 in human nasal epithelial cells. *Respir Res* 2014; 15:21.
344. Wang WC, Tsai JJ, Kuo CY, Chen HM, Kao SH. Non-proteolytic house dust mite allergen, Der p 2, upregulated expression of tight junction molecule claudin-2 associated with Akt/GSK-3beta/beta-catenin signaling pathway. *J Cell Biochem* 2011; 112(6):1544-1551.
345. Lisewski U, Shi Y, Wrackmeyer U, Fischer R, Chen C, Schirdewan A et al. The tight junction protein CAR regulates cardiac conduction and cell-cell communication. *J Exp Med* 2008; 205(10):2369-2379.
346. Chen ML, Ge Z, Fox JG, Schauer DB. Disruption of tight junctions and induction of proinflammatory cytokine responses in colonic epithelial cells by *Campylobacter jejuni*. *Infect Immun* 2006; 74(12):6581-6589.
347. Groschwitz KR, Hogan SP. Intestinal barrier function: molecular regulation and disease pathogenesis. *J Allergy Clin Immunol* 2009; 124(1):3-20.
348. Lei S, Cheng T, Guo Y, Li C, Zhang W, Zhi F. Somatostatin ameliorates lipopolysaccharide-induced tight junction damage via the ERK-MAPK pathway in Caco2 cells. *Eur J Cell Biol* 2014; 93(7):299-307.
349. Muramatsu T. Structure and function of midkine as the basis of its pharmacological effects. *Br J Pharmacol* 2014; 171(4):814-826.

350. Hawkins PT, Stephens LR. PI3K signalling in inflammation. *Biochim Biophys Acta* 2015; 1851(6):882-897.
351. Roh TY, Cuddapah S, Cui K, Zhao K. The genomic landscape of histone modifications in human T cells. *Proc Natl Acad Sci U S A* 2006; 103(43):15782-15787.
352. Burgering BM, Coffey PJ. Protein kinase B (c-Akt) in phosphatidylinositol-3-OH kinase signal transduction. *Nature* 1995; 376(6541):599-602.
353. Franke TF, Yang SI, Chan TO, Datta K, Kazlauskas A, Morrison DK et al. The protein kinase encoded by the Akt proto-oncogene is a target of the PDGF-activated phosphatidylinositol 3-kinase. *Cell* 1995; 81(5):727-736.
354. Faes S, Dormond O. PI3K and AKT: Unfaithful Partners in Cancer. *Int J Mol Sci* 2015; 16(9):21138-21152.
355. Manning BD, Cantley LC. AKT/PKB signaling: navigating downstream. *Cell* 2007; 129(7):1261-1274.
356. Tokuhira N, Kitagishi Y, Suzuki M, Minami A, Nakanishi A, Ono Y et al. PI3K/AKT/PTEN pathway as a target for Crohn's disease therapy (Review). *Int J Mol Med* 2015; 35(1):10-16.
357. Boyd M, Hansen M, Jensen TG, Pearnau A, Olsen AK, Bram LL et al. Genome-wide analysis of CDX2 binding in intestinal epithelial cells (Caco-2). *J Biol Chem* 2010; 285(33):25115-25125.
358. Gunzel D, Fromm M. Claudins and other tight junction proteins. *Compr Physiol* 2012; 2(3):1819-1852.
359. Inai T, Kobayashi J, Shibata Y. Claudin-1 contributes to the epithelial barrier function in MDCK cells. *Eur J Cell Biol* 1999; 78(12):849-855.
360. Zhang YG, Wu S, Xia Y, Sun J. Salmonella infection upregulates the leaky protein claudin-2 in intestinal epithelial cells. *PLoS One* 2013; 8(3):e58606.
361. Bertiaux-Vandaele N, Youmba SB, Belmonte L, Lecleire S, Antonietti M, Gourcerol G et al. The expression and the cellular distribution of the tight junction proteins are altered in irritable bowel syndrome patients with differences according to the disease subtype. *Am J Gastroenterol* 2011; 106(12):2165-2173.
362. Gerova VA, Stoyanov SG, Katsarov DS, Svinarov DA. Increased intestinal permeability in inflammatory bowel diseases assessed by iohexol test. *World J Gastroenterol* 2011; 17(17):2211-2215.
363. Heller F, Florian P, Bojarski C, Richter J, Christ M, Hillenbrand B et al. Interleukin-13 is the key effector Th2 cytokine in ulcerative colitis that affects epithelial tight junctions, apoptosis, and cell restitution. *Gastroenterology* 2005; 129(2):550-564.
364. Weber CR, Raleigh DR, Su L, Shen L, Sullivan EA, Wang Y et al. Epithelial myosin light chain kinase activation induces mucosal interleukin-13 expression to alter tight junction ion selectivity. *J Biol Chem* 2010; 285(16):12037-12046.
365. Nomura K, Obata K, Keira T, Miyata R, Hirakawa S, Takano K et al. *Pseudomonas aeruginosa* elastase causes transient disruption of tight junctions and downregulation of PAR-2 in human nasal epithelial cells. *Respir Res* 2014; 15:21.
366. Amasheh M, Fromm A, Krug SM, Amasheh S, Andres S, Zeitz M et al. TNF α -induced and berberine-antagonized tight junction barrier impairment via tyrosine kinase, Akt and NF κ B signaling. *J Cell Sci* 2010; 123(Pt 23):4145-4155.

367. Inai T, Kobayashi J, Shibata Y. Claudin-1 contributes to the epithelial barrier function in MDCK cells. *Eur J Cell Biol* 1999; 78(12):849-855.
368. Furuse M, Hata M, Furuse K, Yoshida Y, Haratake A, Sugitani Y et al. Claudin-based tight junctions are crucial for the mammalian epidermal barrier: a lesson from claudin-1-deficient mice. *J Cell Biol* 2002; 156(6):1099-1111.
369. Wittchen ES, Haskins J, Stevenson BR. Protein interactions at the tight junction. Actin has multiple binding partners, and ZO-1 forms independent complexes with ZO-2 and ZO-3. *J Biol Chem* 1999; 274(49):35179-35185.
370. Yokoyama S, Tachibana K, Nakanishi H, Yamamoto Y, Irie K, Mandai K et al. alpha-catenin-independent recruitment of ZO-1 to nectin-based cell-cell adhesion sites through afadin. *Mol Biol Cell* 2001; 12(6):1595-1609.
371. Fanning AS, Anderson JM. Zonula occludens-1 and -2 are cytosolic scaffolds that regulate the assembly of cellular junctions. *Ann N Y Acad Sci* 2009; 1165:113-120.
372. Morita K, Furuse M, Fujimoto K, Tsukita S. Claudin multigene family encoding four-transmembrane domain protein components of tight junction strands. *Proc Natl Acad Sci U S A* 1999; 96(2):511-516.
373. Raleigh DR, Boe DM, Yu D, Weber CR, Marchiando AM, Bradford EM et al. Occludin S408 phosphorylation regulates tight junction protein interactions and barrier function. *J Cell Biol* 2011; 193(3):565-582.
374. Fanning AS, Van Itallie CM, Anderson JM. Zonula occludens-1 and -2 regulate apical cell structure and the zonula adherens cytoskeleton in polarized epithelia. *Mol Biol Cell* 2012; 23(4):577-590.
375. Ikenouchi J, Umeda K, Tsukita S, Furuse M, Tsukita S. Requirement of ZO-1 for the formation of belt-like adherens junctions during epithelial cell polarization. *J Cell Biol* 2007; 176(6):779-786.
376. Ngendahayo MC, Dubreuil JD. Escherichia coli heat-stable toxin b impairs intestinal epithelial barrier function by altering tight junction proteins. *Infect Immun* 2013; 81(8):2819-2827.
377. Bruewer M, Hopkins AM, Hobert ME, Nusrat A, Madara JL. RhoA, Rac1, and Cdc42 exert distinct effects on epithelial barrier via selective structural and biochemical modulation of junctional proteins and F-actin. *Am J Physiol Cell Physiol* 2004; 287(2):C327-C335.
378. Tokuda S, Higashi T, Furuse M. ZO-1 knockout by TALEN-mediated gene targeting in MDCK cells: involvement of ZO-1 in the regulation of cytoskeleton and cell shape. *PLoS One* 2014; 9(8):e104994.
379. Van Itallie CM, Fanning AS, Bridges A, Anderson JM. ZO-1 stabilizes the tight junction solute barrier through coupling to the perijunctional cytoskeleton. *Mol Biol Cell* 2009; 20(17):3930-3940.
380. Furuse M, Sasaki H, Fujimoto K, Tsukita S. A single gene product, claudin-1 or -2, reconstitutes tight junction strands and recruits occludin in fibroblasts. *J Cell Biol* 1998; 143(2):391-401.
381. Li D, Mrsny RJ. Oncogenic Raf-1 disrupts epithelial tight junctions via downregulation of occludin. *J Cell Biol* 2000; 148(4):791-800.
382. Li N, Lewis P, Samuelson D, Liboni K, Neu J. Glutamine regulates Caco-2 cell tight junction proteins. *Am J Physiol Gastrointest Liver Physiol* 2004; 287(3):G726-G733.
383. Li N, Neu J. Glutamine deprivation alters intestinal tight junctions via a PI3-K/Akt mediated pathway in Caco-2 cells. *J Nutr* 2009; 139(4):710-714.

384. Shahabuddin S, Ji R, Wang P, Brailoiu E, Dun N, Yang Y et al. CXCR3 chemokine receptor-induced chemotaxis in human airway epithelial cells: role of p38 MAPK and PI3K signaling pathways. *Am J Physiol Cell Physiol* 2006; 291(1):C34-C39.
385. Delgado-Vega AM, Alarcon-Riquelme ME, Kozyrev SV. Genetic associations in type I interferon related pathways with autoimmunity. *Arthritis Res Ther* 2010; 12 Suppl 1:S2.
386. Runkle EA, Rice SJ, Qi J, Masser D, Antonetti DA, Winslow MM et al. Occludin is a direct target of thyroid transcription factor-1 (TTF-1/NKX2-1). *J Biol Chem* 2012; 287(34):28790-28801.
387. Chen J, Xiao L, Rao JN, Zou T, Liu L, Bellavance E et al. JunD represses transcription and translation of the tight junction protein zona occludens-1 modulating intestinal epithelial barrier function. *Mol Biol Cell* 2008; 19(9):3701-3712.
388. Noda S, Tanabe S, Suzuki T. Naringenin enhances intestinal barrier function through the expression and cytoskeletal association of tight junction proteins in Caco-2 cells. *Mol Nutr Food Res* 2013; 57(11):2019-2028.
389. Wang HB, Wang PY, Wang X, Wan YL, Liu YC. Butyrate enhances intestinal epithelial barrier function via up-regulation of tight junction protein Claudin-1 transcription. *Dig Dis Sci* 2012; 57(12):3126-3135.
390. Prasad S, Mingrino R, Kaukinen K, Hayes KL, Powell RM, MacDonald TT et al. Inflammatory processes have differential effects on claudins 2, 3 and 4 in colonic epithelial cells. *Lab Invest* 2005; 85(9):1139-1162.
391. Terry S, Nie M, Matter K, Balda MS. Rho signaling and tight junction functions. *Physiology (Bethesda)* 2010; 25(1):16-26.

9 Acknowledgment

I am greatly indebted for my research and success to Merciful and Almighty “ALLAH” Who blessed me with the ability to achieve this milestone, and all respects are for the Holy Prophet, Hazrat Muhammad (PBUH).

I would like to express my deepest and sincere gratitude to Prof. Dr. Abdul R. Asif and Dr. Lutz Binder for offering the opportunity to do Ph.D, for their constant encouraging guidance, support, and invaluable suggestions. They provide me inspiring energy and have always been ready for both scientific and social discussions during this period. Their creativity and expertise in research, patience, and motivational skills are exceptional.

I would like to thank and express my profound gratitude to Prof. Dr. Uwe Groß and Prof. Dr. Stefenne Pöggeler for serving on my thesis committee, and for their tremendous scientific suggestions, constructive scientific criticisms which kept me on the right tract during my research project and endless help throughout my PhD research.

I was blessed to work in such a fantastic, inspiring and friendly atmosphere of nice and lovely colleagues Misbah Tauseef, Sonia Ziegler, Sabika Farasat, Saba Khaliq, Muhammad Qasim, Hazir Rahman, Alexander Ziegler, Sidra Shahid, Marlena Pantakani, Jenny Gao, Ivana Markovic and Bharat Singh for giving me critical advice during our discussions and helped me to turn results into science. They were with me through the thick and thin of this long and arduous PhD journey.

I offer special thanks to Dr. Krishna Pantakani and Dr. Christof Lenz, for his consistent scientific guidance, motivation, and inspiring discussion of research work. They are brilliant mentors and always friendly to all colleagues.

I sincerely thank all of the laboratory technicians, especially Susanne Goldmann, Rainer Andaq, Ulrike Bonitz, Sandra Hartung, Lisa Neuenroth, and Jan Schrader for their technical support, expertise and always available kind help.

I express gratitude to my parents, friends, relatives and family members for supporting me in difficult moments and understanding my needs. Wholehearted thanks to the peoples of Göttingen especially Pakistani community for all the good care and great help throughout the way. May God bless you all.

10 Curriculum Vitae - Niamat Khan

Apartment No. 108
Albrecht-Thaer-Weg 12
Deutschland
37075 Goettingen, Germany
E-Mail: niamat.khattak@gmail.com
Date of birth: 01-02-1975
Place of birth: Kohat, Pakistan
Nationality: Pakistani

EDUCATION:

2013_todate: PhD Student. Department of Clinical Chemistry, UMG, Goettingen, Germany.
(PhD student grant funded by the HEC/DAAD)

2011 – 2012: Laboratory for Molecular Hematology and Oncology, Dept. of Medicine II, Hematology and Oncology, University Hospital Frankfurt am Main. Topic: “The degradation of receptor tyrosine kinases in leukemia” (PhD student grant funded by the HEC/DAAD)

2005 – 2007 Degree/Diploma: MPhil (Genetics),
Quaid-i- Azam University, Islamabad, Pakistan
Diploma thesis: Estimation of genetic diversity among commercial varieties and primitive cultivars of Pakistani Rice (*Oryza sativa* L.) on the basis of Morphological characteristics, Molecular and Biochemical markers.

2000 – 2002 Degree/Diploma: M.Sc (Genetics)
University of Karachi, Karachi, Pakistan

1996 – 1998 Degree/Diploma: B.Sc (Pre- Medical)
University of Karachi, Karachi, Pakistan

CURRENT AFFILIATION:

2007 – date Department of Biotechnology & Genetic Engineering,
Kohat University of Science & Technology, Kohat, NWFP, Pakistan.

TEACHING EXPERIENCE:

2007 – 2011 Lecturer in the Department of Biotechnology & Genetic Engineering,
Kohat University of Science & Technology, Kohat, KPK, Pakistan.

Scientific Contribution:

Published

Khan N, Asif AR (2014) Tight Junction Integrity: Need for Non-Invasive Markers. *J Clin Cell Immunol* 5:e115. doi: 10.4172/2155-9899.1000e115

Khan N and Abdul R. Asif, “Transcriptional Regulators of Claudins in Epithelial Tight Junctions,” *Mediators of Inflammation*, vol. 2015, Article ID 219843, 6 pages, 2015. doi:10.1155/2015/219843

Mufti FU, Ullah H, Bangash A, **Khan N**, Hussain S, Ullah F, Jamil M, Jabeen M. Antimicrobial activities of *Aerva javanica* and *Paeonia emodi* plants, *Pak J Pharm Sci.* 2012 Jul; 25(3):565-9.

Submitted

Khan N, Pantakani DVK, Binder L, Qasim M and Asif AR (2015). Immunosuppressant MPA modulate tight junction through epigenetic activation of MLCK/MLC-2 pathway via p38MAPK. (Accepted in *Frontiers in Physiology*)

Khan N, Zahur M, Asif AR (2015). Mechanism of Tight Junction Regulation in Leak-Flux Diarrhea (Submitted)

List of Manuscripts in Submission Stage

Khan N, Lenz C, Binder L, Pantakani DVK, Asif AR (2015). Active and repressive chromatin associated proteome profiling after MPA treatment and the role of midkine in epithelial monolayer permeability. (To be submitted)

Khan N, Binder L, Pantakani DVK, Asif AR (2015). MPA modulates tight junctions' permeability via midkine/PI3K pathway in Caco-2 cells: A possible mechanism of leak-flux diarrhea in organ transplanted patients. (To be submitted)